CMIP experimental results from the CSIRO Mk3 climate system model: Comparison with reanalysis and observations

M.A. Collier, A.C. Hirst, M.R. Dix, R.P. Cechet, H.B. Gordon, E.A. Kowalczyk, S.P. O'Farrell and L.D. Rotstayn

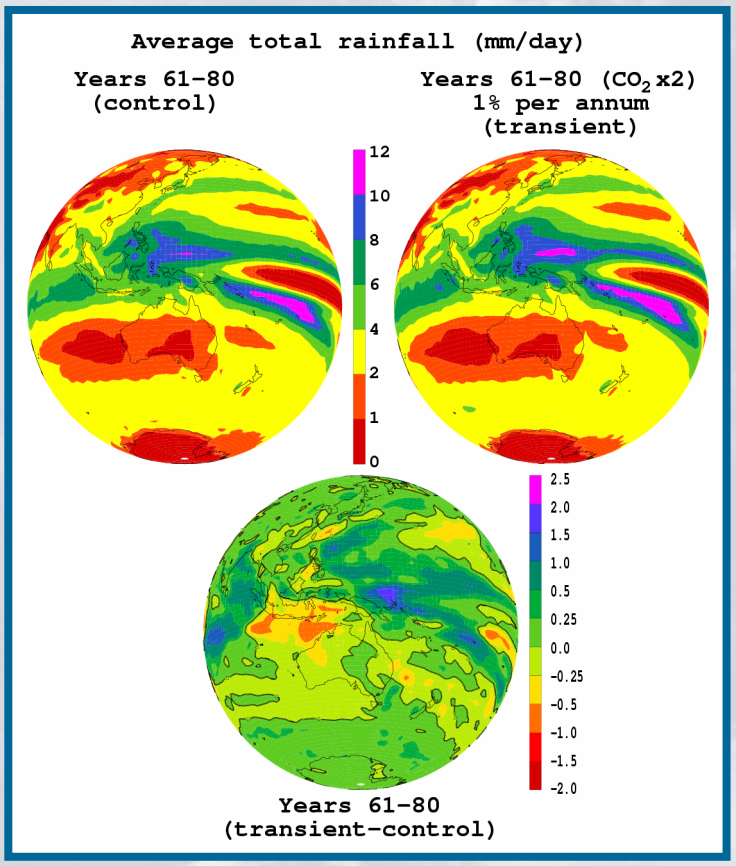

CSIRO

Atmospheric Research

CSIRO Atmospheric Research Technical Paper 69

CMIP experimental results from the CSIRO Mk3 climate system model: comparison with reanalysis and observations

M.A. Collier, A.C. Hirst, M.R. Dix, R.P. Cechet, H.B. Gordon, E.A. Kowalczyk, S.P. O'Farrell and L.D. Rotstayn

CSIRO Atmospheric Research Technical Paper No. 69

The National Library of Australia Cataloguing-in-Publication entry

CMIP experimental results from the CSIRO Mk3 climate system
Model: comparison with reanalysis and observations

ISBN 0 643 06888 0.

1. Atmospheric circulation - Computer simulation. 2. Ocean circulation - Computer simulation. 3. Numerical weather forecasting - Mathematical models. 4. Atmospheric circulation - Mathematical models. 5. Climatology - Mathematical models. I. Collier, M. A. II. CSIRO. Division of Atmospheric Research. (Series : CSIRO Atmospheric Research technical paper (Online) ; no. 69).

551.524

Address and contact details: CSIRO Atmospheric Research
Private Bag No. 1 Aspendale Victoria 3195 Australia
Ph: (+61 3) 9239 4400; fax: (+61 3) 9239 4444
e-mail: ar-enquiries@csiro.au

CSIRO Atmospheric Research Technical Papers may be issued out of sequence. From July 2000 all new Technical Papers will appear on the web site of CSIRO Atmospheric Research. Some Technical Papers will also appear in paper form.

Contents

Index to figures

Index to figures (cont.)

CMIP experimental results from the CSIRO Mk3 Climate System Model: comparison with reanalysis and observations

M.A. Collier, A.C. Hirst, M.R. Dix, R.P. Cechet, H.B. Gordon, E.A. Kowalczyk, S.P. O'Farrell and L.D. Rotstayn

CSIRO Atmospheric Research
PMB 1, Aspendale, Victoria 3195
Australia

July 2004

Abstract

This document lists the CSIRO Mk3 Climate System Model experimental data that have been contributed to the Climate Model Intercomparison Project (CMIP), and in particular, a realisation of CMIP known as CMIP2+ (the positive sign indicating an expansion on the original CMIP2 proposal). Included are a brief description of the monthly and daily fields that form the list of the core variables required for acceptance of a individual coupled climate model. Two experiments are described, one a control experiment with fixed constituents (CO_2, ozone, sulfate aerosols) and the other where the CO_2 level is increased at one percent per annum compounding. Together they both form an eighty year archive of model experiments following the COORDS netCDF convention. Annual, winter and summertime fields from the control experiment are compared to a climatology of the NCEP/NCAR R-1 reanalysis, where possible. Details on accessing fields are given in Section 6.

1 Technical aspects of the CSIRO Mk3 CSM

Technical aspects of the CSIRO Mk3 Climate System Model (hereafter CSIRO Mk3), have been comprehensively described in *Gordon et al.* (2002), and where relevant, details will be reiterated here. Topics on weather and climate have been addressed from detailed analysis of the CSIRO Mk3 CSM (*Cai et al.*, 2002, 2003, 2004; *Watterson and Dix*, 2004) and it is expected that a (stepwise improving) version of CSIRO Mk3 CSM will be active for several years to come. CSIRO has been involved in the Climate Model Intercomparison Project (CMIP[1]) activity since its inception in 1995, as it provides a unique international forum for the collection and objective comparison of simulations from global coupled climate models (*Meehl et al.*, 2003).

1.1 Anthropogenic forcings

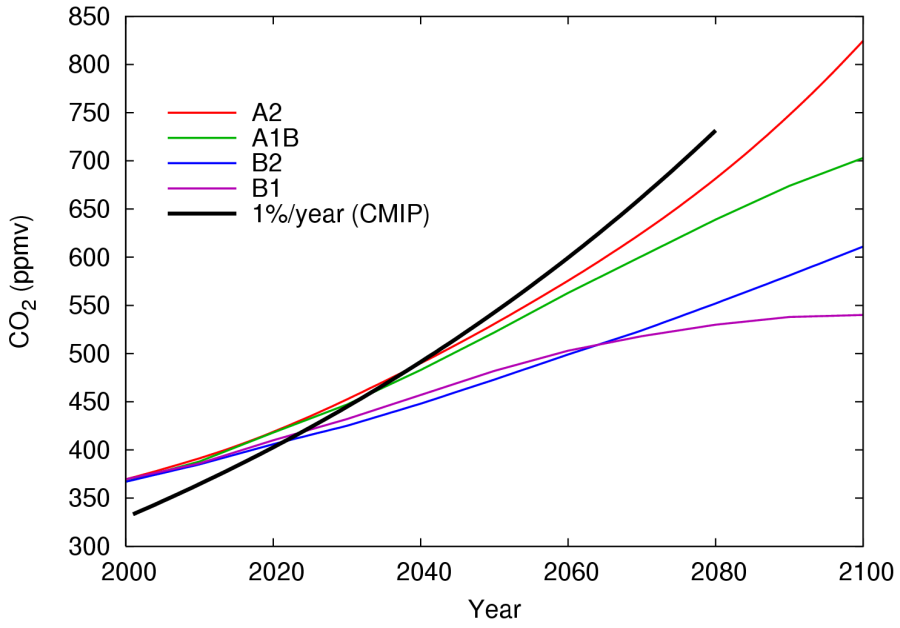

Figure 1: Actual CO_2 concentration scenario for 1% per annum compounding compared with that for equivalent CO_2 for commonly used scenarios.

The CMIP transient experiment uses a 1% per annum compounding carbon-dioxide series, as indicated in Figure 1. The rate of increase in the CMIP experiment is larger than of the SRES cases. However when other greenhouse

[1] http://www-pcmdi.llnl.gov/cmip/

gases (methane, nitrous oxide, chloro-fluorocarbons) are taken into account, the CMIP radiative forcing is quite similar to the A2 total GHG forcing. All other forcing, namely ozone and sulfate aerosols, are held constant.

1.2 Model component spin-up and coupled model initialisation

A general discussion on CSIRO Mk3 CSM initialisation and spin-up is covered in *Gordon et al.* (2002, Section 20), and will be briefly reexamined here. The oceanic component of CSIRO Mk3 CSM was integrated for about 1500 years using asynchronous time-stepping. That is, time-steps for the tracer integration (8 hours) were chosen to be much larger than the dynamics (15 minutes) to reduce wall clock time to reach a quasi-equilibrium thermohaline solution. Monthly climatological forcings of zonal and meridional wind stress, precipitation (or salt equivalent) and solar radiation were generated off-line by the atmosphere model and interpolated to the ocean model time-step during model integration. The ocean model was integrated for a further 10 years with synchronous time-stepping. The AGCM spinup used seasonally varying climatological sea-surface temperatures for about 100 years. The coupled model was then initialised using the spun-up ocean fields, and integrated for 120 years to allow the coupled climate to recover from the initial "shock" and reach a new, relatively stable, climate state. The CMIP simulations described here are commenced from the atmospheric and oceanic conditions at the 120 year mark of the coupled run.

1.3 Coupled model grid

A detailed description of the atmospheric and ocean model grids are described in *Gordon et al.* (2002, Section 7, 20.1, 20.2 and 20.3), only pertinent details are presented here and tabulated in Section 4. The oceanic component of the CSIRO Mk3 CSM has a horizontal grid referred to as an Arakawa "B-grid", where the tracer and velocity variables are solved on separate staggered grids, the ocean bathymetry is shown in Figure 2a.

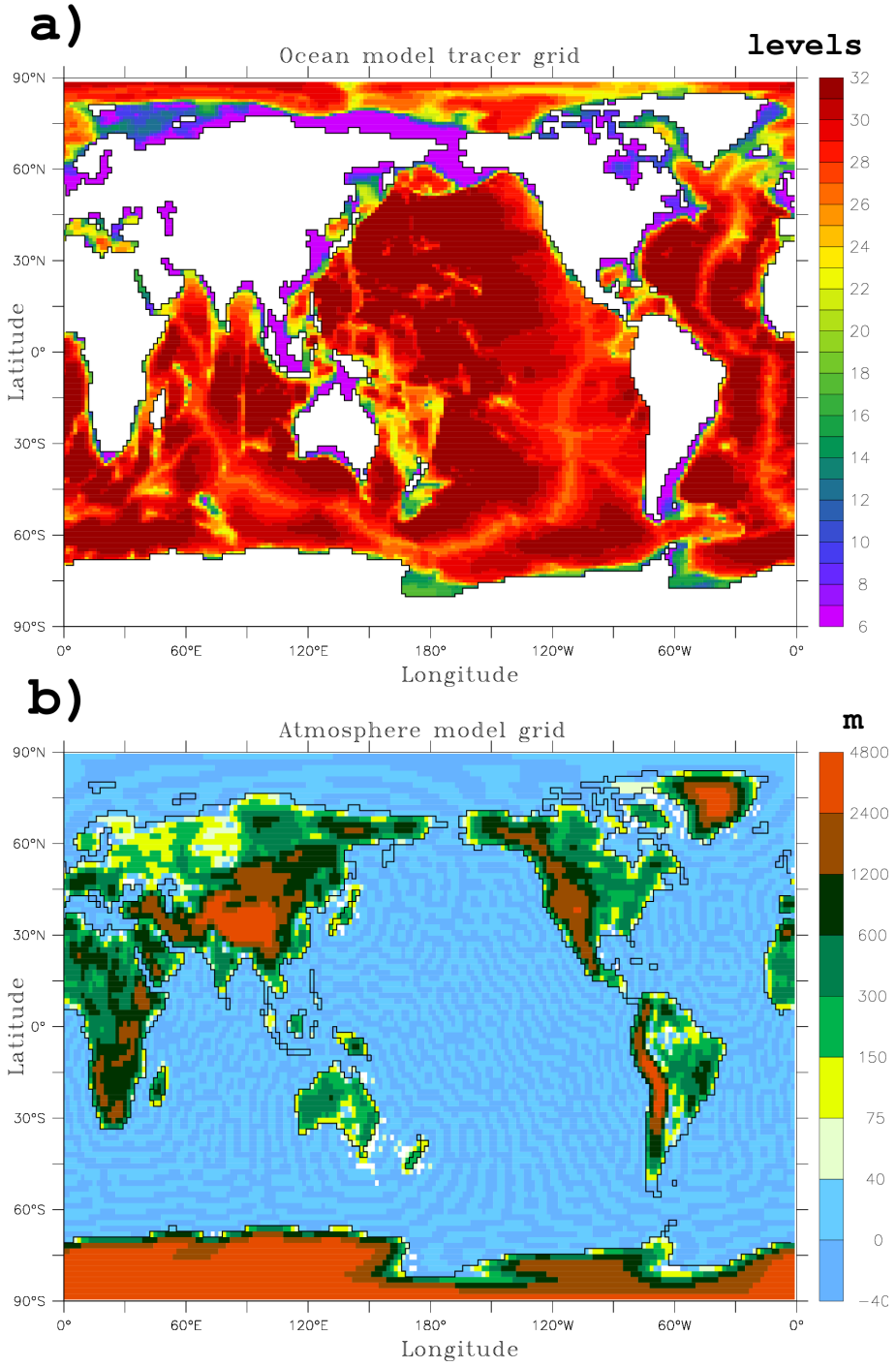

Figure 2: Outline of the CSIRO-Mk3 T63_2 (192 × 196) a) ocean and b) atmosphere model component grid, with bathymetry and topography shaded for each.

The real depth values of these so called kmt levels (shaded in the figure) can be looked up in the table headed "Depth levels" in Section 4.2. For example, a kmt level of 6 corresponds to a depth of 78.54 metres for both tracer and velocity grids. Note that all ocean columns have a minimum of 6 levels depth. The ocean depths were chosen to enhance the seasonally varying part of the upper ocean (13 of the 31 vertical levels represent the upper 400 metres), and to aid in better communication of exchanges of heat, moisture and momentum with the atmosphere. The ETOPO5 5-minute data set was used in the initial bathymetry construction. The automatically generated oceanic component bathymetry was then modified to ensure realistic depths of key sills not well resolved in the original construction.

The atmospheric component features dynamics at spectral truncation T63 and physics grid of approximately 1.875° longitude by 1.875° latitude, and 18 vertical levels. The ocean component has the horizontal resolution of 1.875° longitude by 0.9375° latitude. The horizontal resolution of the ocean component matches the atmospheric component in the zonal direction, but twice that in the meridional direction. Several variables are computed (e.g. cloud amounts and surface radiative and turbulent heat fluxes) on the so-called physics grid of the atmospheric model. Key model variables (e.g. temperature and velocities) represented in the model are defined in spectral space, however, are transformed to the physics grid for further caluclations in physics space and written out to average and instantaneous files for post-processing. History files, used primarily for initialisation of the coupled model, have a combination of spectral and horizontal fields so that, if necessary a model can be rerun from any point in the model experiment and replicate the results on any given machine architecture.

Because two ocean grid points match a single atmosphere grid point, an average of the fields (wind, heat and water) is communicated between the corresponding model component grid-points during coupling. The land-sea mask for both the ocean and atmosphere match exactly to avoid any inaccurate interpolation of data that would be otherwise required. As the atmospheric model is spectral, the mountains are spectrally analysed from raw high resolution grid-point data, this data transformed back into grid-point space is shown in Figures 2b. When spectral topography is transformed to a regular horizontal grid small negative values appear. The model physics includes a parameterisation for sub-grid scale topography (gravity-wave drag) and adjustment of lowest level temperature fields to compensate for the spurious effects of series truncation on the topography field.

1.4 Land surface characteristics

Parameterization of the land-surface scheme has been significantly improved in the CSIRO Mk3 CSM compared with Mk2 *McGregor et al.* (1993), an overview is presented in *Gordon et al.* (2002, Section 7, 9 and 19). The snow model has three snowpack layers where temperature, density and thickness are computed. The soil model has six layers where temperature, liquid water amount and ice amount are computed. Each land grid box has surface properties derived from the products of *Dorman et al.* (1989), including monthly albedo, stomatal resistence and roughness length.

1.5 Ocean and sea-ice model

The sea-ice model resides in the atmospheric model code and simulates both ice dynamics and ice thermodynamics as described in *Gordon et al.* (2002, Section 19). Model grid points with sea-ice are allowed to have a fraction of open water (leads/polynyas) to improve the simulation of the effects of turbulent heat fluxes from the ocean to the atmosphere. The oceanic code of the CSIRO Mk3 CSM is based on version 2.2 of the GFDL Modular Ocean Model (MOM) and the implementation is described in *Gordon et al.* (2002, Section 20).

2 CMIP contribution

Listed in tables in Section 2.1 are the main set of variables, available in CO-ORDS[2] conforming netCDF form, which are further examined in subsequent sections of this paper. We have chosen as our set the same set of variables as is required by the 20^{th} Century Climate in Coupled Model (20C3M) pilot project, originally specified in November 2002[3]. We make this choice because the 20C3M project requires more comprehensive set of fields than the original CMIP2, but a much smaller set of fields when compared to the CMIP2+[4] project. The CMIP2+ charter required all archive monthly data from a one century control and transient experiment, and daily data for limited decades. These were an extremely large and difficult collection of data to assemble and submit.

[2] http://www.unidata.ucar.edu/packages/netcdf/conventions.html

[3] http://www-pcmdi.llnl.gov/cmip/ann_20c3m.html

[4] CSIRO was involved in this project, which is now closed to new submissions. CSIRO expects to make contributions to future CMIP activities

In Section 2.2 the CSIRO Mk3 CSM CMIP control experiment is described by way of diagrams of ANN (annual average), DJF (December, January and February) and JJA (June, July and August) ocean and atmosphere climatologies, both for horizontally defined variables and cross-sections of variables that are a function of height or depth. These have been compared, where possible, to the NCEP/NCAR R-1[5] reanalysis climatologies (Kalnay et al., 1996; Kanamitsu et al., 2002; Kislter et al., 2001; *Collier*, 2000, 2004) in the case of atmospheric variables, and against the NODC World Ocean Atlas (WOA) for the oceanic variables (*Conkright et al.*, 2002; *Collier*, 2003). In Section 3.1 time-series of results averaged over the globe surface (or land or ocean-only, or where they are defined) are averaged with a 121-month running mean to illustrate the response to changing atmospheric forcings and compared to the control experiment to provide an indication of inter-annual variability and model sensitivity.

2.1 Core variables

It is not possible to provide all variables exactly as requested by the 20CM3 activity. The absence of some variables is due to a CSIRO Mk3 CSM diagnostic limitation or a treatment of certain physical processes in the model which dosen't allow for it. Three-dimensional cloud amounts are predicted by the model, however, only lower, middle and upper cloud amounts are available as monthly averages[6]. Sea-level rise is not predicted in the model (a rigid-lid approximation is employed in the ocean component, where the surface vertical velocity is zero), however, techniques are available to diagnostic it implicitly.

In the comparison with NCEP/NCAR R-1 reanalysis, it may not be possible to find the equivalent CSIRO Mk3 CSM model variable. This is particularly true for a number of variables described by the land-surface scheme. Lower and upper level soil moisture[7]. fall into this category and therefore in Section 2.2 of this paper figures are drawn for qualitative purposes and no difference field figures, model versus observations, are generated. Ice depth is not available in NCEP R-1 and so ice concentration is presented in the comparison instead.

[5] the original 1996 reanalysis. The version released in 2002 is referred to as R-2 "Reanalysis-2"

[6] these are derived using a random overlap approach for cloud amounts at the atmospheric levels 1-6, 7-11 and 12-18 listed in Section 4.1, respectively

[7] in NCEP soil moisture is described by volumetric ratio i.e. ratio of water volume to total soil volume. In Mk3 soil moisture is describe by volumetric ratio of water available for evapotranspiration i.e. ratio of water volume minus wilting point to total soil volume. For NCEP and Mk3 upper is a value averaged over 0-0.10 and 0-0.022 m of the soil model column, respectively, and lower averaged over 0.10-2.0 and 0-4.6 m, respectively

The spatial patterns of fields which cannot directly be compared, may still be of interest to readers, and to some degree give an indication of model sensitivity to external forcings. However, in Section 3.1, the control and transient response of the CSIRO Mk3 CSM core variables are compared through a set of x-y time-series. The control and transient experiments have the experimental label of ct3 and cm3, respectively. The variables presented in the tables found in this section have been extracted from model diagnostic history files. A full set of variables contained in these history files is presented in Section 5.

For each monthly diagnostic field, either from the atmosphere or ocean component, there are 960 temporal fields (80 years of monthly data). Note that this model has a fixed year length of 365 days (i.e. no leap years). The atmosphere pressure level variables have 18 levels, 192 longitudes and 96 latitudes listed in Section 4.1. The ocean depth level variables have 31 levels, 194 longitudes and 189 latitudes on the tracer grid, and 194 longitudes and 189 latitudes on the velocity grid as shown in Section 4.2. Note that all CSIRO Mk3 CSM variables described within this paper are available at the full vertical and horizontal resolution of the coupled model.

For each daily diagnostic field, for which there are only atmospheric variables, there are 29200 temporal fields 80 years of daily data, with underlying calendar years of 1961-2040 [8]). The horizontal resolution remains at 192 by 96.

[8]the year range in the control experiment ct3 is purely for convenience as the choice is arbitrary and not fixed to our real calendar

Field	Variable	Unit	Experiment label	$x \times y \times z \times t$
total cloud	clm	fraction	ct3/cm3	192 96 1 960
ice concentration	ico	fraction	ct3/cm3	192 96 1 960
mean sea level pressure	psl	hPa	ct3/cm3	192 96 1 960
surface screen temperature	tsc	°C	ct3/cm3	192 96 1 960
surface temperature	tsu	°C	ct3/cm3	192 96 1 960
lower level available soil moisture	wfb	volumetric ratio	ct3/cm3	192 96 1 960
upper level available soil moisture	wfg	volumetric ratio	ct3/cm3	192 96 1 960
air temperature	t4d	°C	ct3/cm3	192 96 18 960
ocean salinity	Salt	ppt	ct3/cm3	194 189 31 960
ocean in-situ temperature	Temp	°C	ct3/cm3	194 189 31 960

Table 1: Eighty years of monthly data from the CSIRO Mk3 CSM CMIP control (ct3) and transient (cm3) experiments.

Field	Variable	Unit	Experiment label	x × y × z × t
mean sea level pressure	psl	hPa	ct3/cm3	192 96 1 29200
total precipitation	rnd	mm	ct3/cm3	192 96 1 29200
maximum surface temperature	thd	°C	ct3/cm3	192 96 1 29200
minimum surface temperature	tld	°C	ct3/cm3	192 96 1 29200

Table 2: Eighty years of daily data from the CSIRO Mk3 CSM CMIP control (ct3) and transient (cm3) experiments.

A full list of variables available from the CSIRO Mk3 CSM CMIP experiments is given in Sections 5.1 and 5.2. From these raw variables, the variables found in Tables 1 and 2 have been created. Core variables are an improved version of the raw variables, specifically in terms of the netCDF conventions that are used, designed to be easy to read by CMIP investigators. Other diagnostic variables may be derived from the core or raw variables, for example, meridional overturning stream-function on a basin basis, or pressure level variables at specific levels other than those already available.

2.2 CSIRO Mk3 CSM CMIP control climatology

2.2.1 ANN

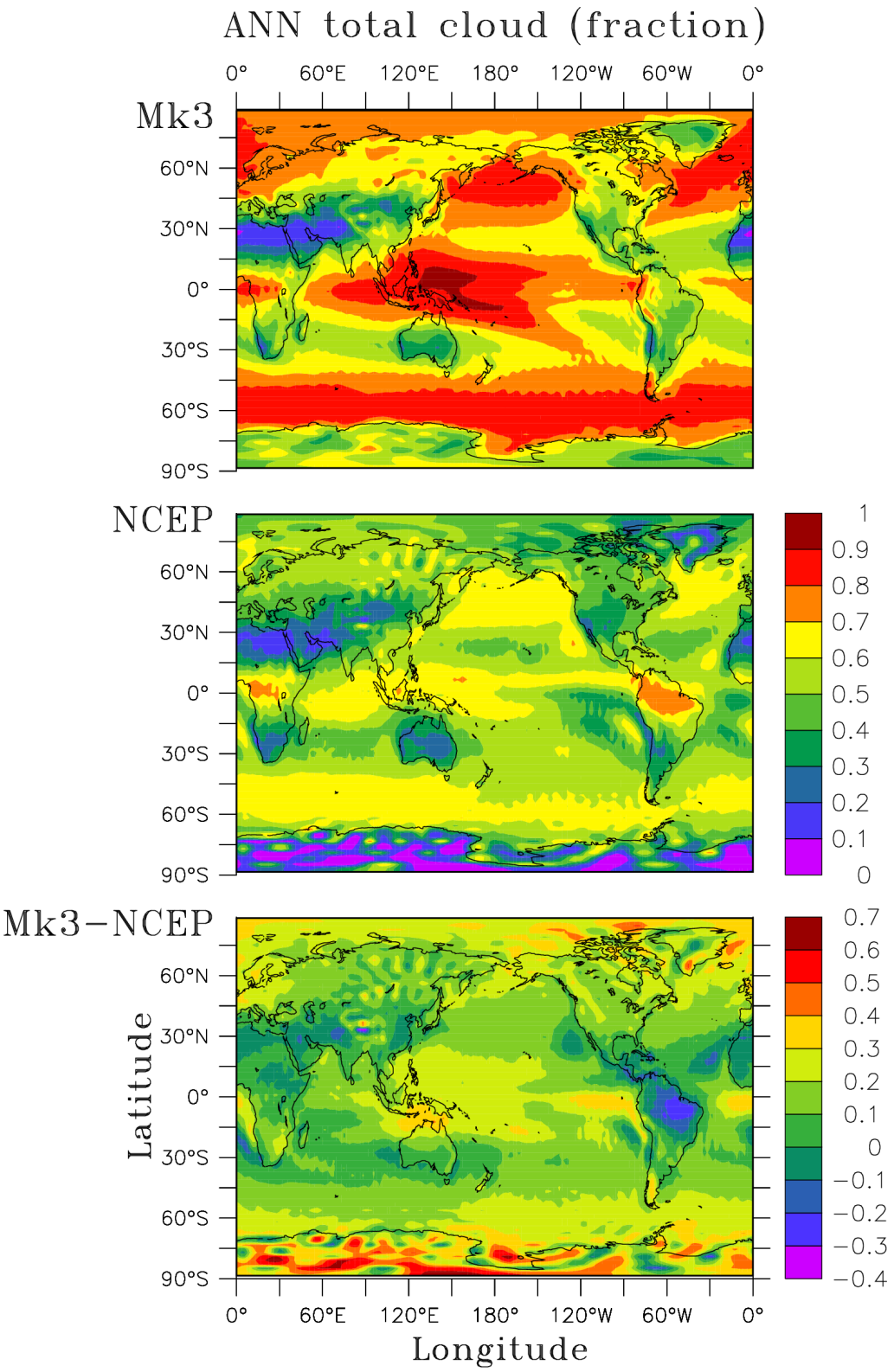

Figure 3: CSIRO-Mk3 CMIP control experiment (top), NCEP reanalysis (middle) and difference (bottom) of ANN total cloud climatology (fraction).

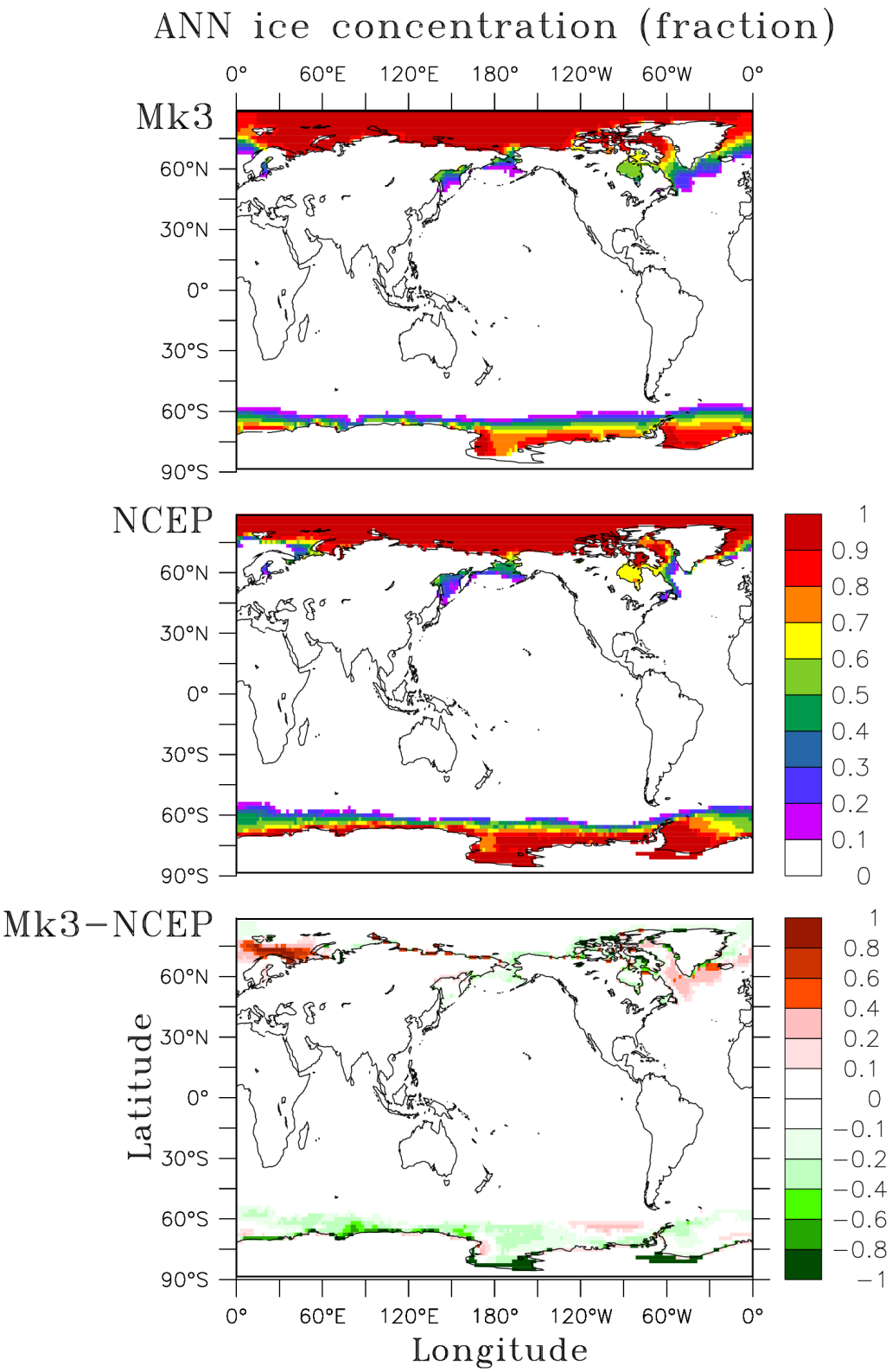

Figure 4: CSIRO-Mk3 CMIP control experiment (top), NCEP reanalysis (middle) and difference (Mk3-NCEP, bottom) of ANN ice concentration climatology (fraction).

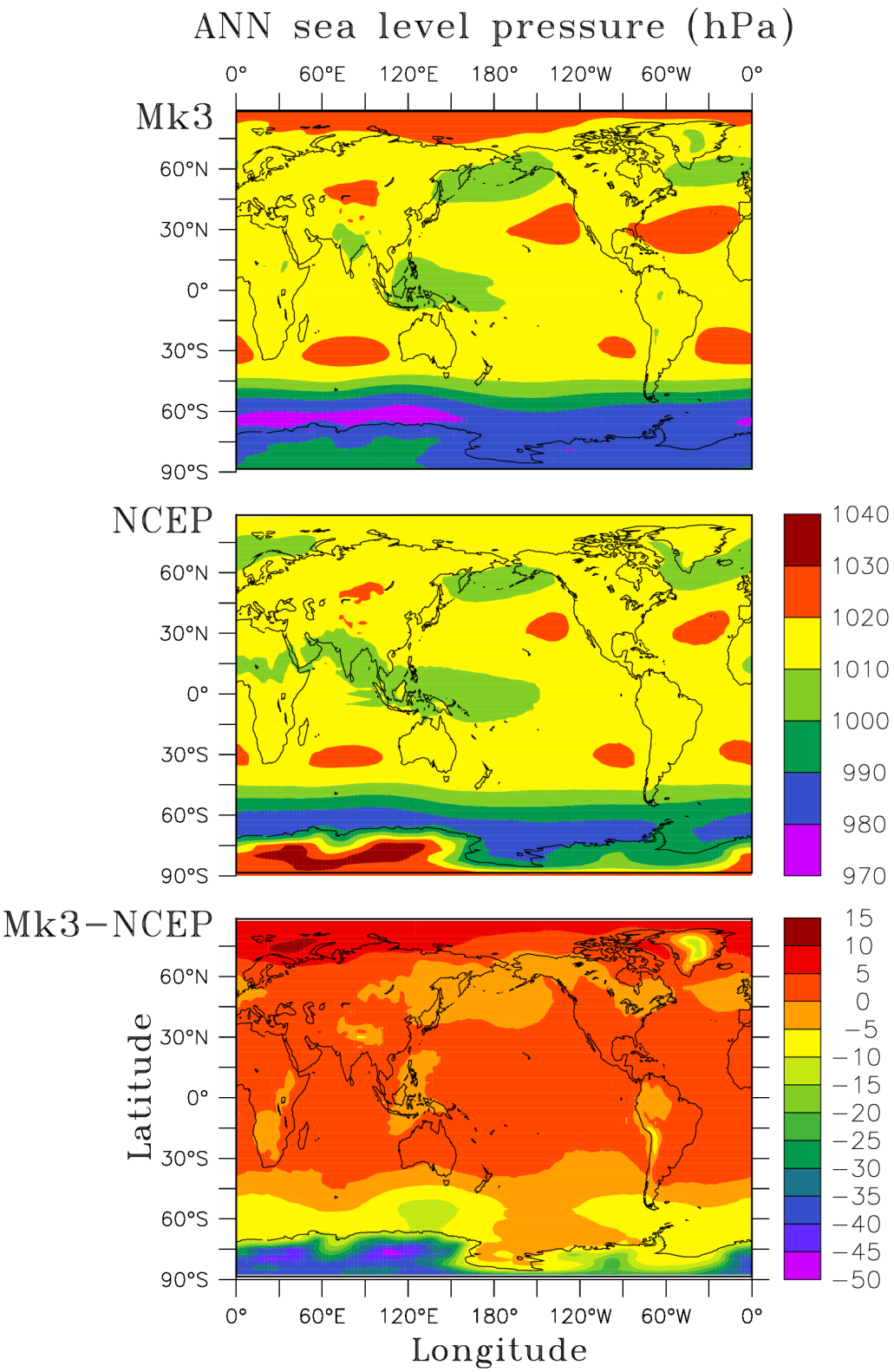

Figure 5: CSIRO-Mk3 CMIP control experiment (top), NCEP reanalysis (middle) and difference (Mk3-NCEP, bottom) of ANN mean sea level pressure climatology (hPa).

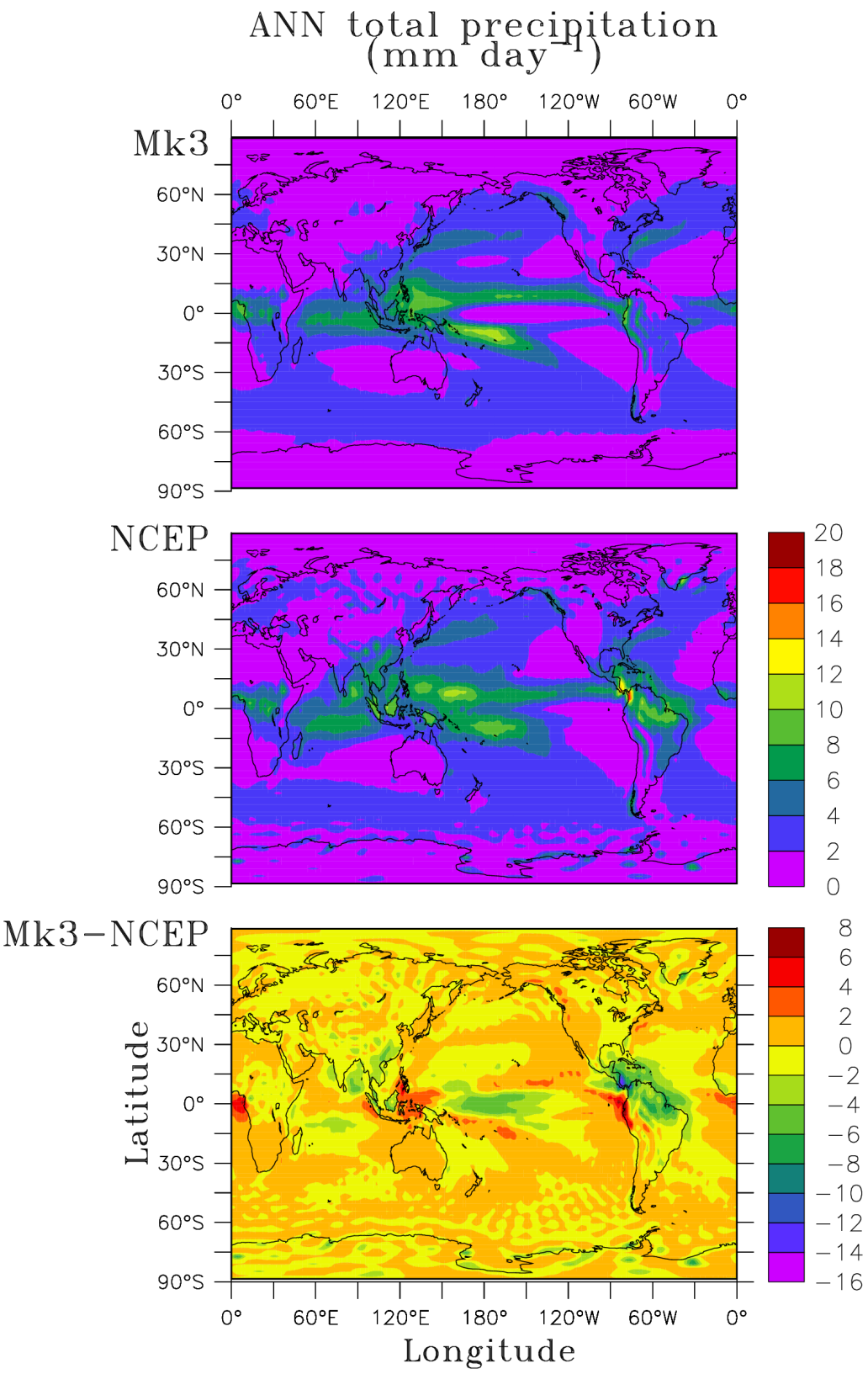

Figure 6: CSIRO-Mk3 CMIP control experiment (top), NCEP reanalysis (middle) and difference (Mk3-NCEP, bottom) of ANN precipitation climatology (mm day^{-1}).

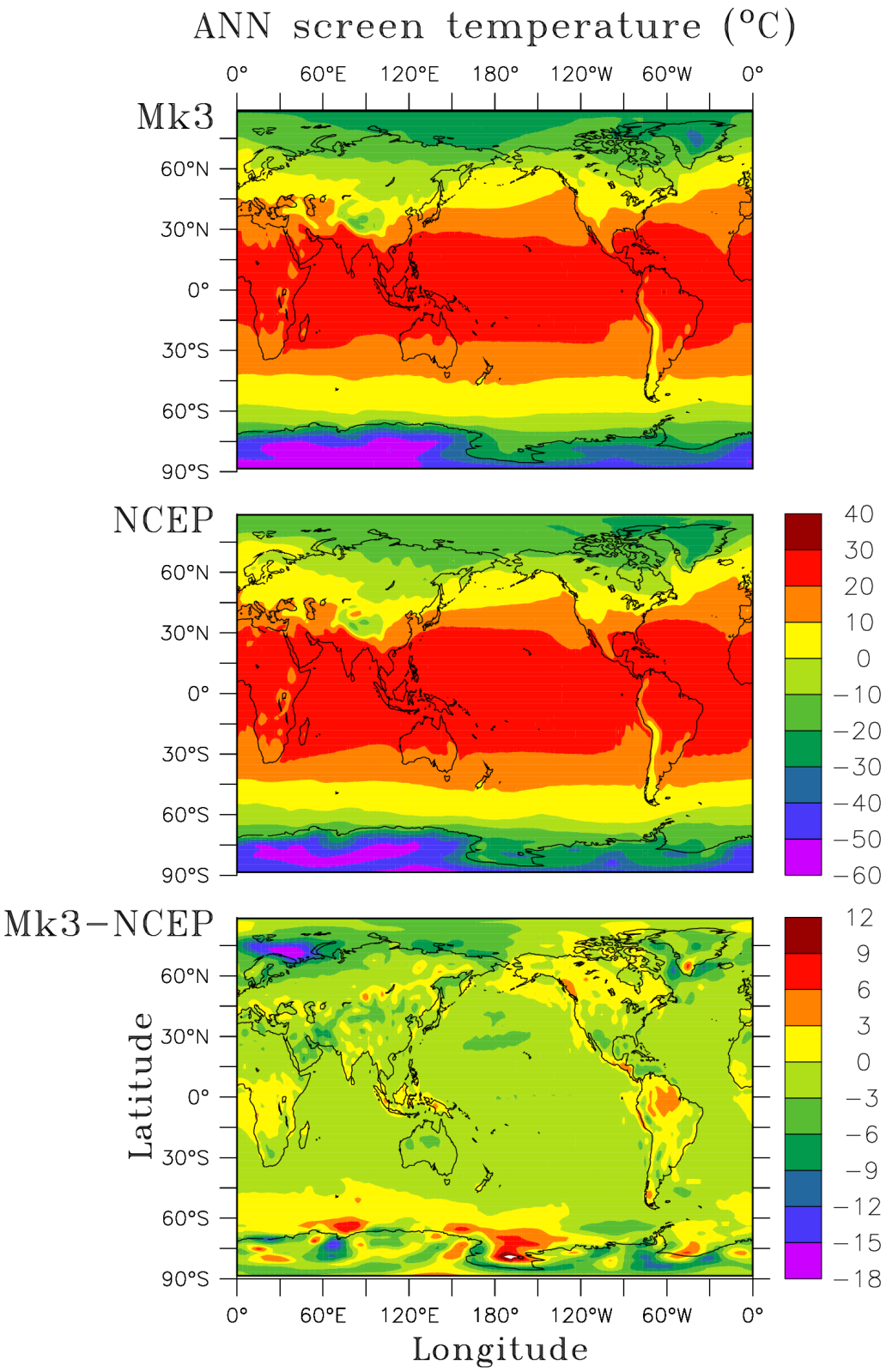

Figure 7: CSIRO-Mk3 CMIP control experiment (top), NCEP reanalysis (middle) and difference (Mk3-NCEP, bottom) of ANN surface screen temperature climatology (°C).

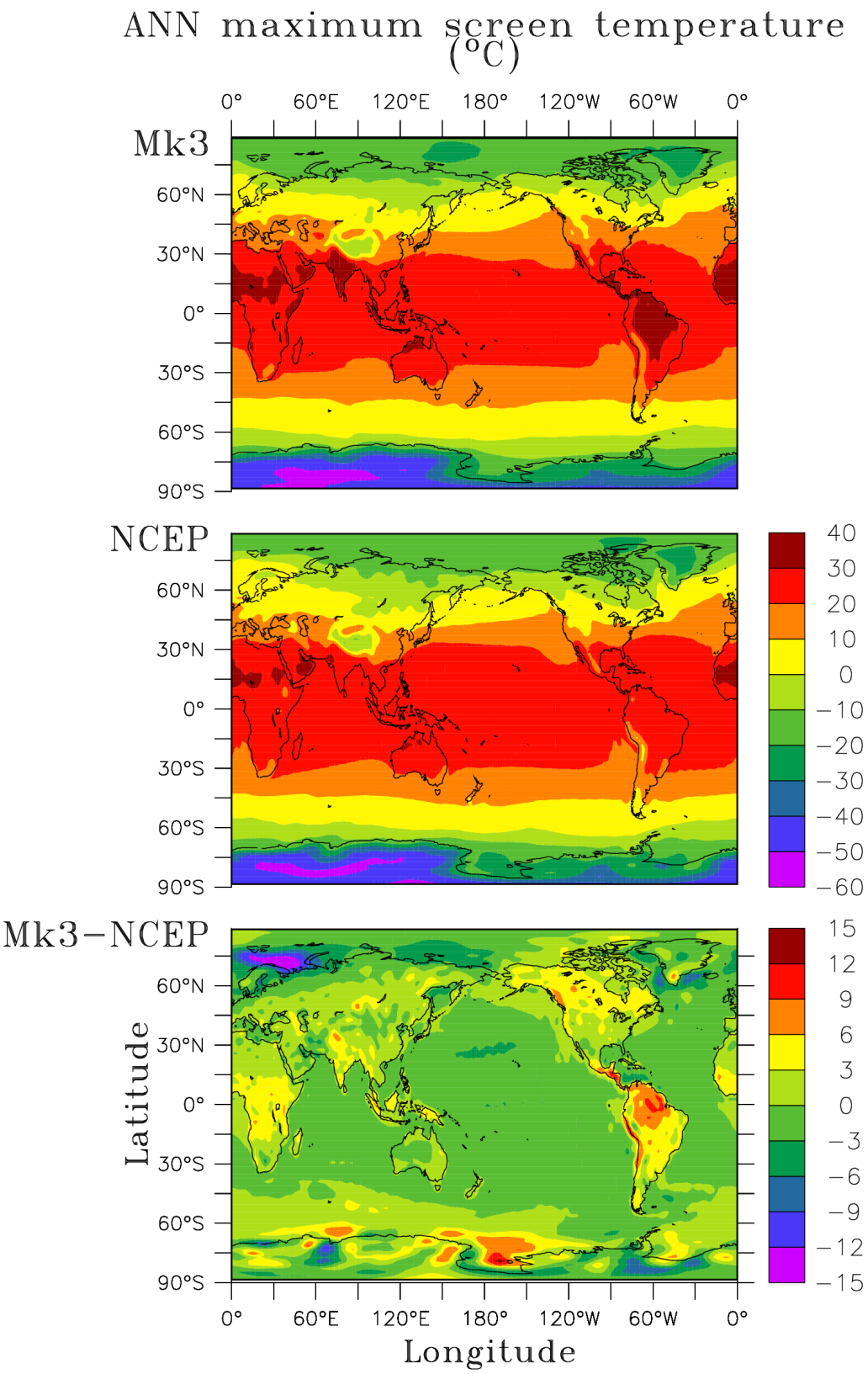

Figure 8: CSIRO-Mk3 CMIP control experiment (top), NCEP reanalysis (middle) and difference (Mk3-NCEP, bottom) of ANN maximum screen temperature climatology (°C).

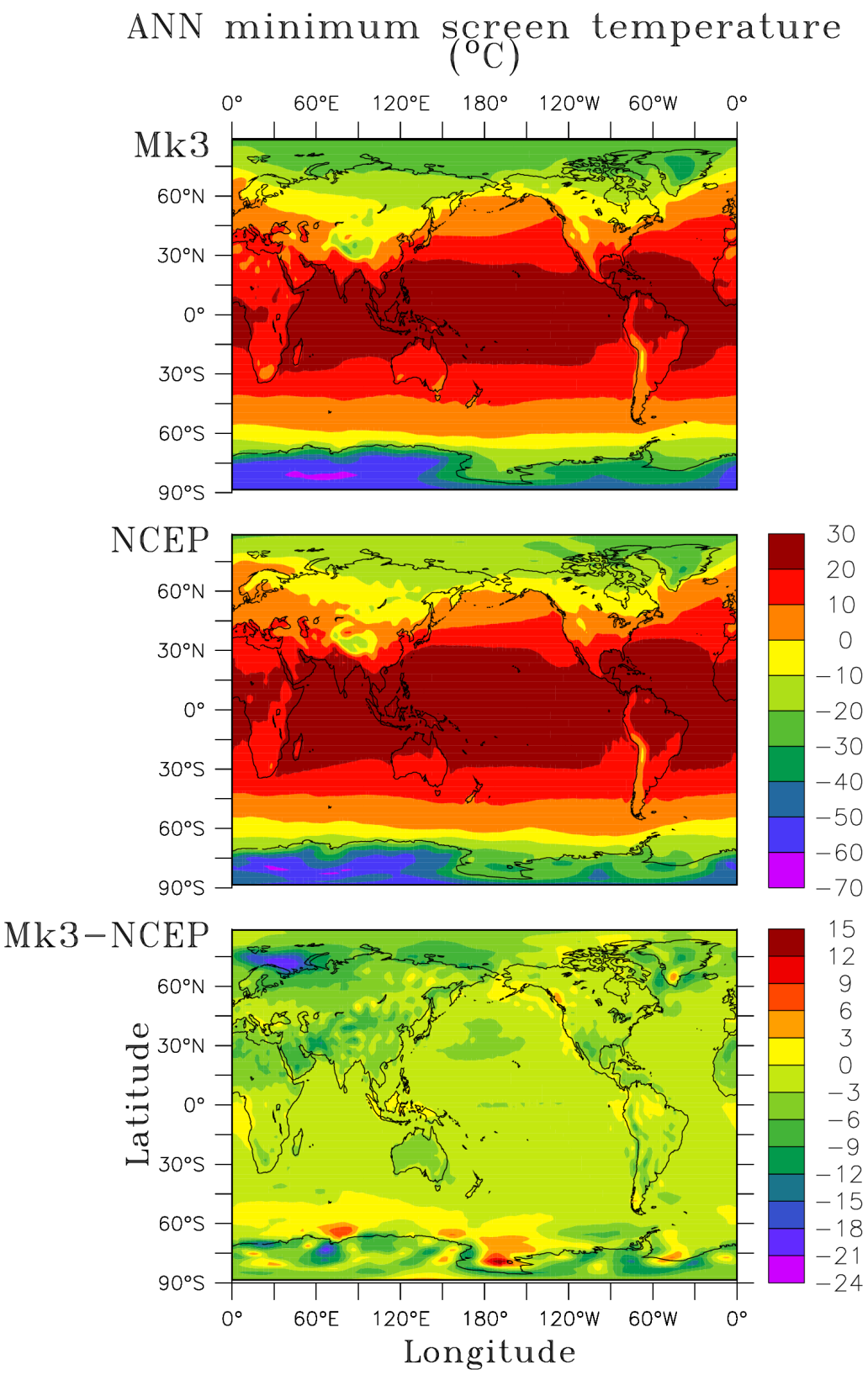

Figure 9: CSIRO-Mk3 CMIP control experiment (top), NCEP reanalysis (middle) and difference (Mk3-NCEP, bottom) of ANN minimum screen temperature climatology (°C).

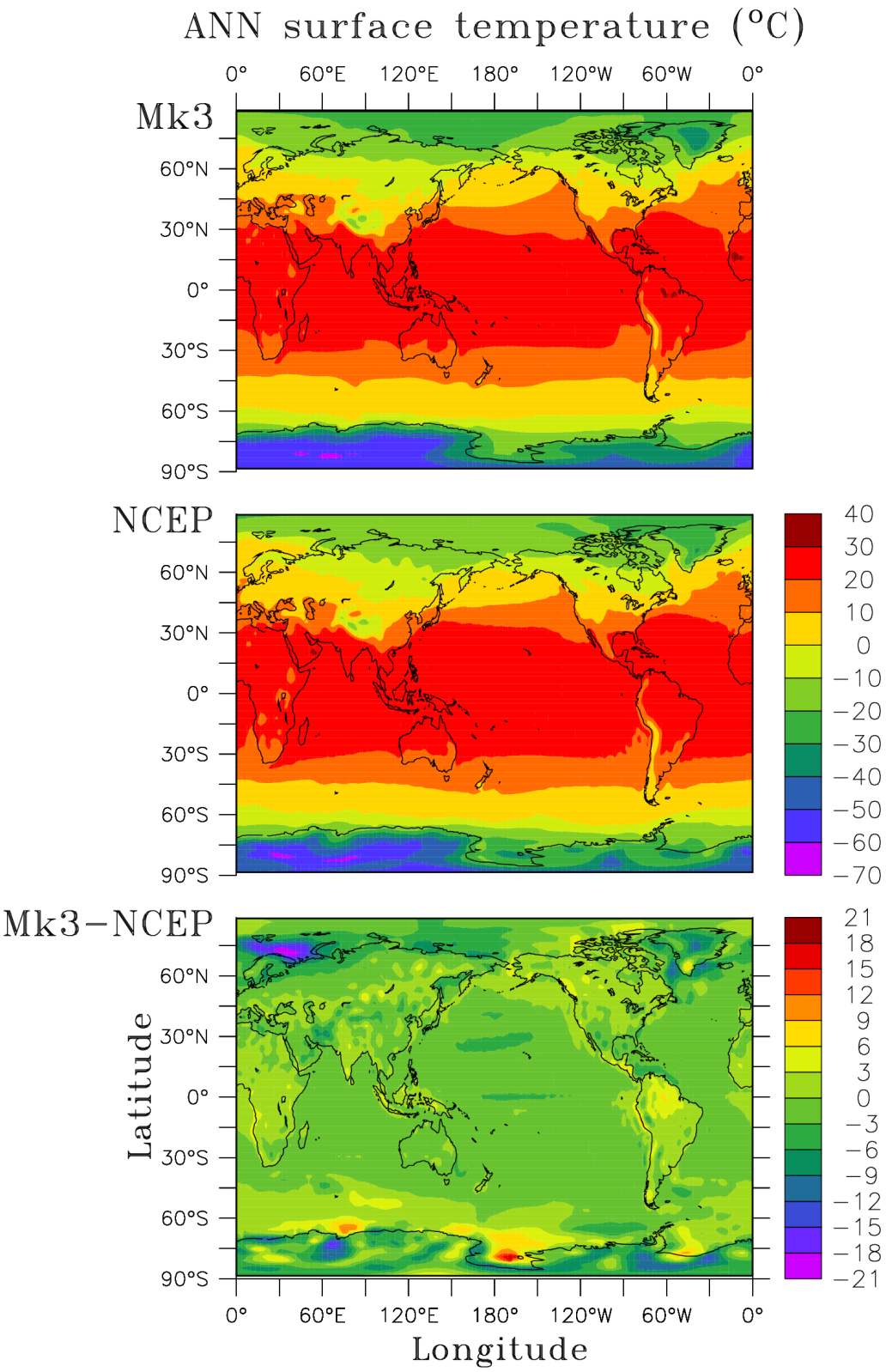

Figure 10: CSIRO-Mk3 CMIP control experiment (top), NCEP reanalysis (middle) and difference (Mk3-NCEP, bottom) of ANN surface temperature climatology (∘C).

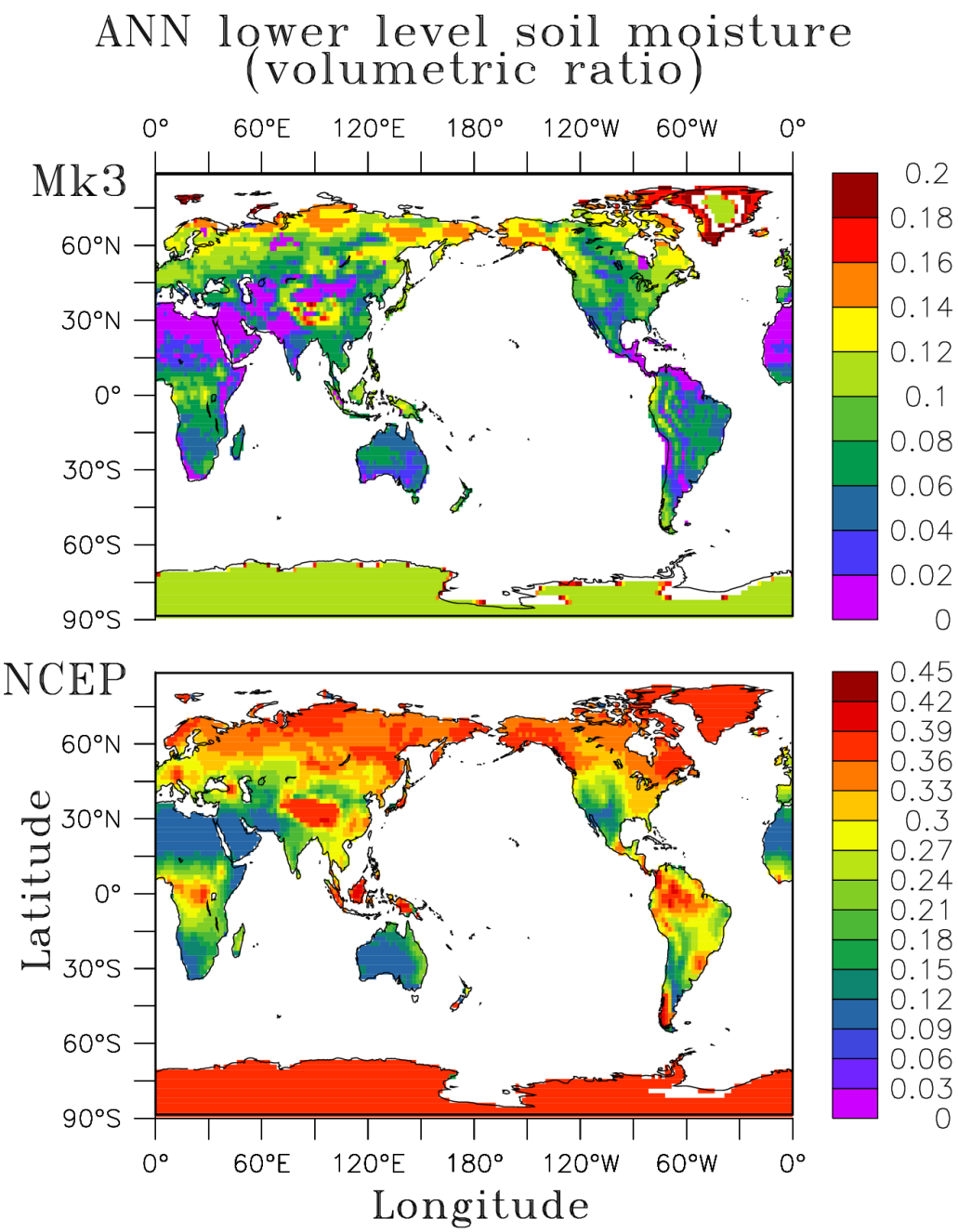

Figure 11: CSIRO-Mk3 CMIP control experiment (top) and NCEP reanalysis (bottom) of ANN lower level available soil moisture climatology (volumetric ratio). In CSIRO-Mk3 and NCEP, the soil depth range is 0-4.6 and 0.1-2.0 m, respectively.

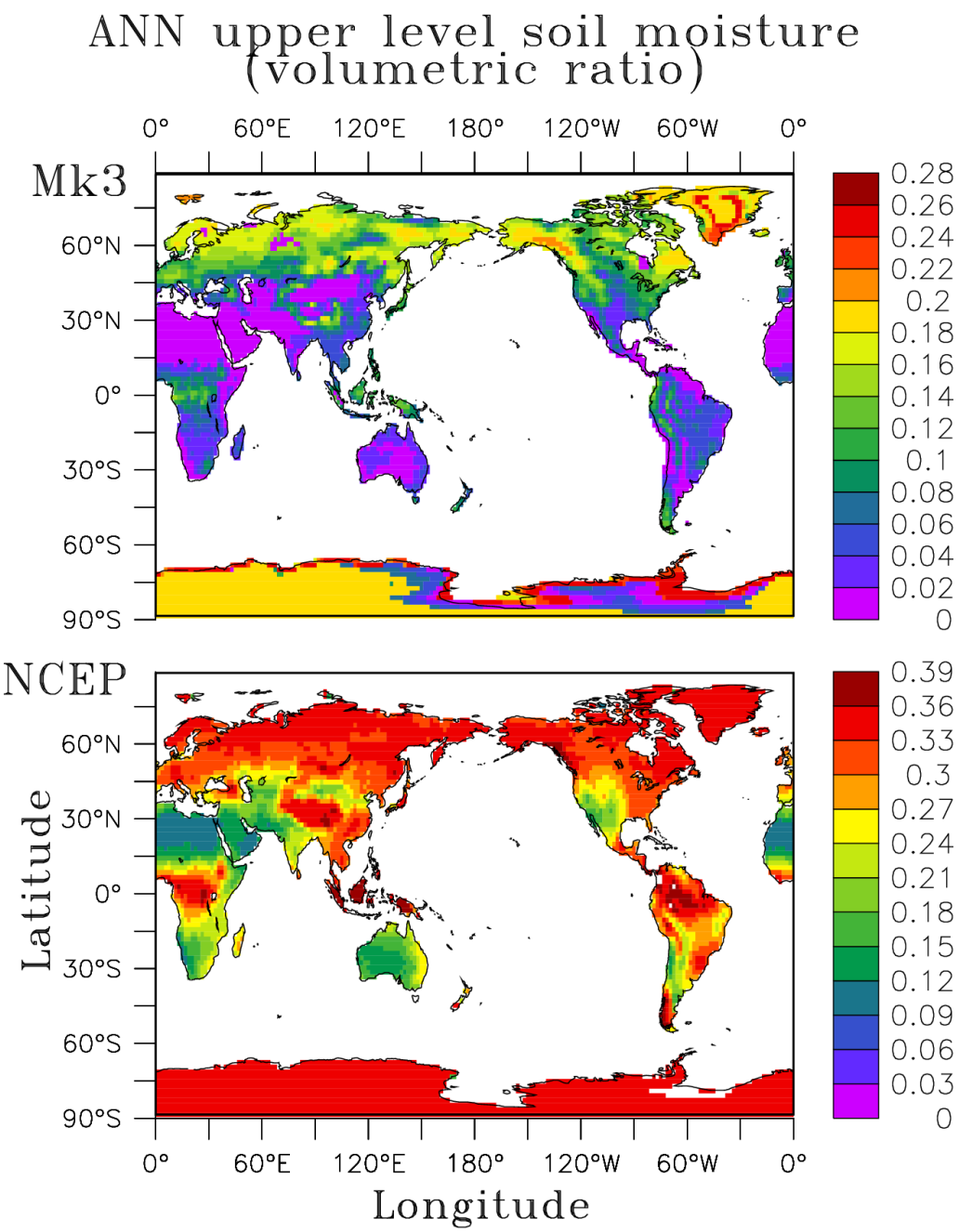

Figure 12: CSIRO-Mk3 CMIP control experiment (top) and NCEP reanalysis (bottom) of ANN upper level available soil moisture climatology (volumetric ratio). In CSIRO-Mk3 and NCEP, the soil depth range is 0-0.02 and 0-0.1 m, respectively.

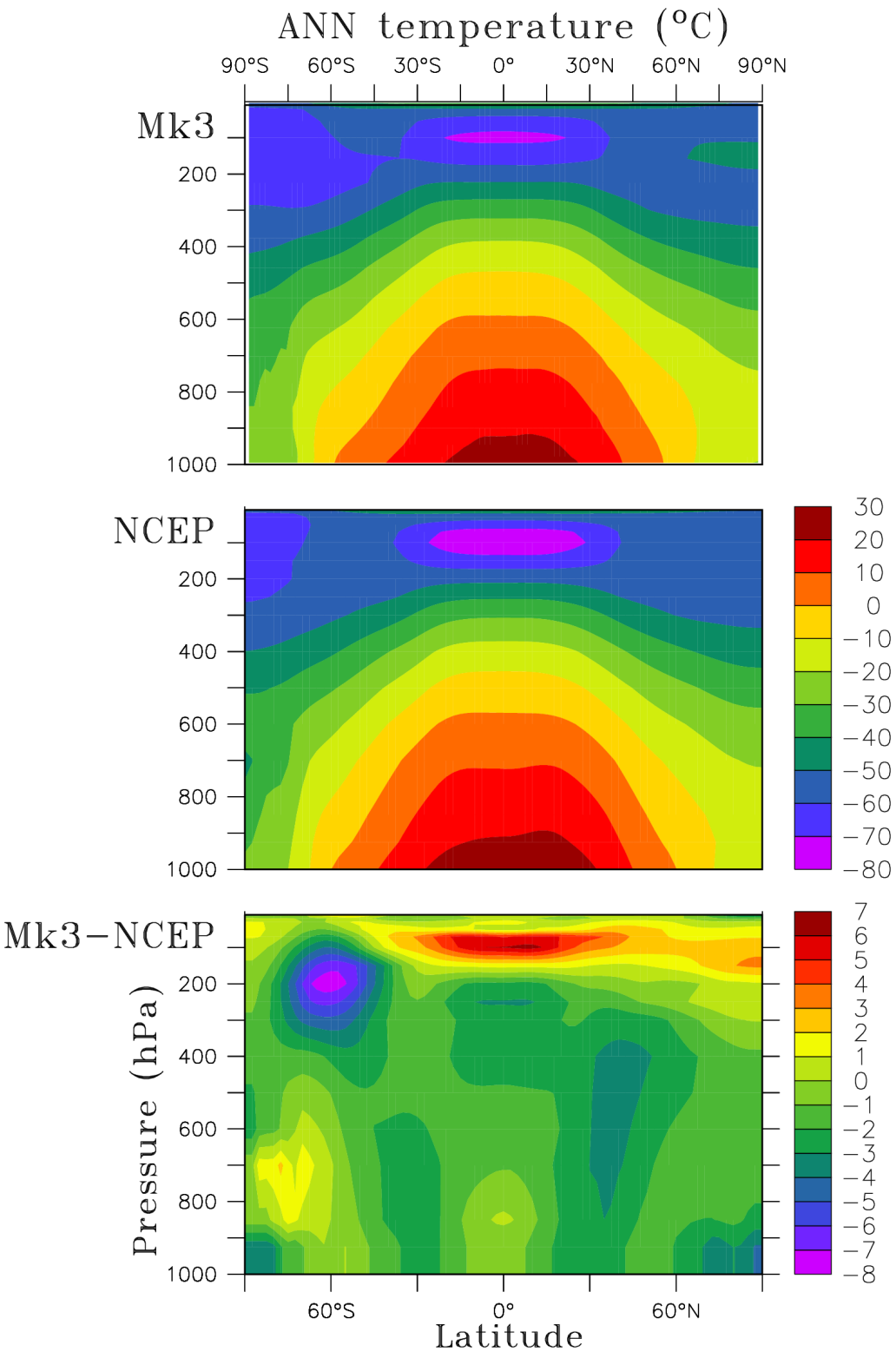

Figure 13: CSIRO-Mk3 CMIP control experiment (top), NCEP reanalysis (middle) and difference (Mk3-NCEP, bottom) of ANN atmosphere temperature climatology (°C).

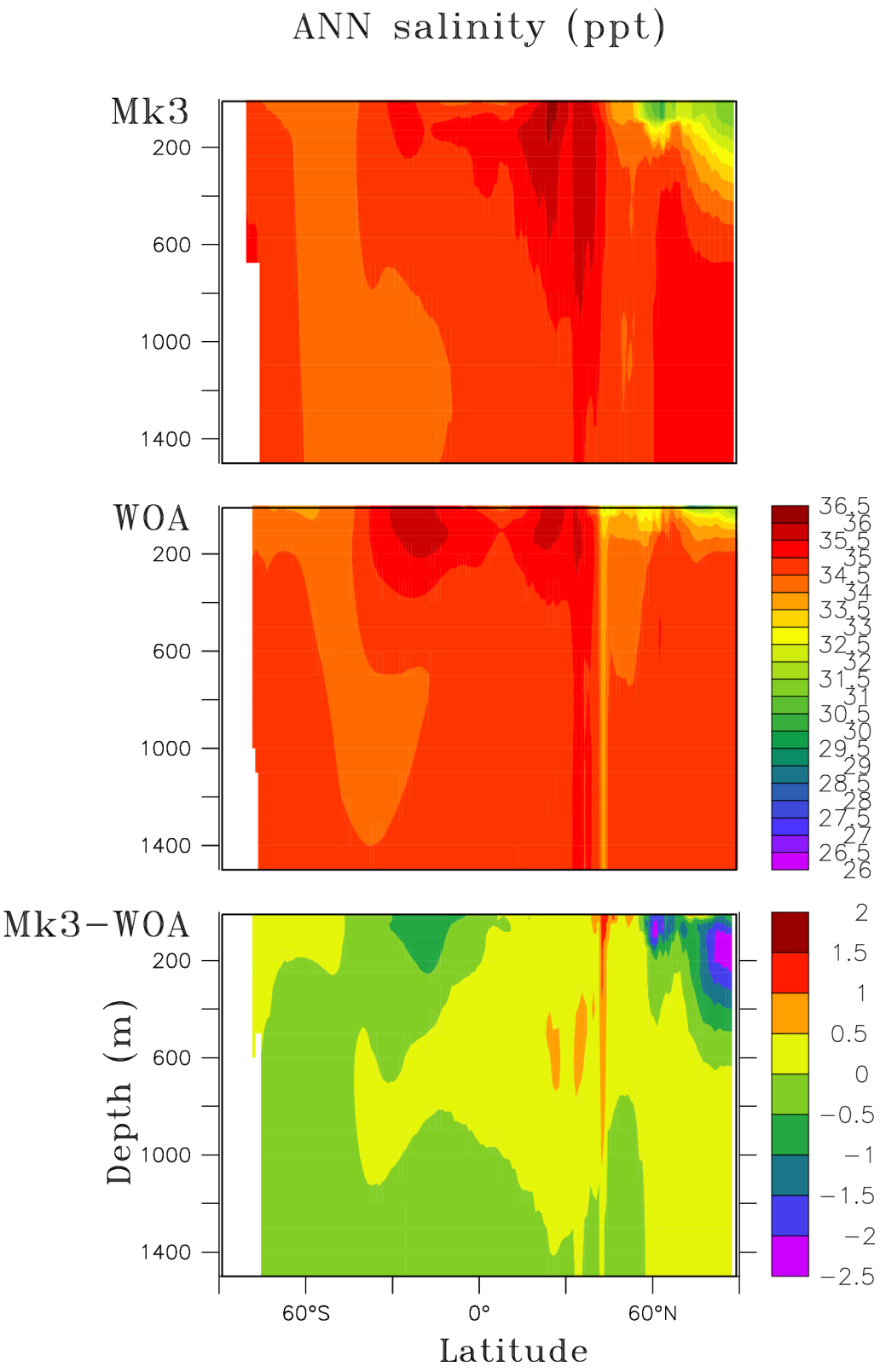

Figure 14: CSIRO-Mk3 CMIP control experiment (top), WOA observations (middle) and difference (Mk3-WOA, bottom) of ANN ocean salinity climatology (ppt).

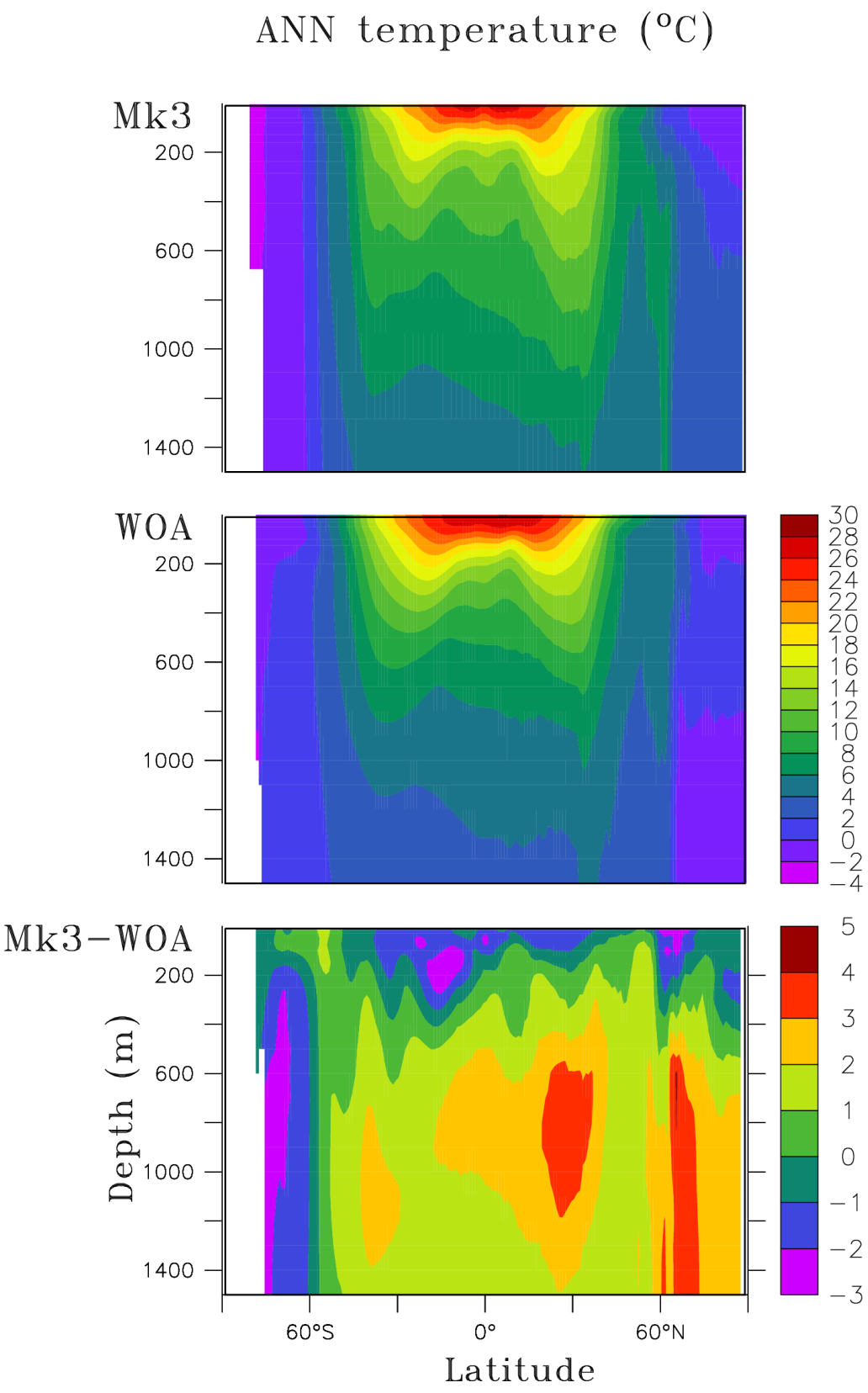

Figure 15: CSIRO-Mk3 CMIP control experiment (top), WOA observations (middle) and difference (Mk3-WOA, bottom) of ANN ocean temperature climatology (°C).

2.2.2 DJF

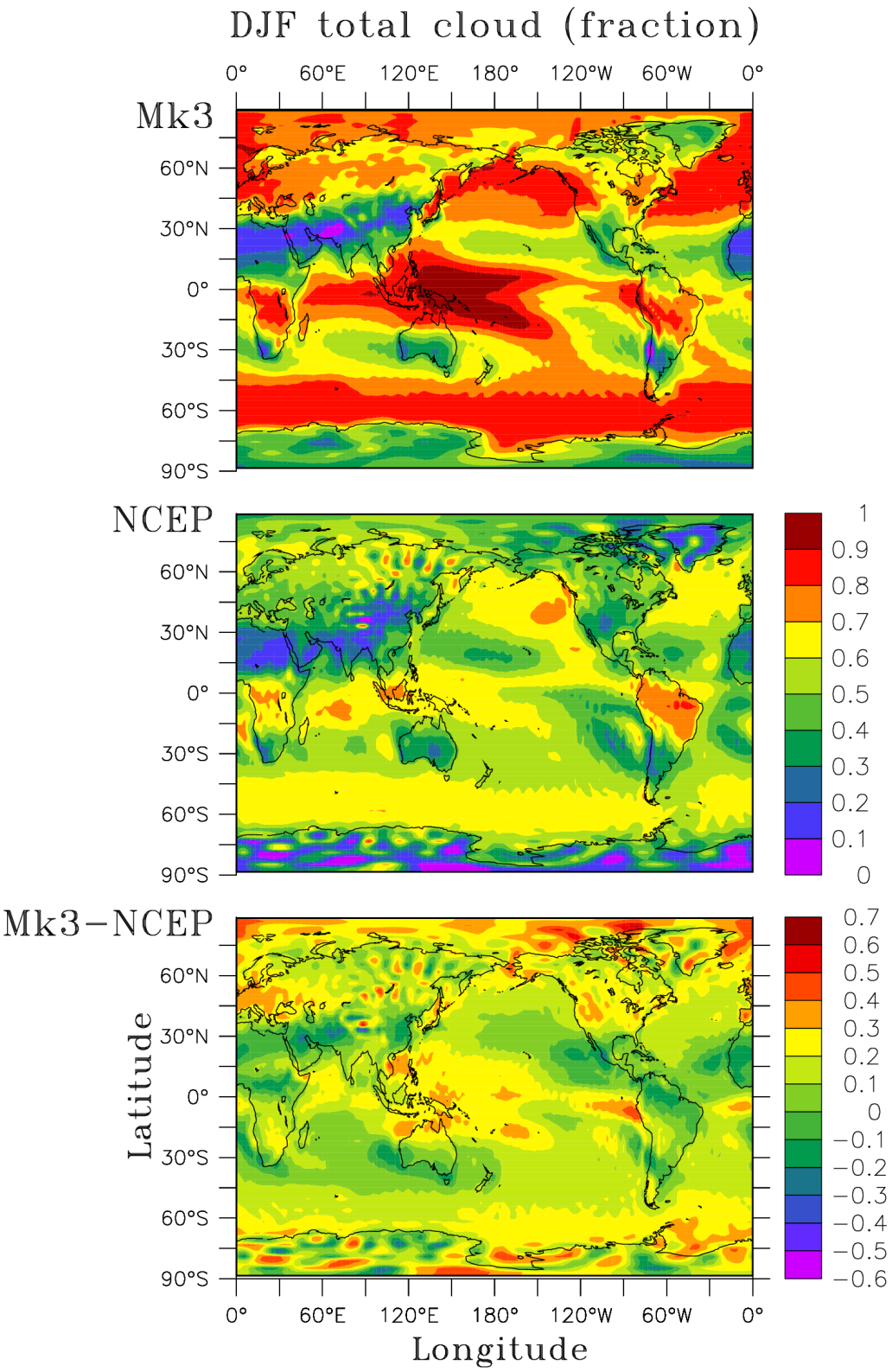

Figure 16: CSIRO-Mk3 CMIP control experiment (top), NCEP reanalysis (middle) and difference (bottom) of DJF total cloud climatology (fraction).

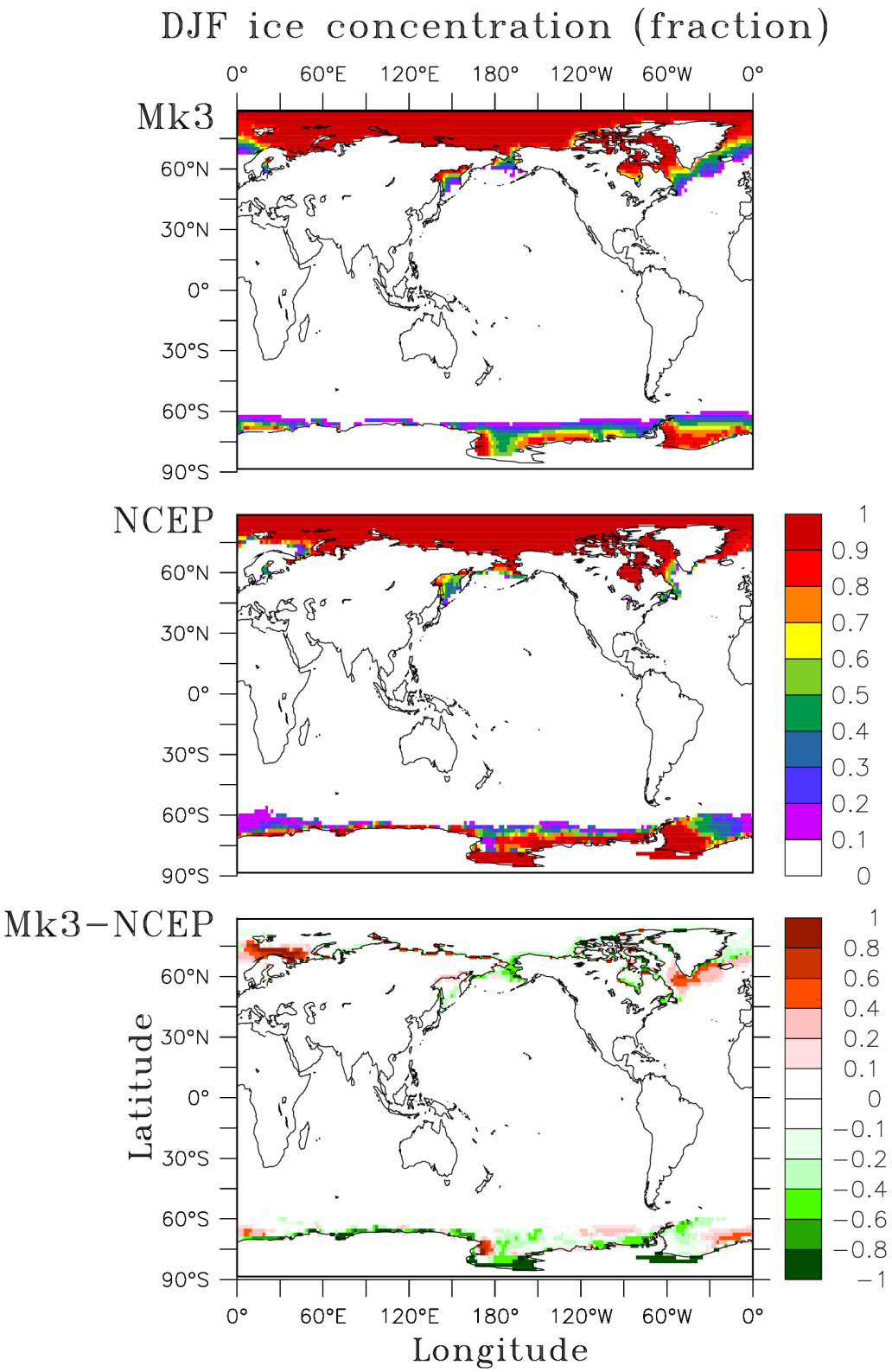

Figure 17: CSIRO-Mk3 CMIP control experiment (top), NCEP reanalysis (middle) and difference (bottom) of DJF ice concentration climatology (fraction).

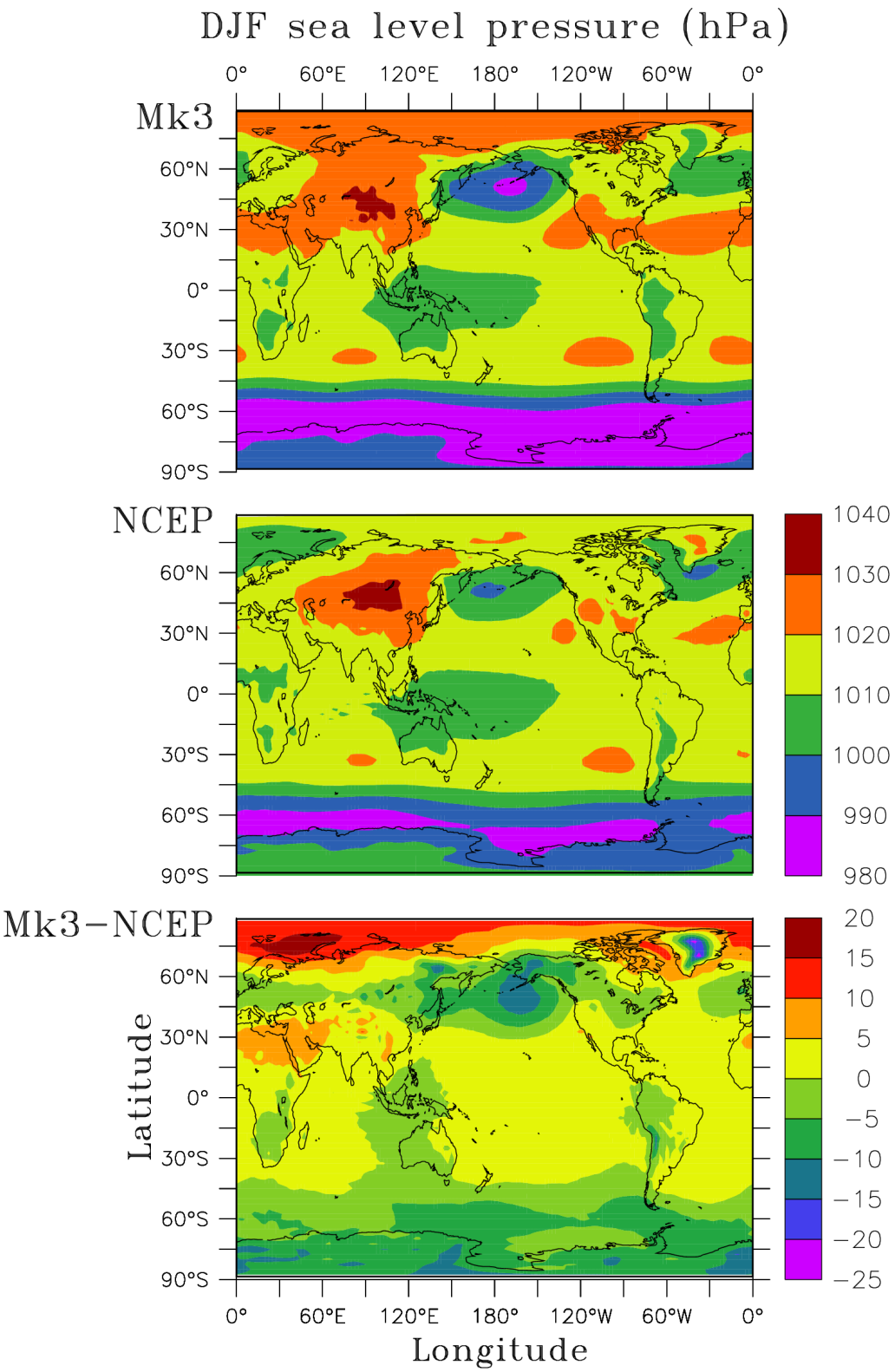

Figure 18: CSIRO-Mk3 CMIP control experiment (top), NCEP reanalysis (middle) and difference (bottom) of DJF mean sea level pressure climatology (hPa).

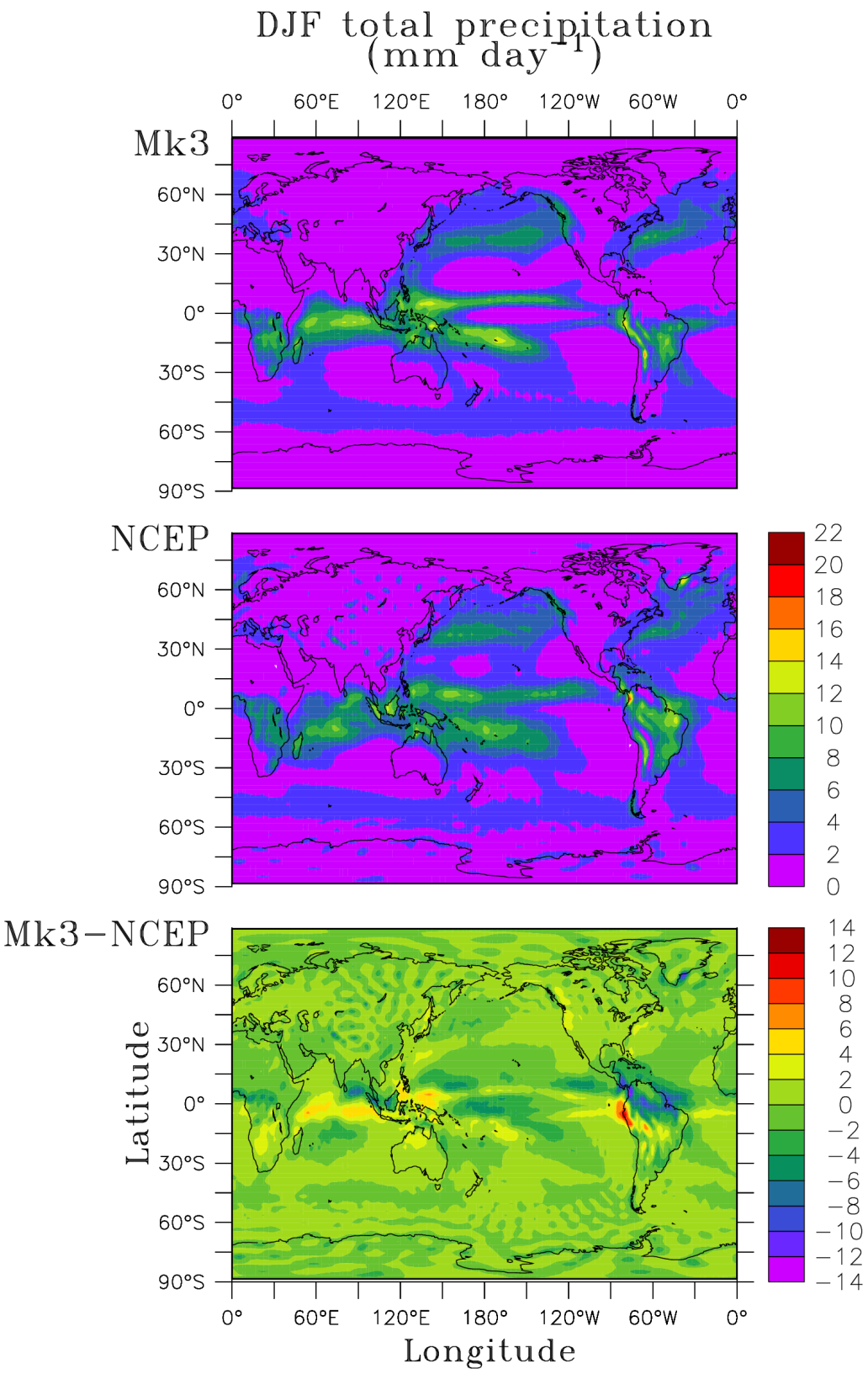

Figure 19: CSIRO-Mk3 CMIP control experiment (top), NCEP reanalysis (middle) and difference (bottom) of DJF precipitation climatology (mm day^{-1}).

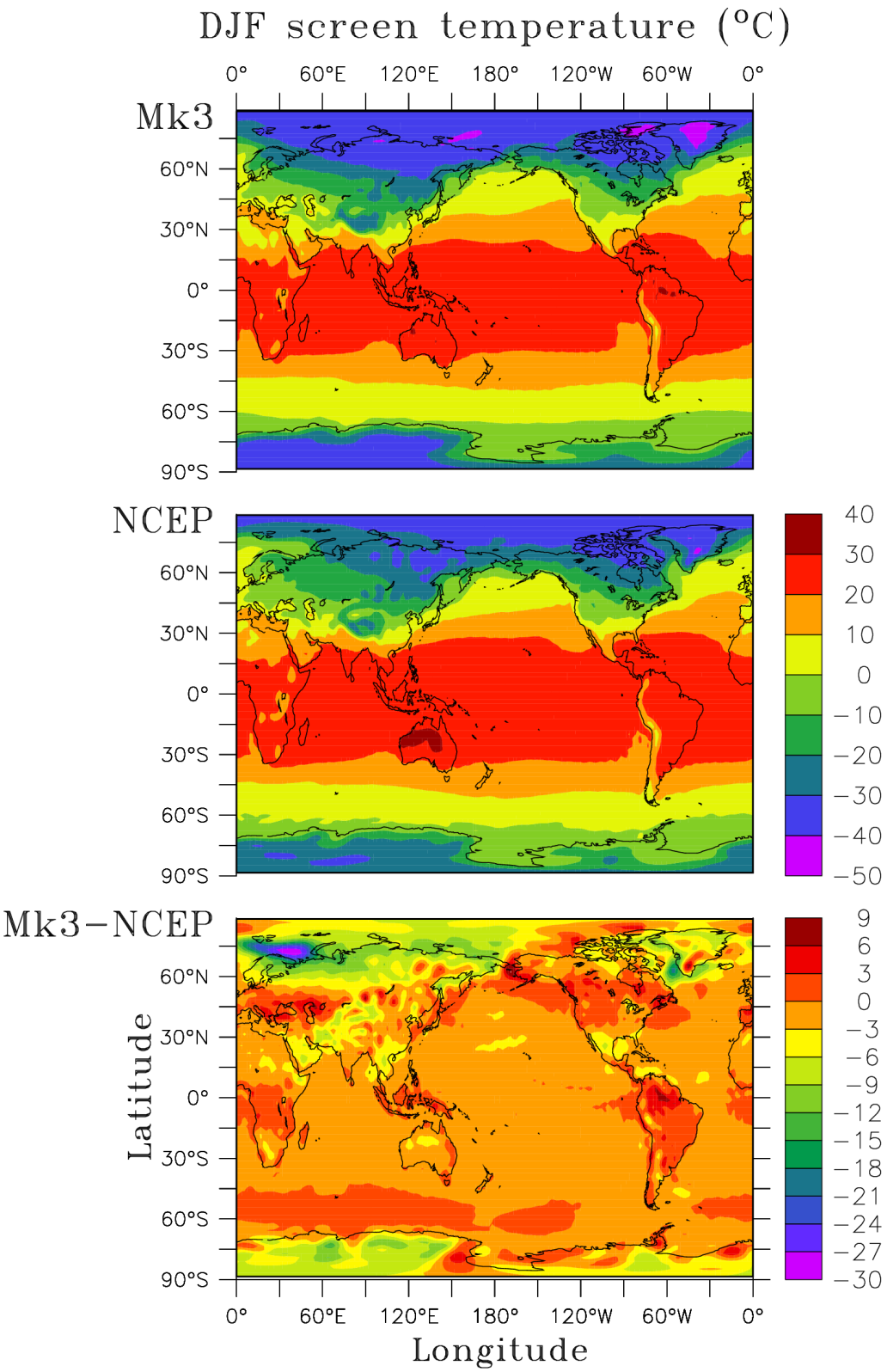

Figure 20: CSIRO-Mk3 CMIP control experiment (top), NCEP reanalysis (middle) and difference (bottom) of DJF surface screen temperature climatology (°C).

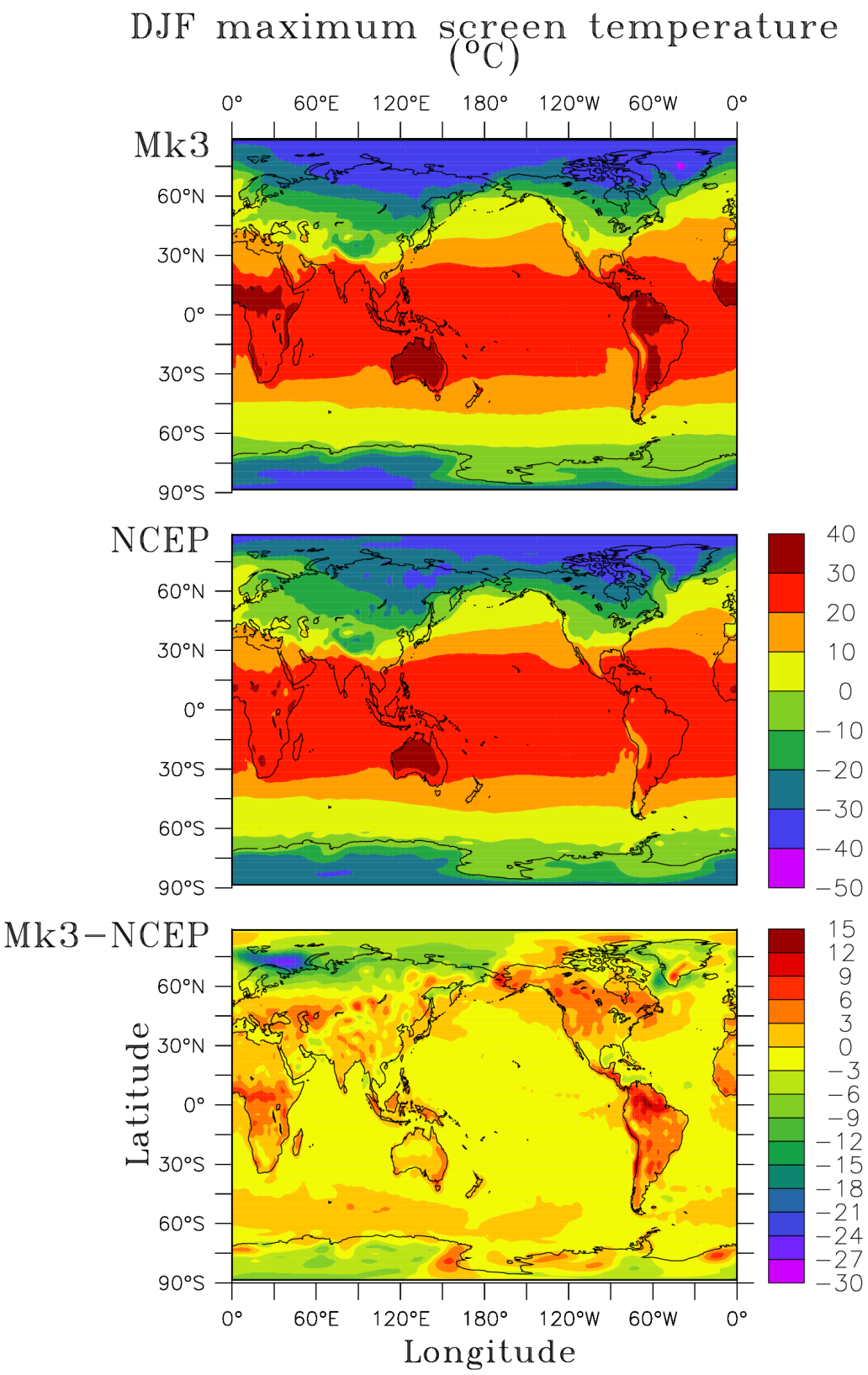

Figure 21: CSIRO-Mk3 CMIP control experiment (top), NCEP reanalysis (middle) and difference (bottom) of DJF maximum screen temperature climatology (°C).

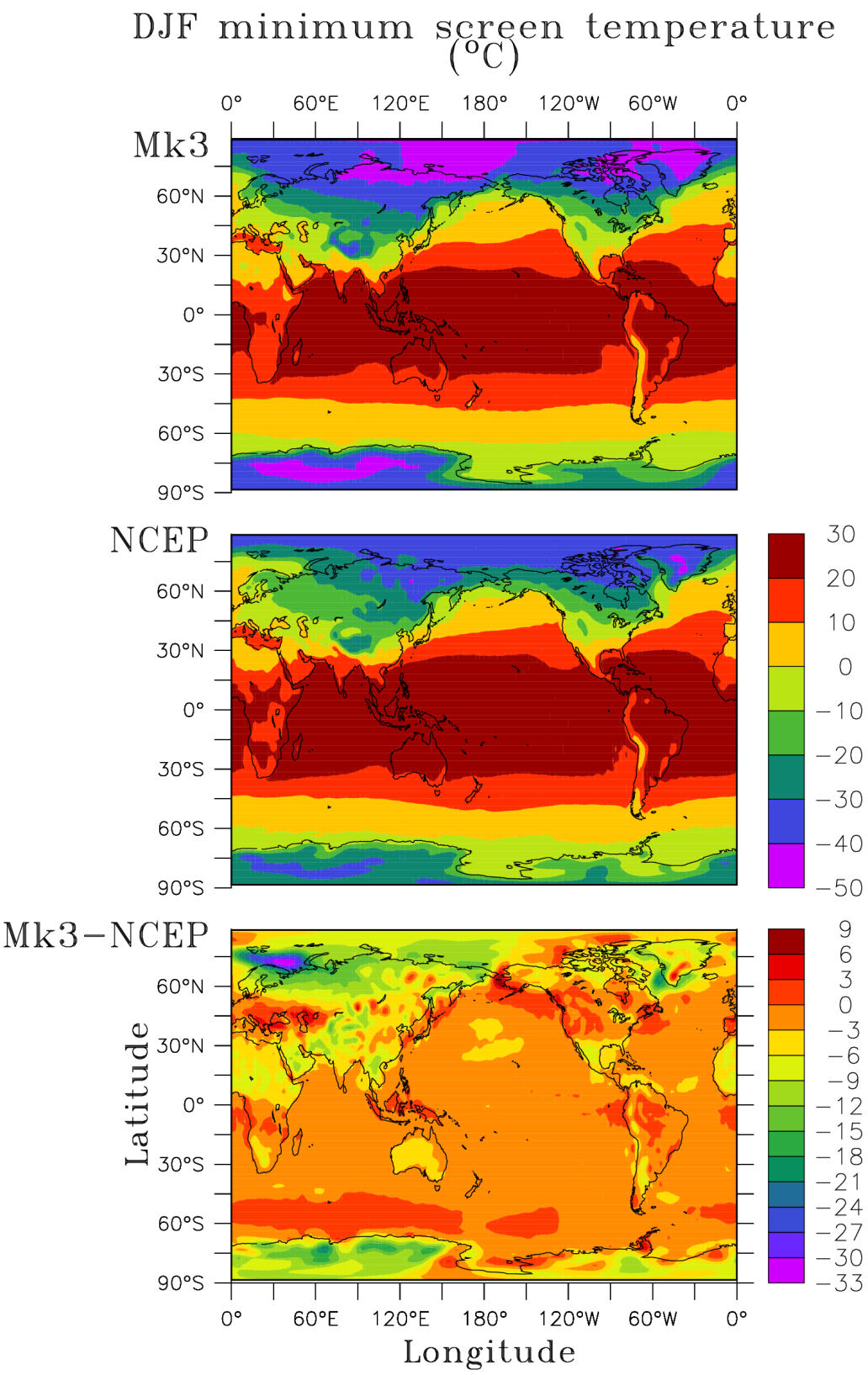

Figure 22: CSIRO-Mk3 CMIP control experiment (top), NCEP reanalysis (middle) and difference (bottom) of DJF minimum screen temperature climatology (°C).

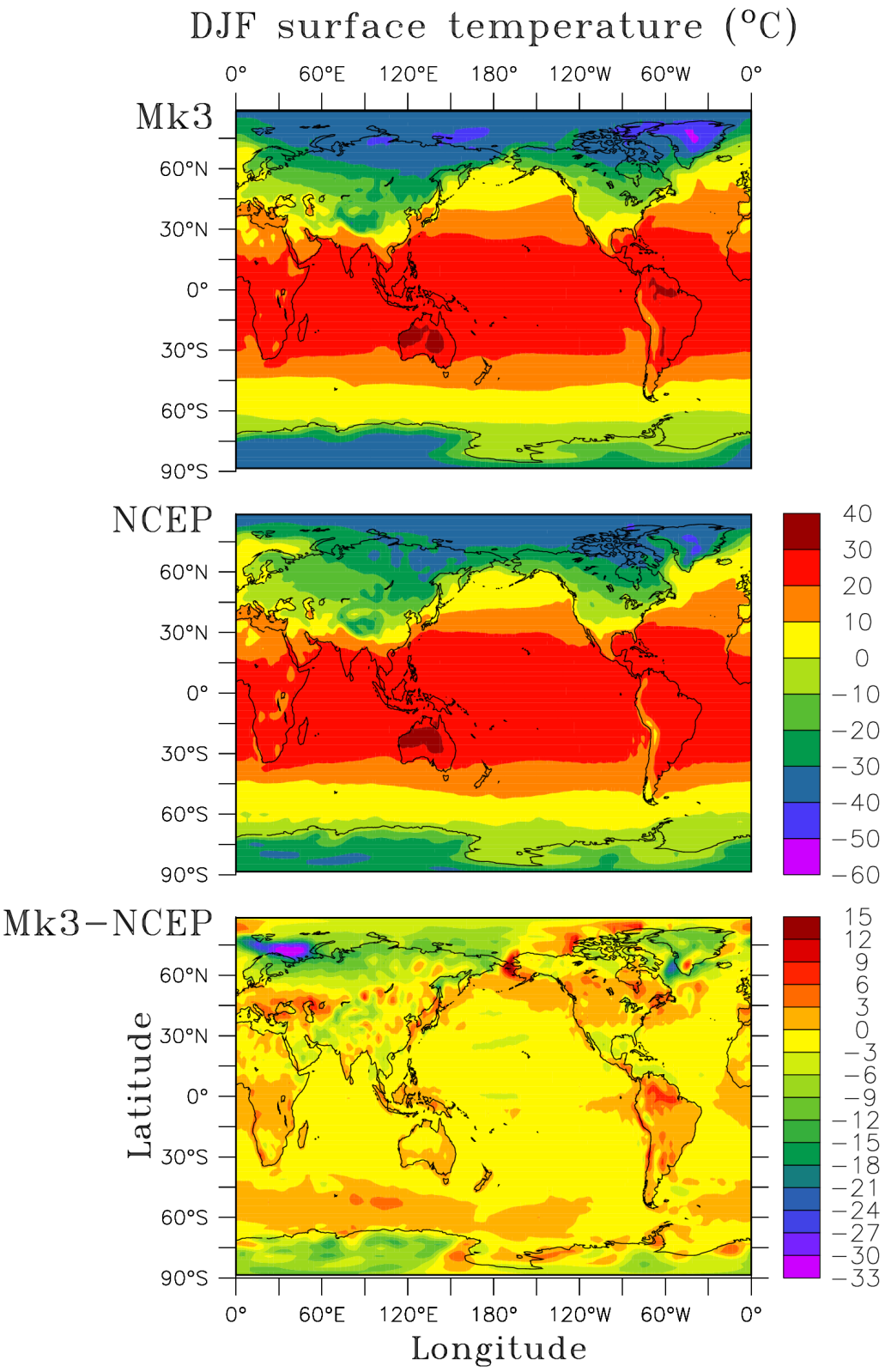

Figure 23: CSIRO-Mk3 CMIP control experiment (top), NCEP reanalysis (middle) and difference (bottom) of DJF surface temperature climatology (°C).

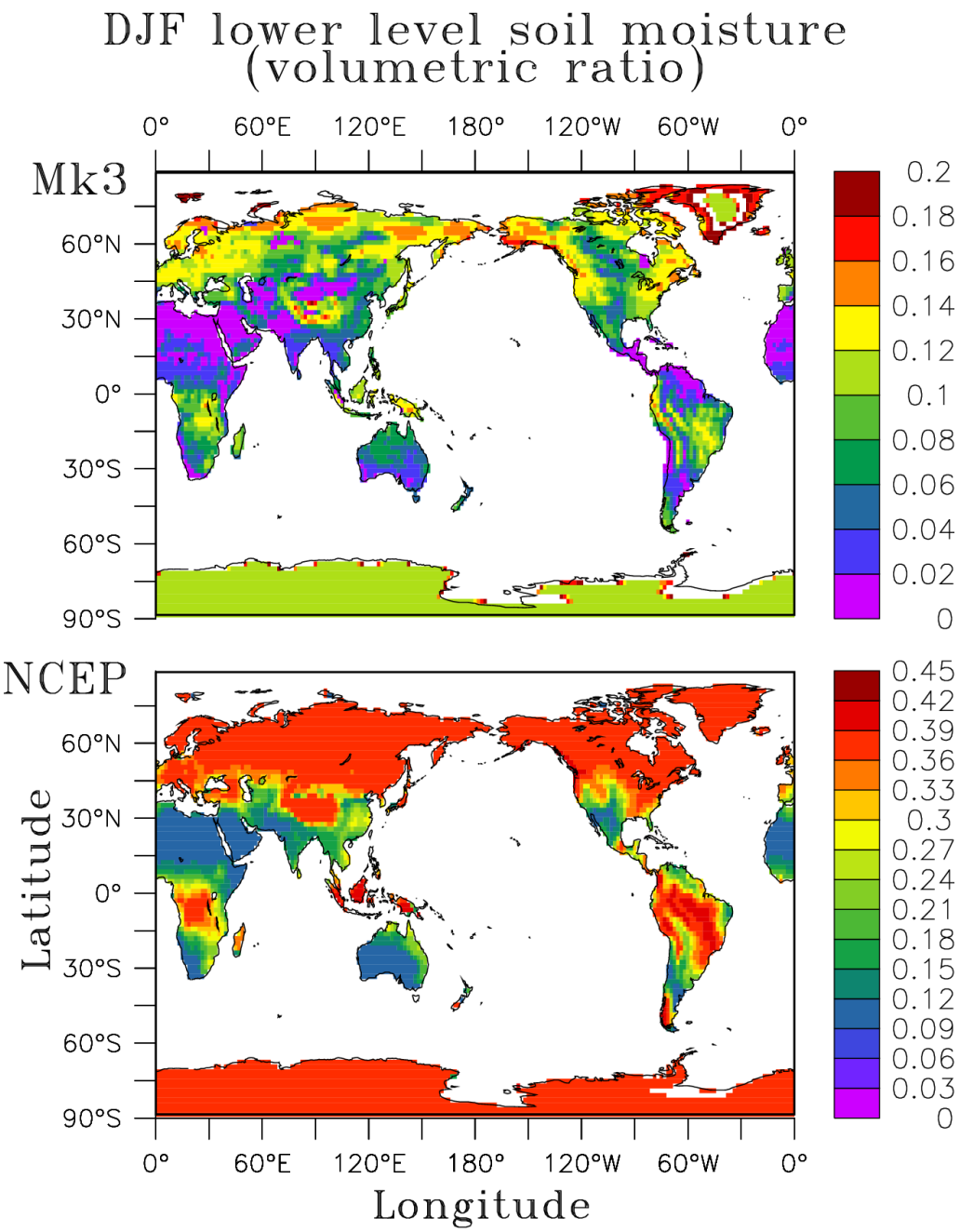

Figure 24: CSIRO-Mk3 CMIP control experiment (top) and NCEP reanalysis (bottom) of DJF lower level available soil moisture climatology (volumetric ratio). In CSIRO-Mk3 and NCEP, the soil depth range is 0-4.6 and 0.1-2.0 m, respectively.

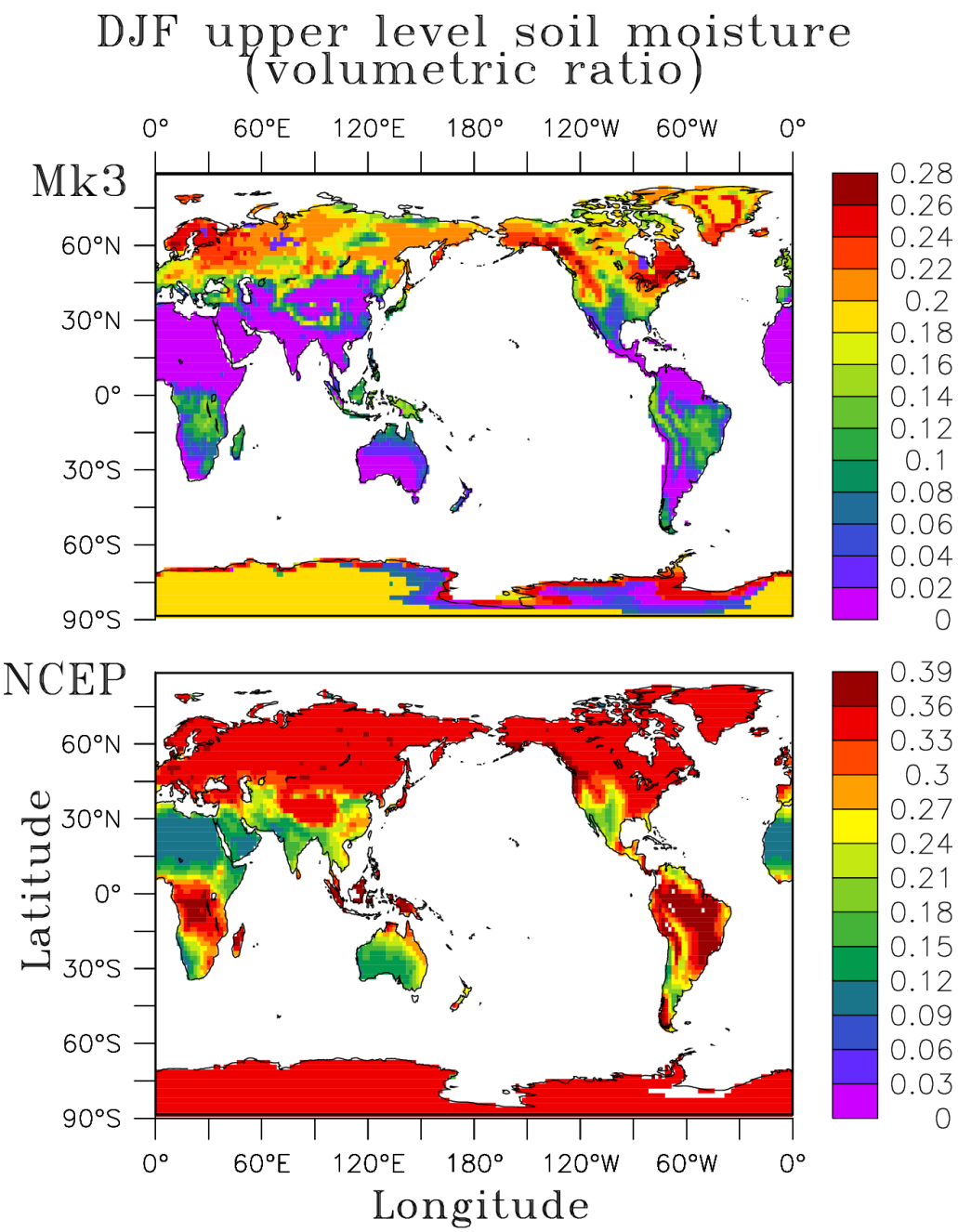

Figure 25: CSIRO-Mk3 CMIP control experiment (top) and NCEP reanalysis (bottom) of JJA upper level available soil moisture climatology (volumetric ratio). In CSIRO-Mk3 and NCEP, the soil depth range is 0-0.02 and 0-0.1 m, respectively.

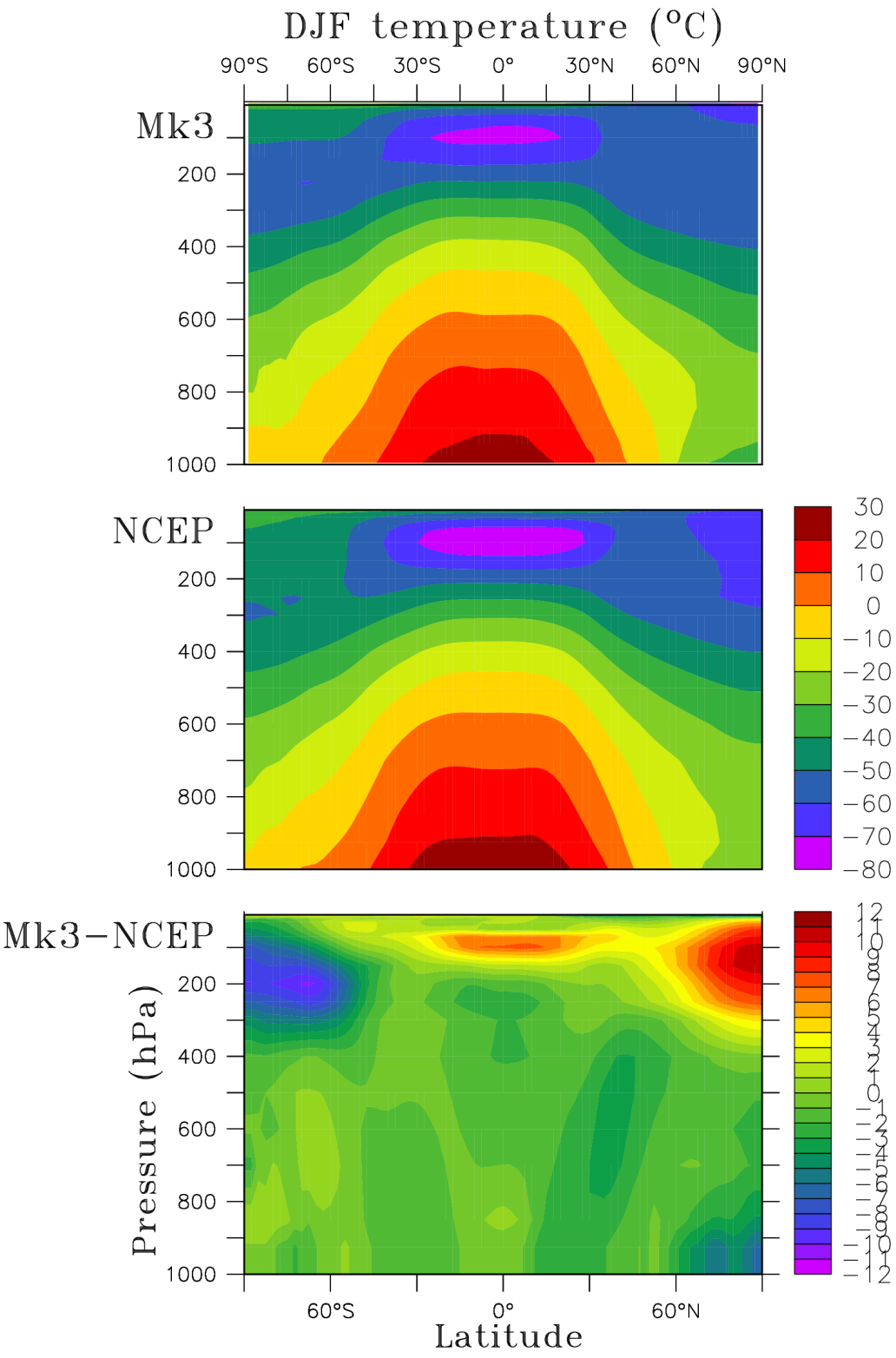

Figure 26: CSIRO-Mk3 CMIP control experiment (top), NCEP reanalysis (middle) and difference (bottom) of DJF atmosphere temperature climatology (°C).

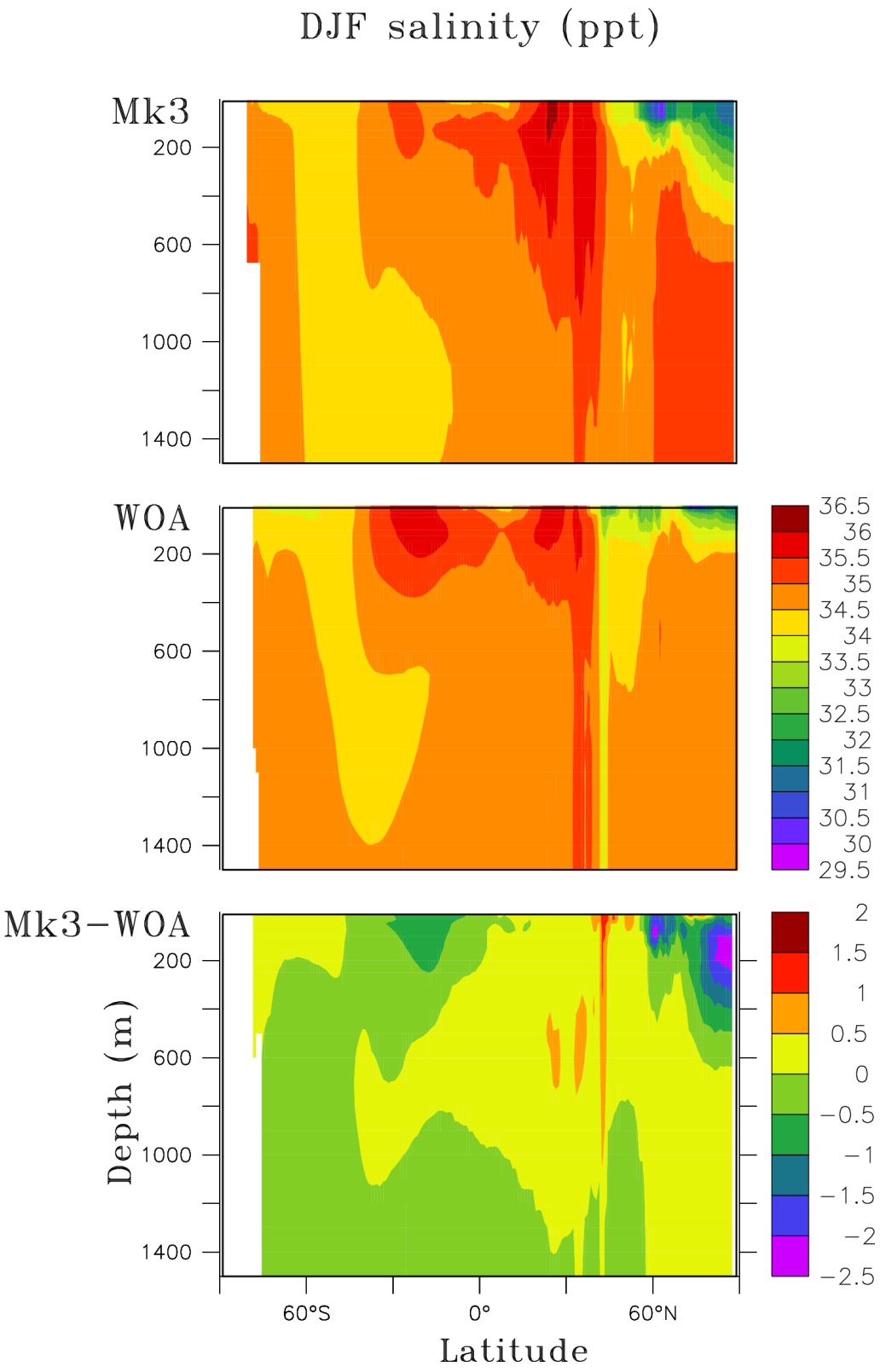

Figure 27: CSIRO-WOA CMIP control experiment (top), WOA observations (middle) and difference (bottom) of DJF ocean salinity climatology (PPS).

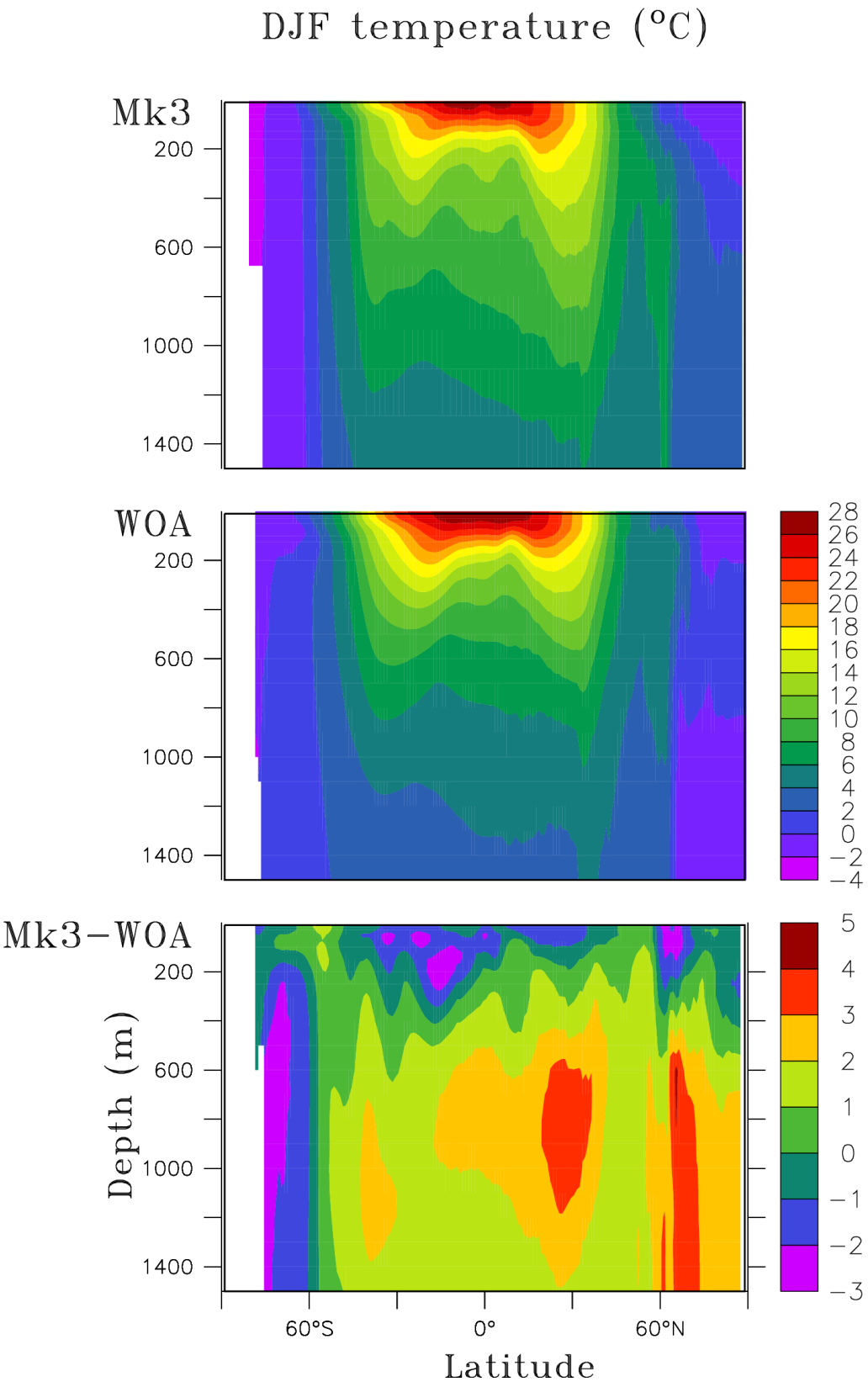

Figure 28: CSIRO-WOA CMIP control experiment (top), WOA observations (middle) and difference (bottom) of DJF ocean temperature climatology (°C).

2.2.3 JJA

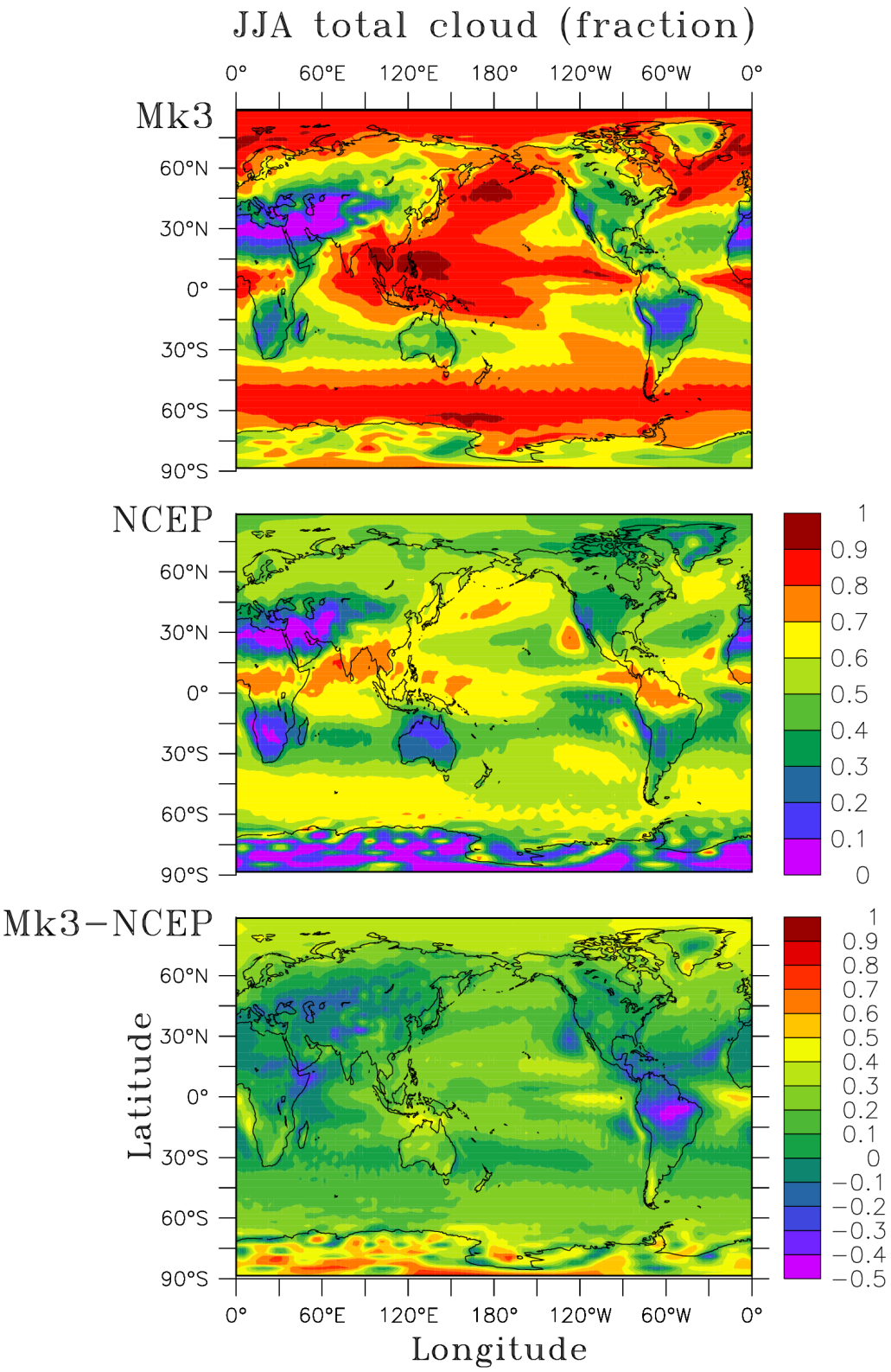

Figure 29: CSIRO-Mk3 CMIP control experiment (top), NCEP reanalysis (middle) and difference (bottom) of JJA total cloud climatology (fraction).

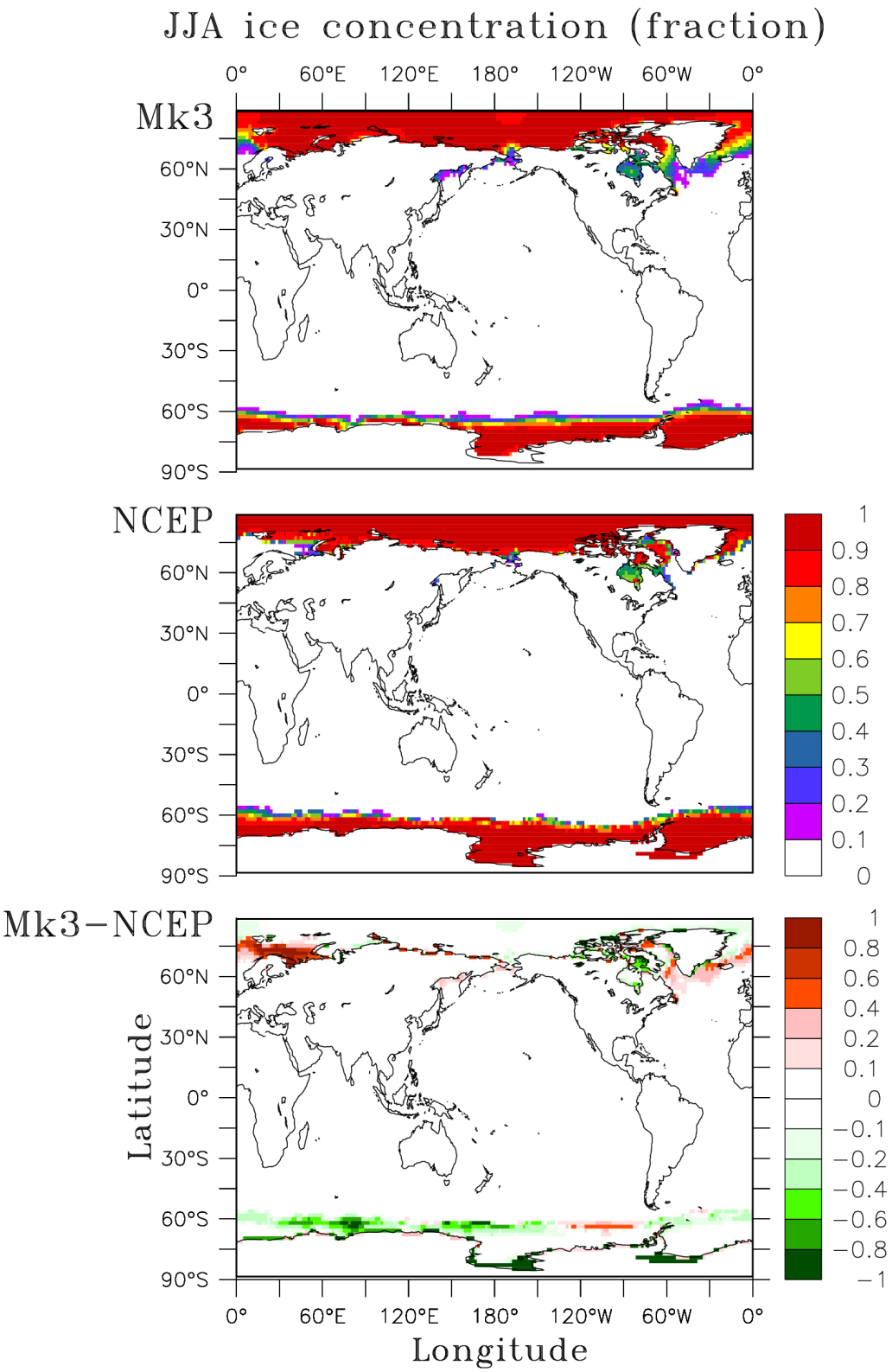

Figure 30: CSIRO-Mk3 CMIP control experiment (top), NCEP reanalysis (middle) and difference (bottom) of JJA ice concentration climatology (m).

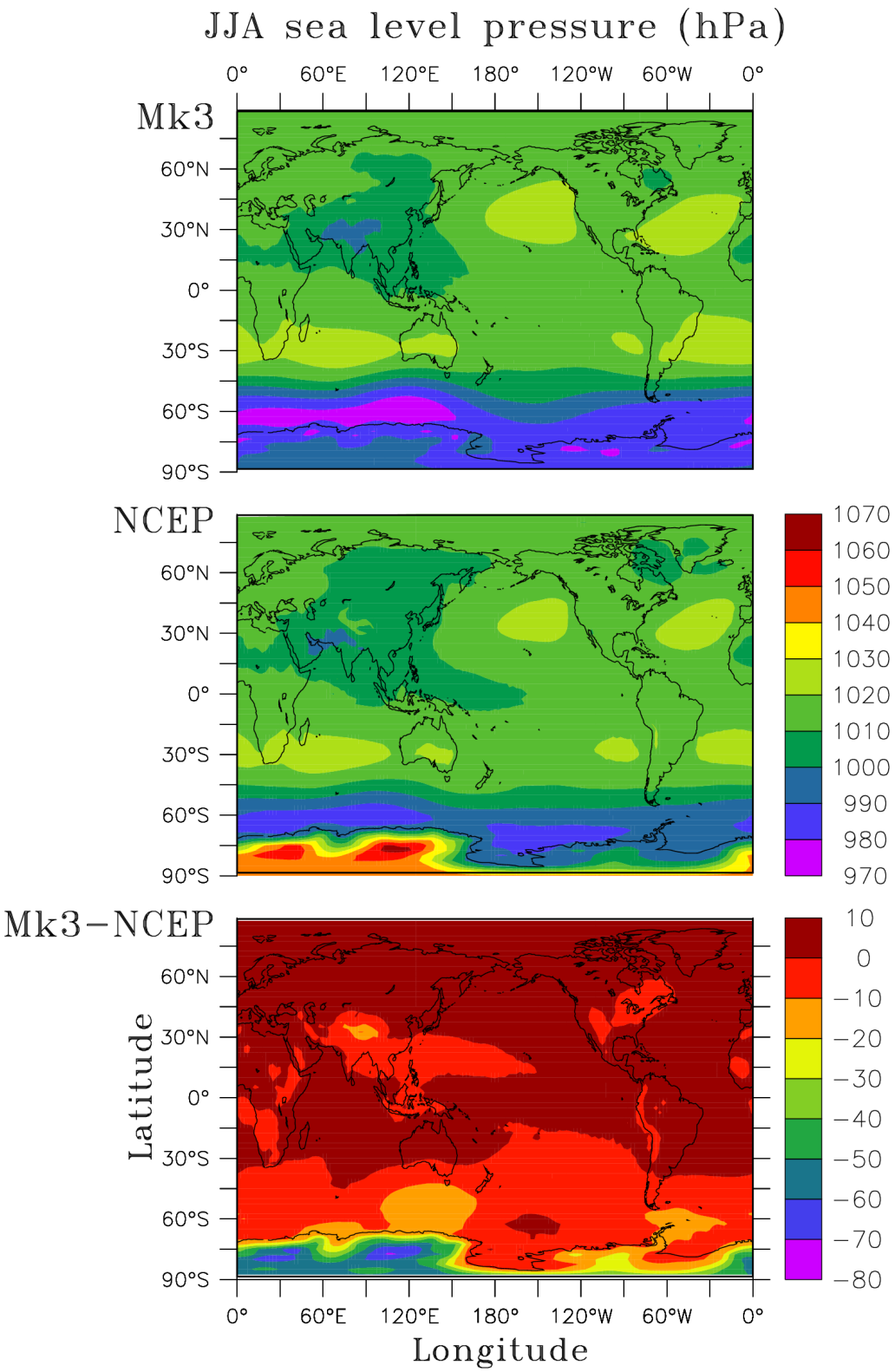

Figure 31: CSIRO-Mk3 CMIP control experiment (top), NCEP reanalysis (middle) and difference (bottom) of JJA mean sea level pressure climatology (hPa).

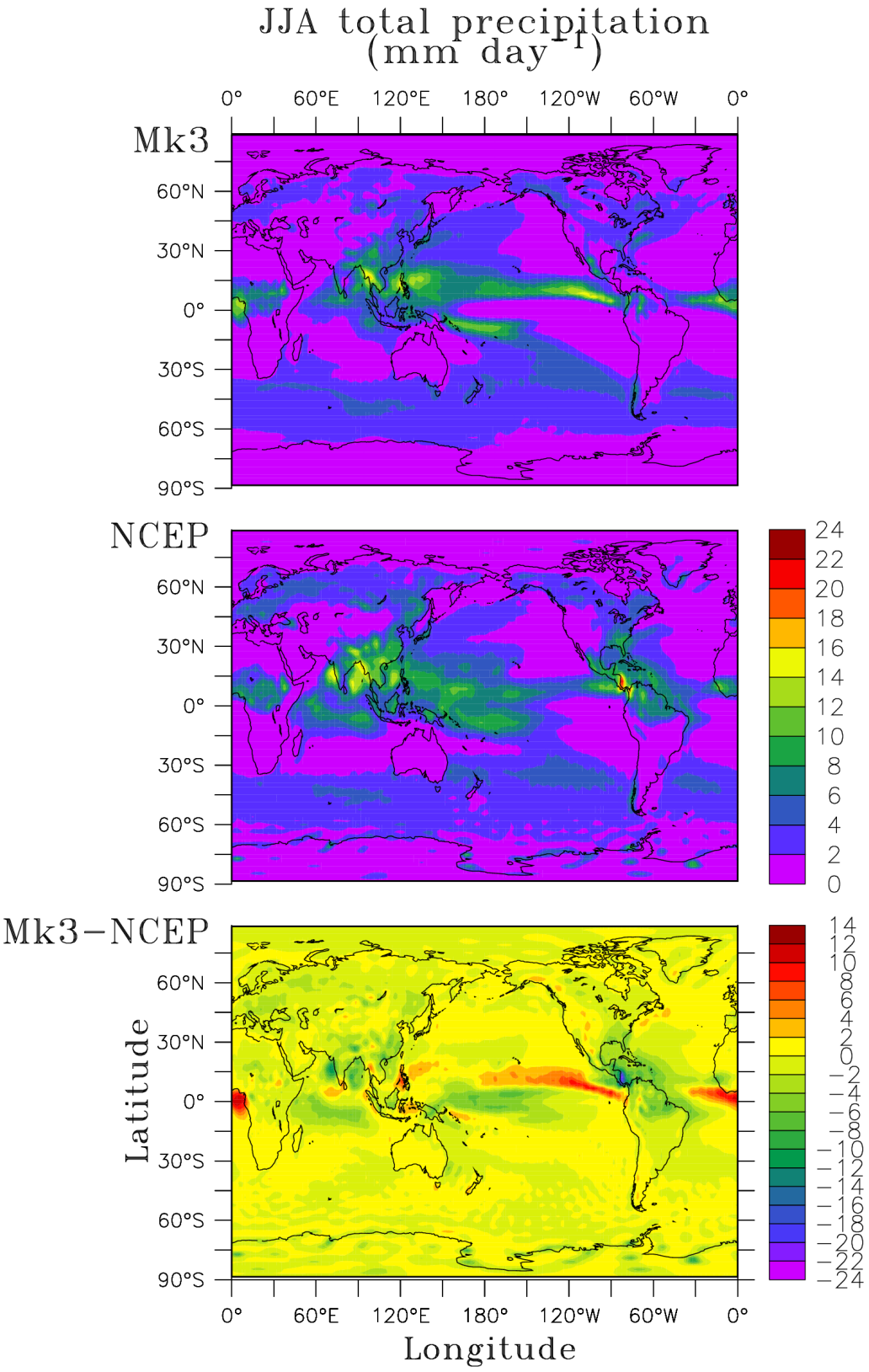

Figure 32: CSIRO-Mk3 CMIP control experiment (top), NCEP reanalysis (middle) and difference (bottom) of JJA precipitation climatology (mm day^{-1}).

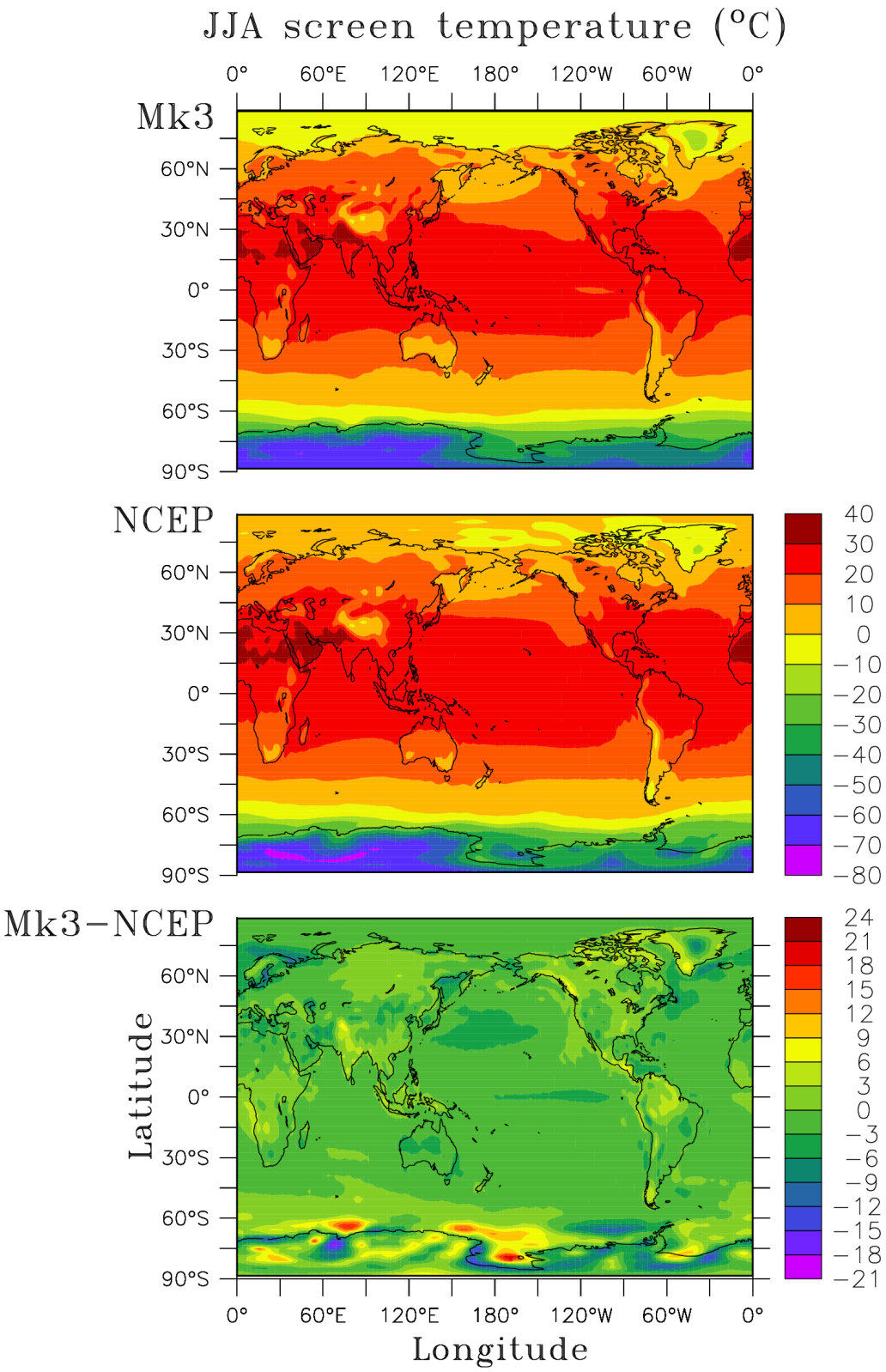

Figure 33: CSIRO-Mk3 CMIP control experiment (top), NCEP reanalysis (middle) and difference (bottom) of JJA surface screen temperature climatology (°C).

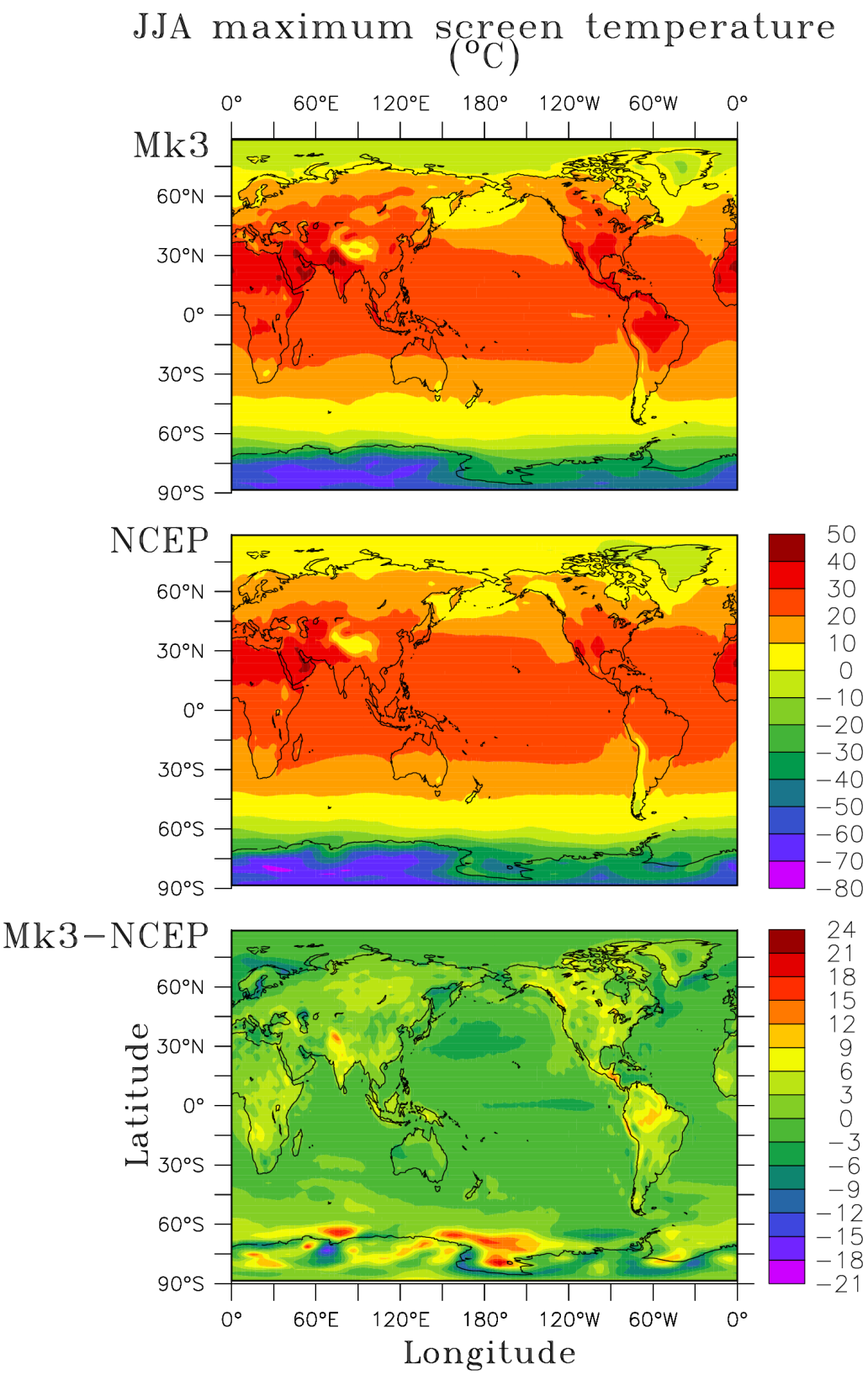

Figure 34: CSIRO-Mk3 CMIP control experiment (top), NCEP reanalysis (middle) and difference (bottom) of JJA maximum screen temperature climatology (°C).

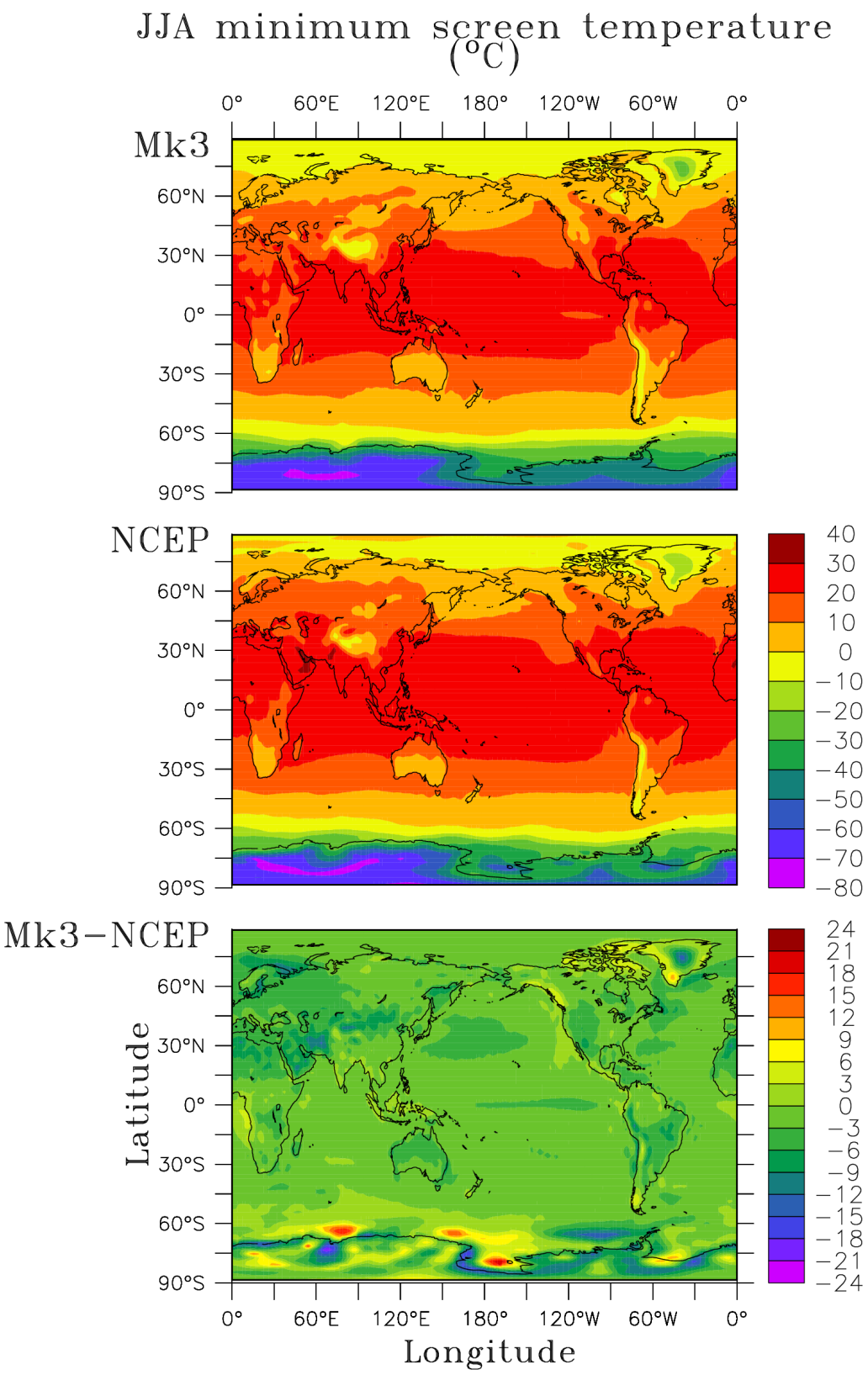

Figure 35: CSIRO-Mk3 CMIP control experiment (top), NCEP reanalysis (middle) and difference (bottom) of JJA minimum screen temperature climatology (◦C).

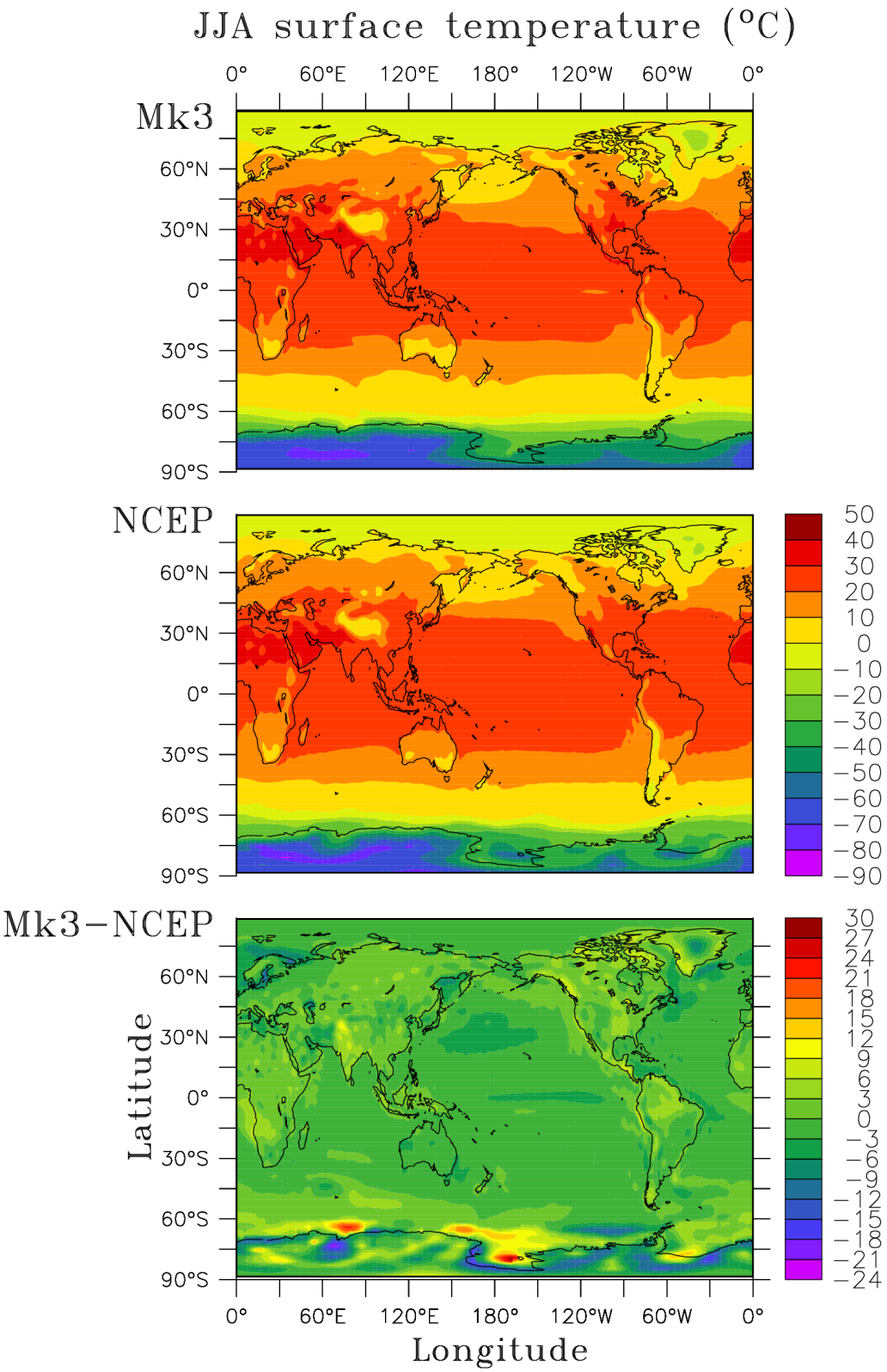

Figure 36: CSIRO-Mk3 CMIP control experiment (top), NCEP reanalysis (middle) and difference (bottom) of JJA surface temperature climatology (°C).

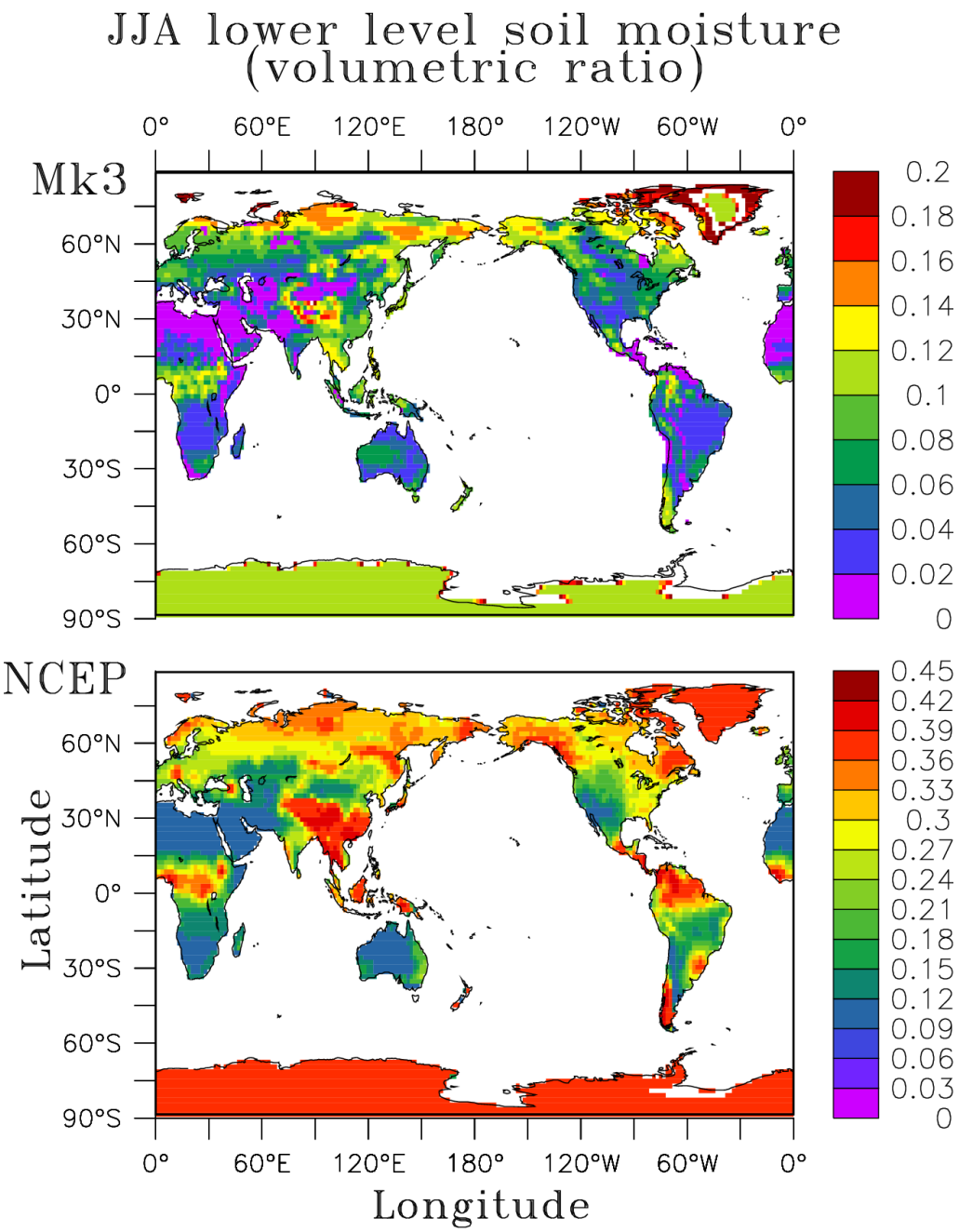

Figure 37: CSIRO-Mk3 CMIP control experiment (top) and NCEP reanalysis (bottom) of JJA lower level available soil moisture climatology (volumetric ratio). In CSIRO-Mk3 and NCEP, the soil depth range is 0-4.6 and 0.1-2.0 m, respectively.

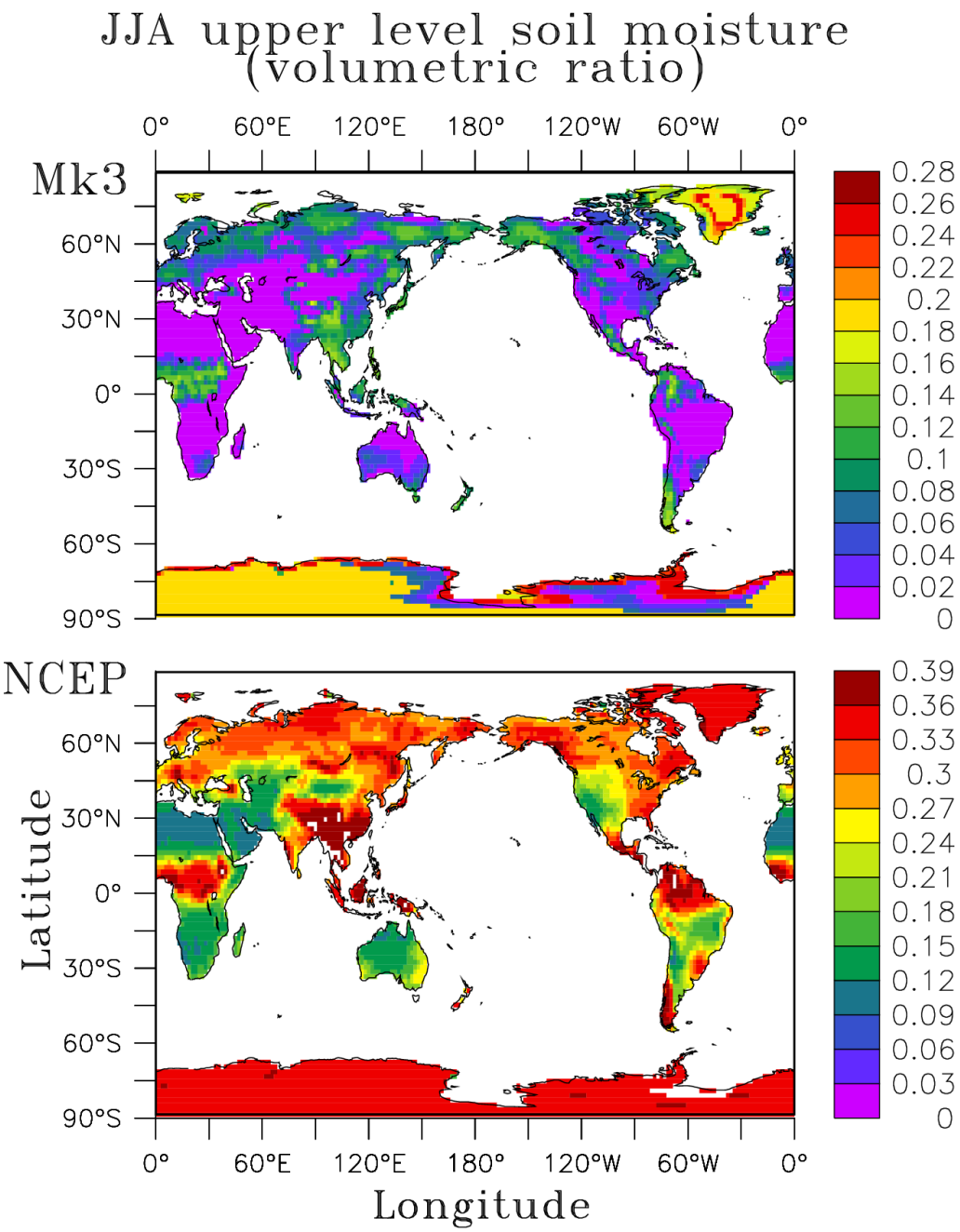

Figure 38: CSIRO-Mk3 CMIP control experiment (top) and NCEP reanalysis (bottom) of JJA upper level available soil moisture climatology (volumetric ratio). In CSIRO-Mk3 and NCEP, the soil depth range is 0-0.02 and 0-0.1 m, respectively.

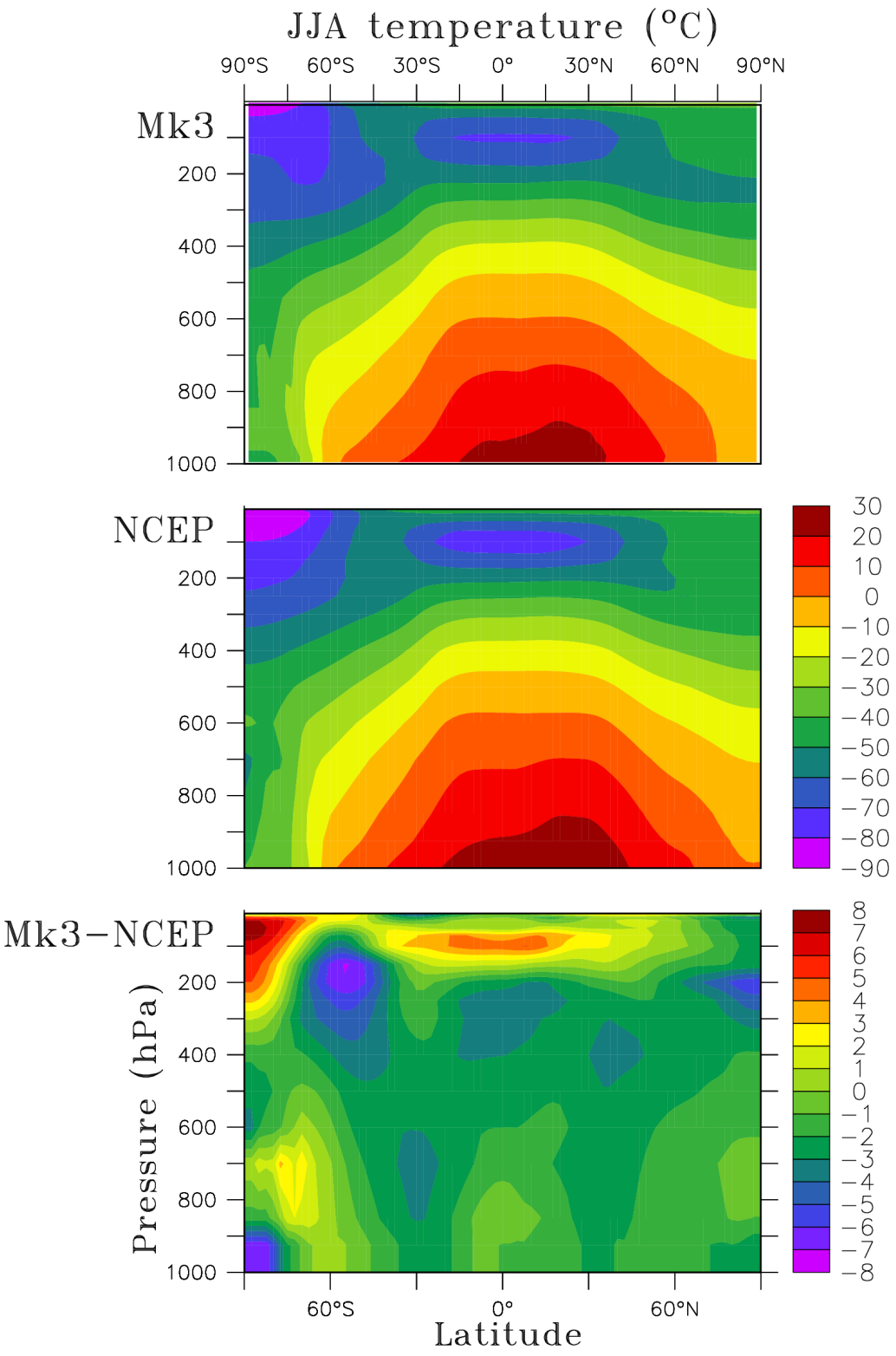

Figure 39: CSIRO-Mk3 CMIP control experiment (top), WOA observations (middle) and difference (bottom) of JJA atmosphere temperature climatology (°C).

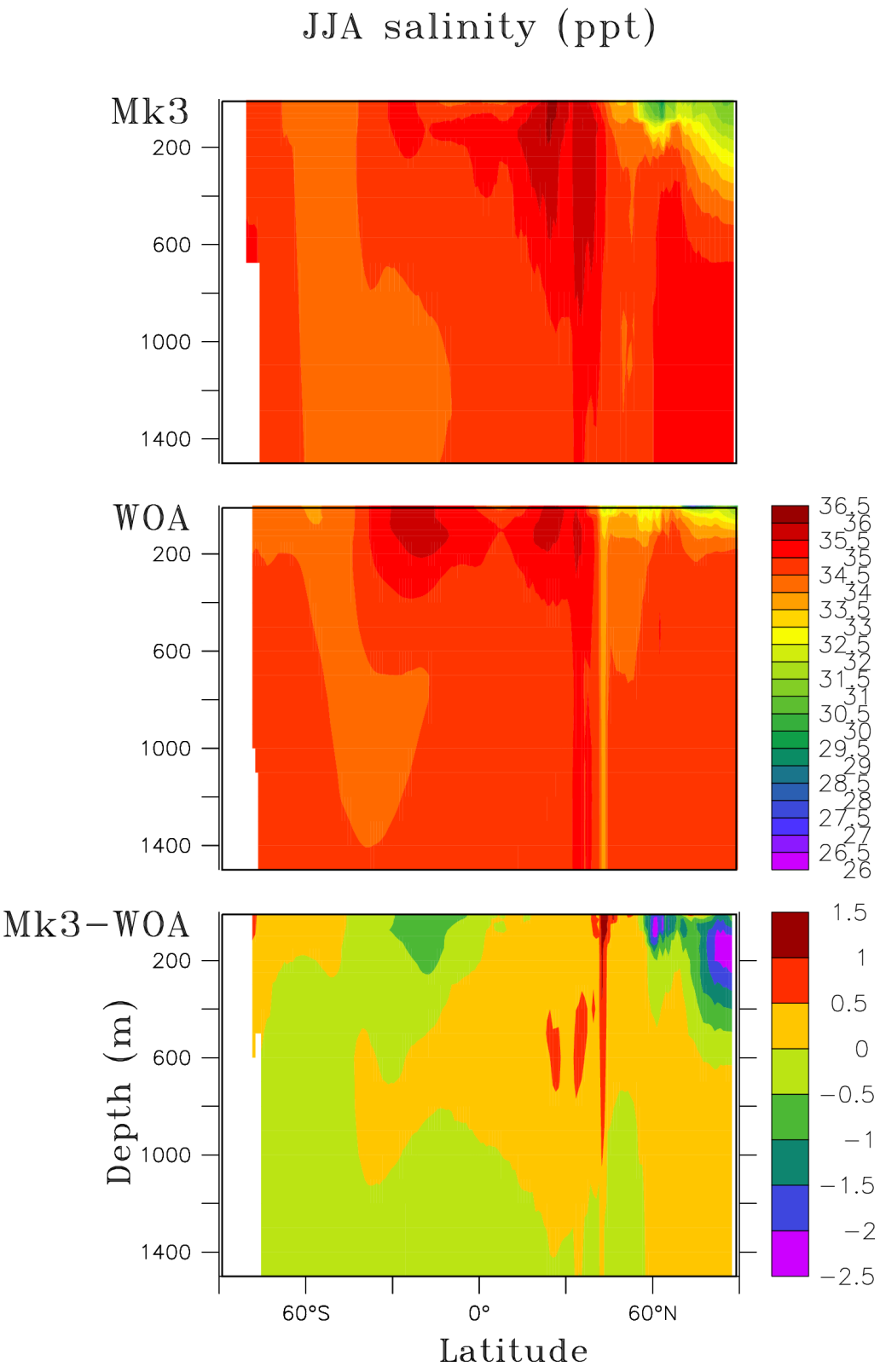

Figure 40: CSIRO-WOA CMIP control experiment (top), WOA observations (middle) and difference (bottom) of JJA ocean salinity climatology (PPS).

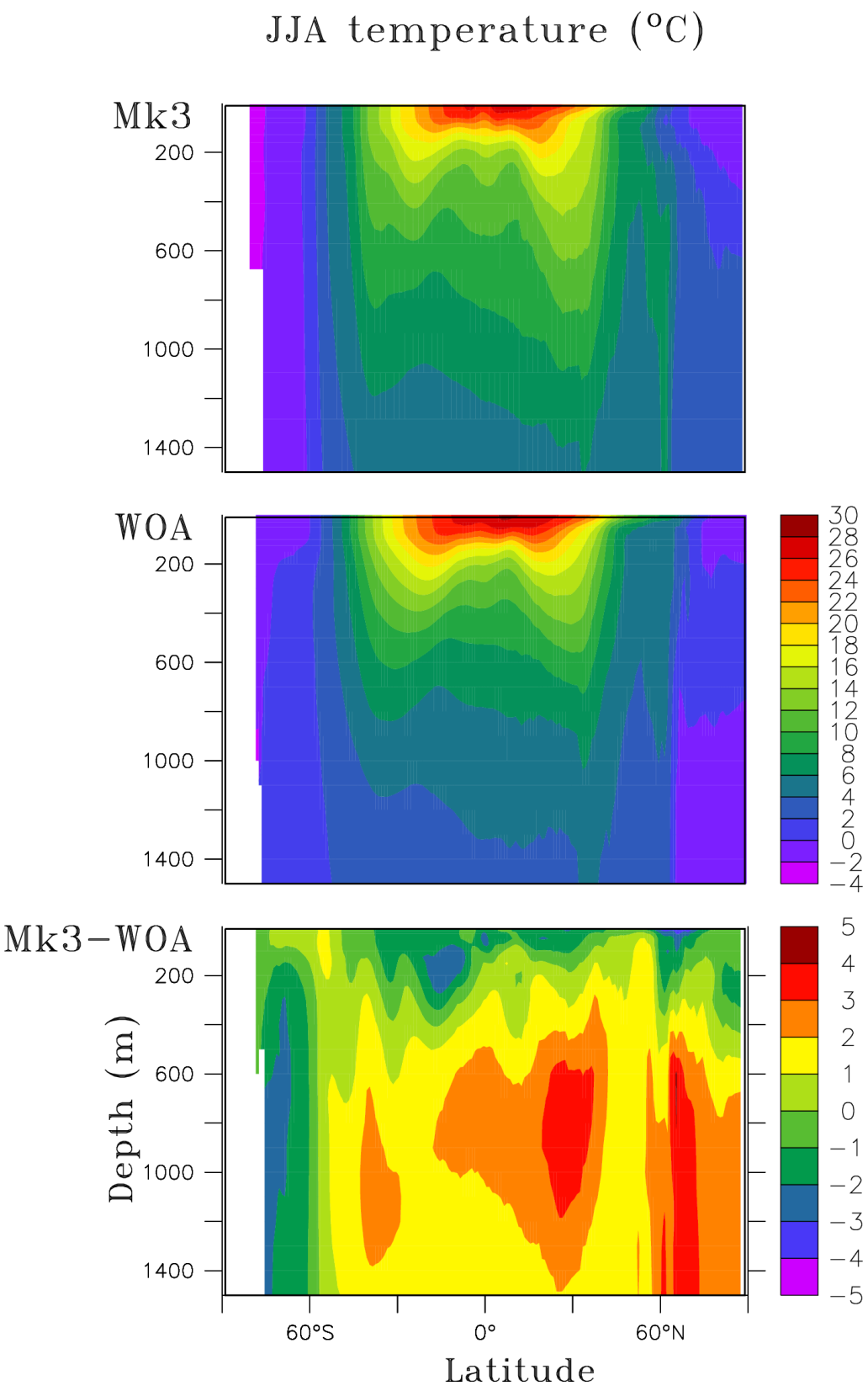

Figure 41: CSIRO-WOA CMIP control experiment (top), NCEP reanalysis (middle) and difference (bottom) of JJA ocean temperature climatology (°C).

3 CSIRO Mk3 CSM CMIP transient results

3.1 CSIRO Mk3 CSM Temporal response

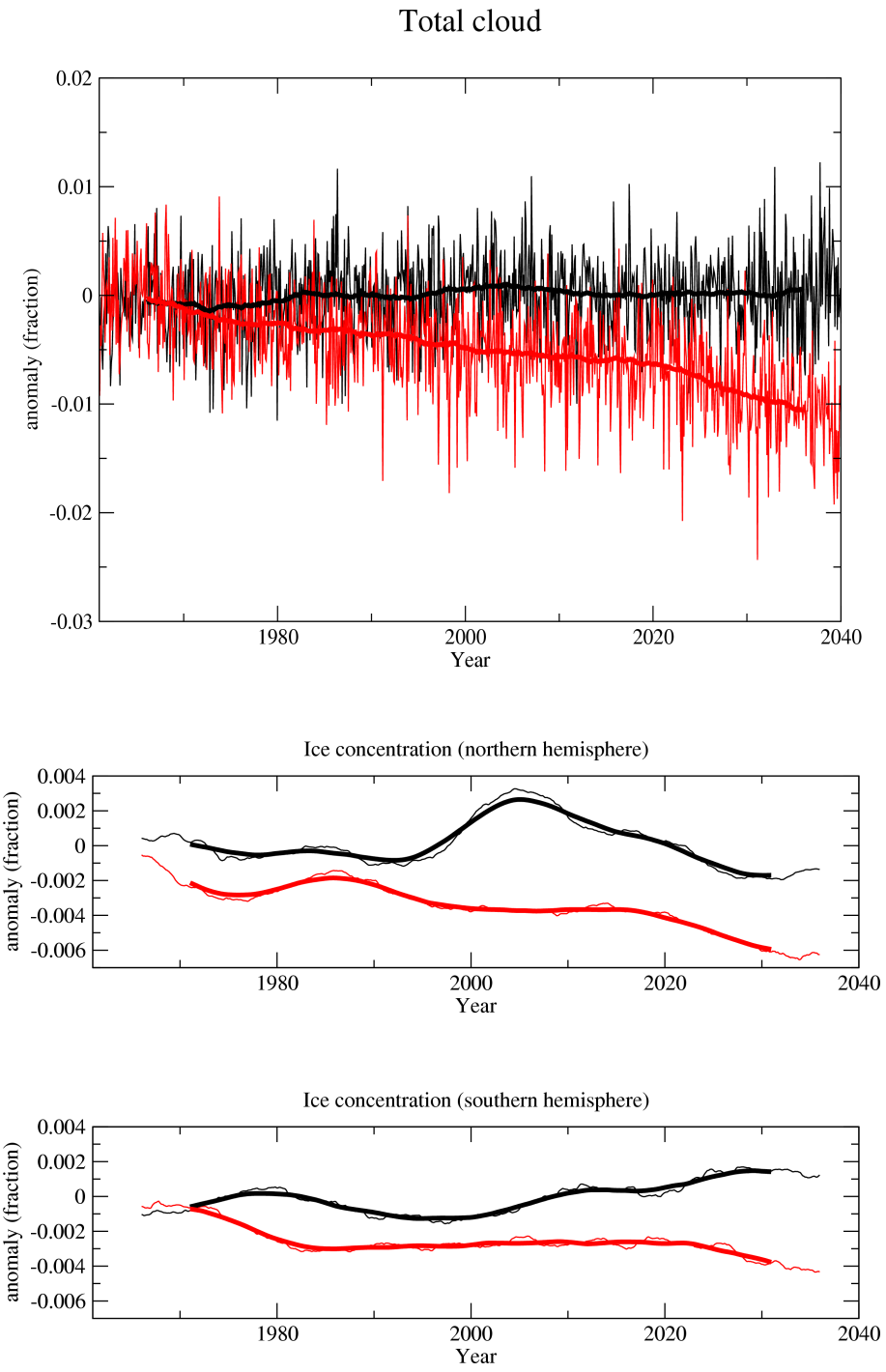

Figure 42: Area weighted monthly anomaly of global total cloud (fraction, upper panel), northern (fraction, middle panel) and southern (lower panel) hemisphere ice concentration for control (black curve) and transient (red curve) experiments. For each monthly time-series a 121-month running average has been overlaid.

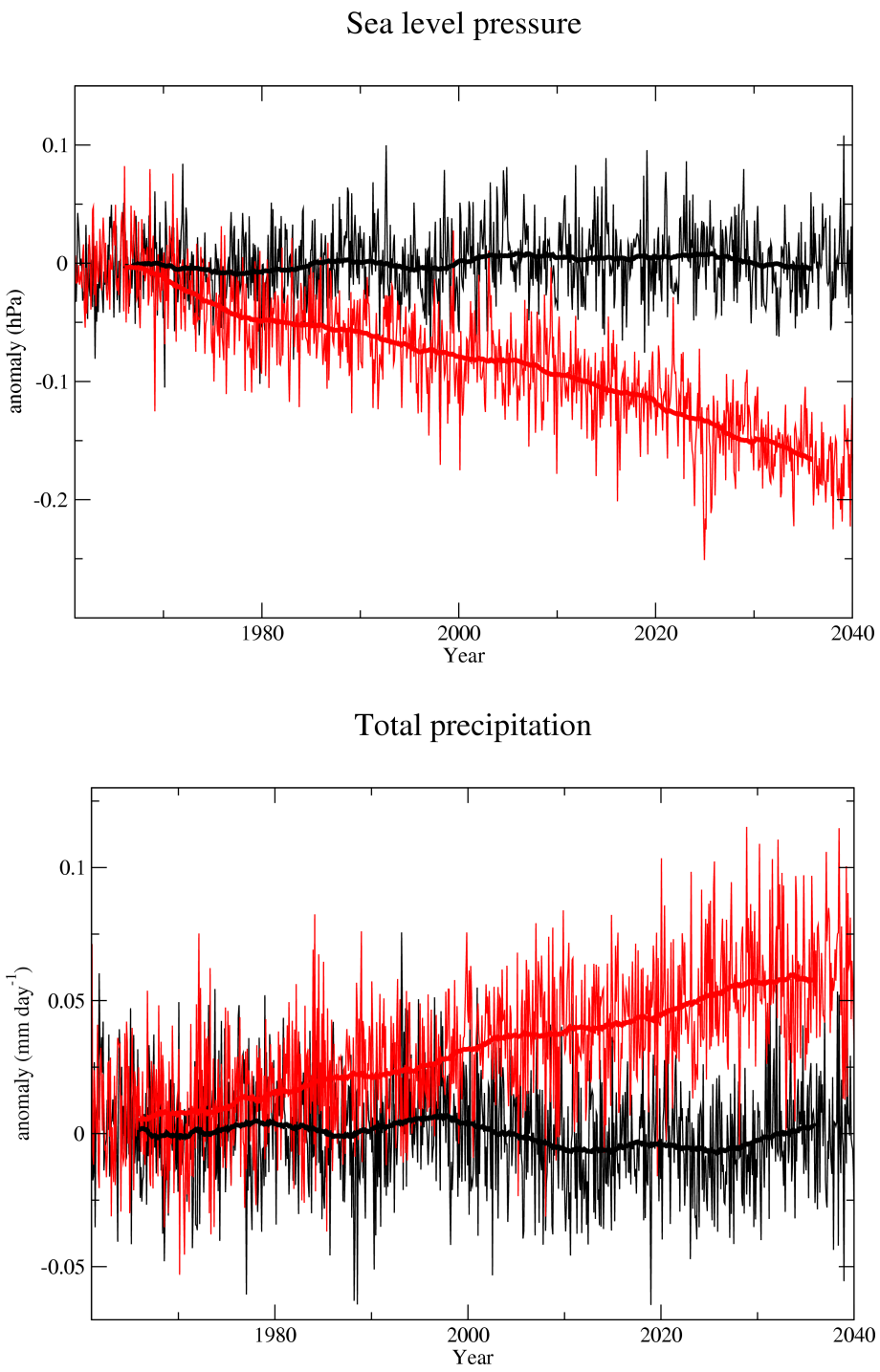

Figure 43: Global area weighted monthly anomaly of mean sea level pressure (hPa, upper panel) and precipitation (mm day^{-1}, lower panel) for control (black curve) and transient (red curve) experiments. For each monthly time-series a 121-month running average has been overlaid.

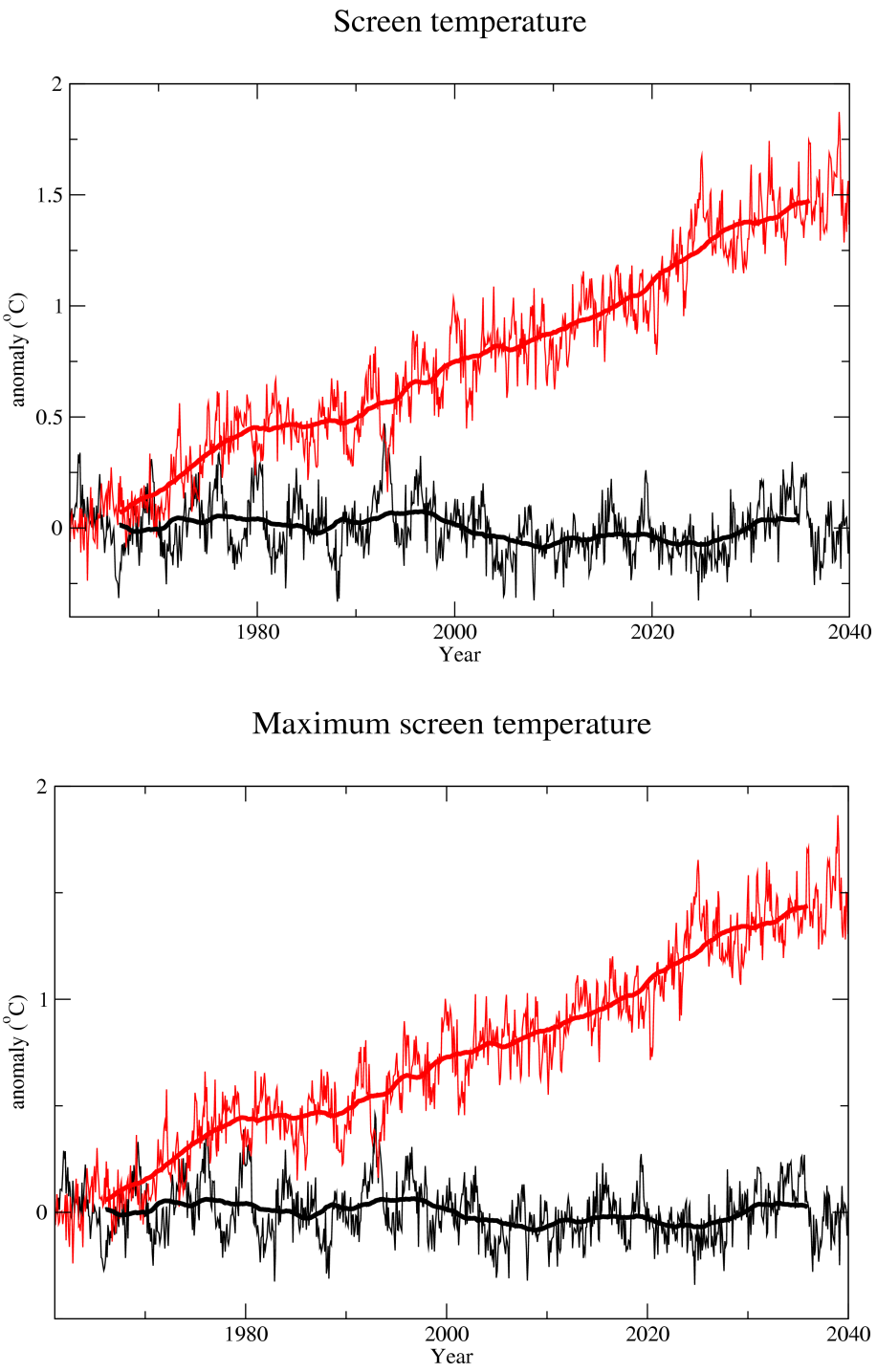

Figure 44: Global area weighted monthly anomaly of surface screen temperature anomaly (°C, upper panel) and maximum screen temperature ($°C$, lower panel) for control (black curve) and transient (red curve) experiments. For each monthly time-series a 121-month running average has been overlaid.

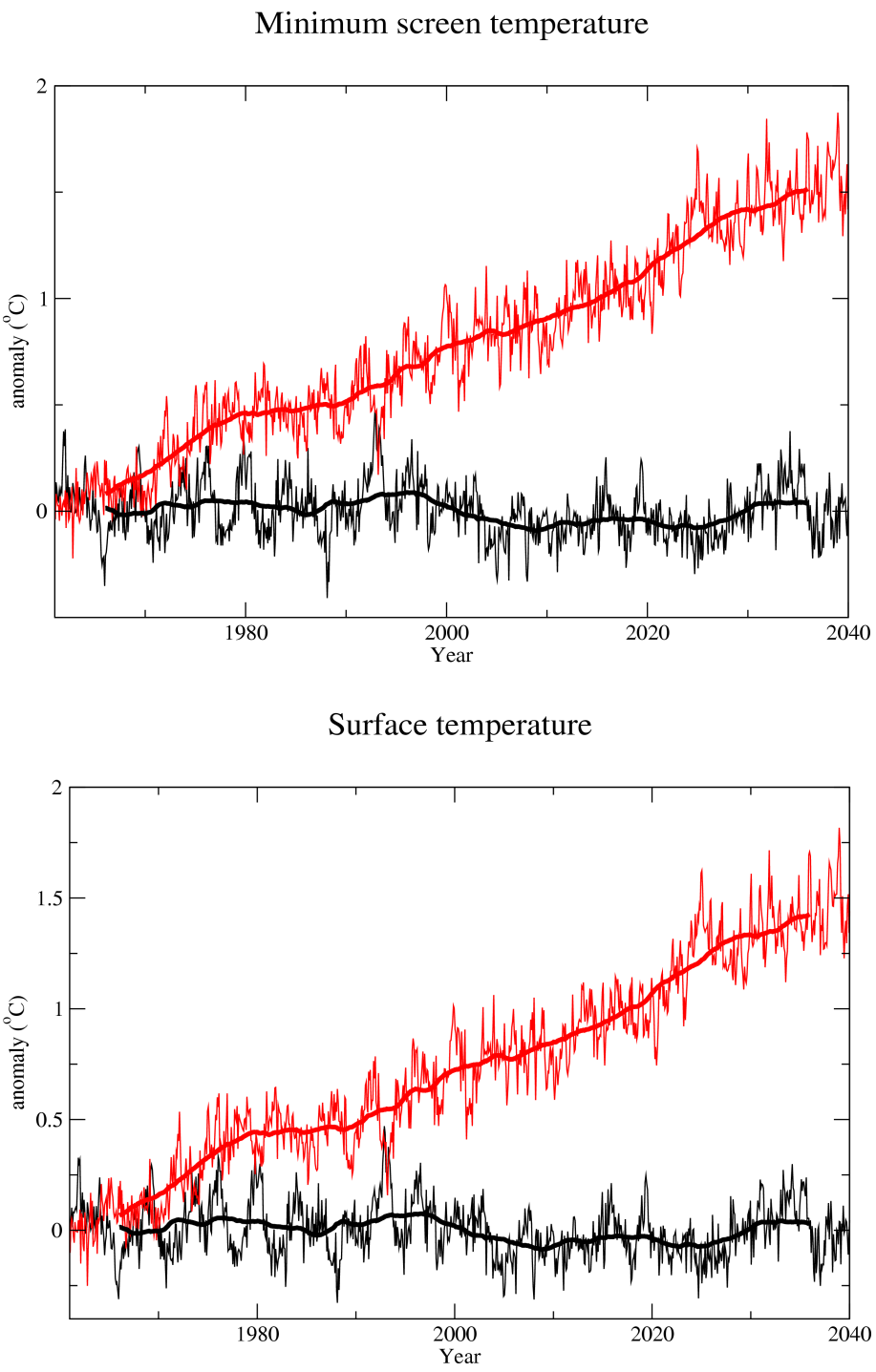

Figure 45: Global area weighted monthly anomaly of minimum screen temperature (°C, upper panel) and surface temperature (°C, lower panel) for control (black curve) and transient (red curve) experiments. For each monthly time-series a 121-month running average has been overlaid.

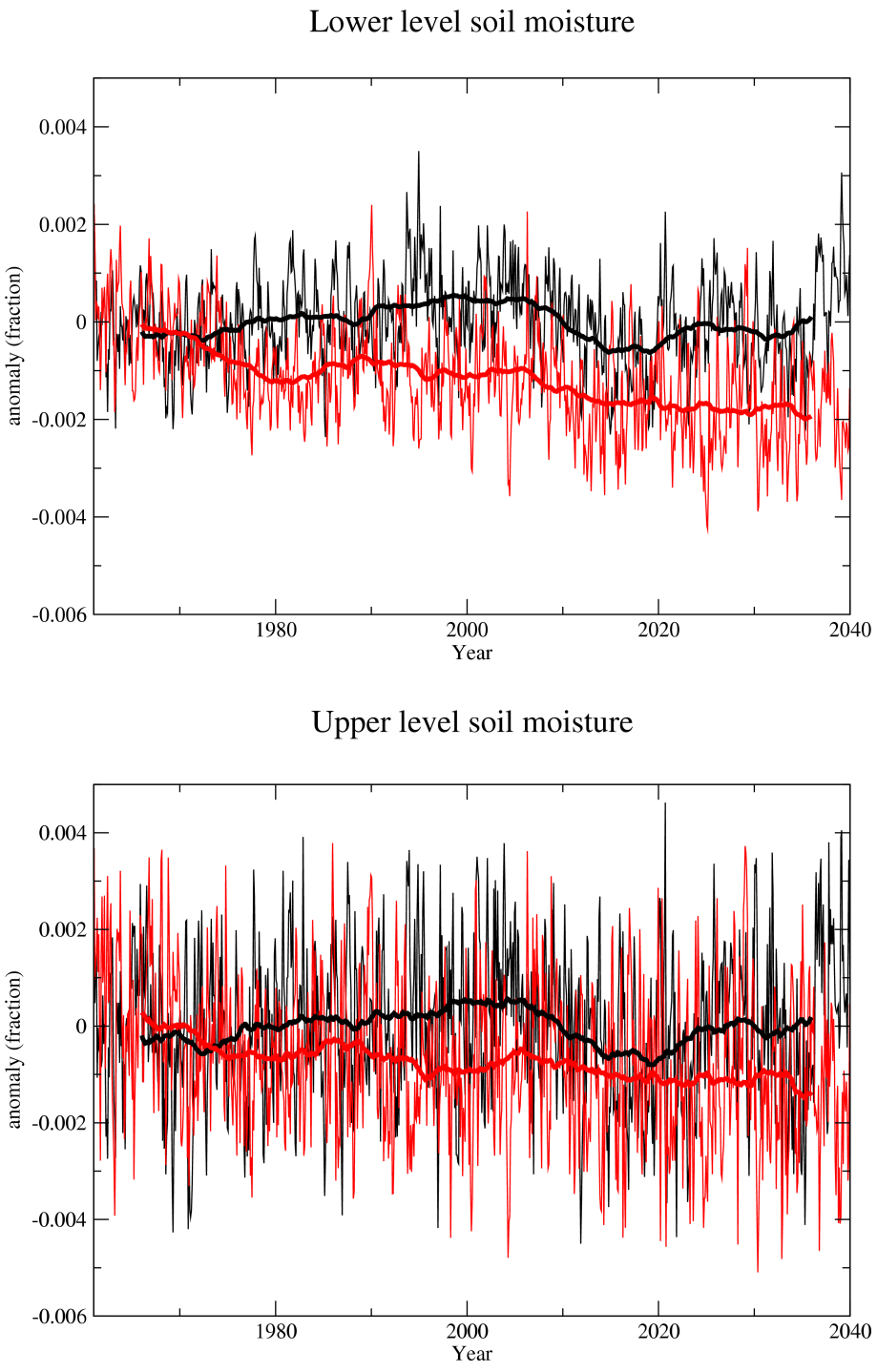

Figure 46: Global area weighted monthly anomaly of lower (upper panel) and upper (lower panel) level available soil moisture (volumetric ratio) for control (black curve) and transient (red curve) experiments. For each monthly The soil depth range is 0-0.022 and 0-4.6 m for the upper and lower soil moisture fields, respectively.

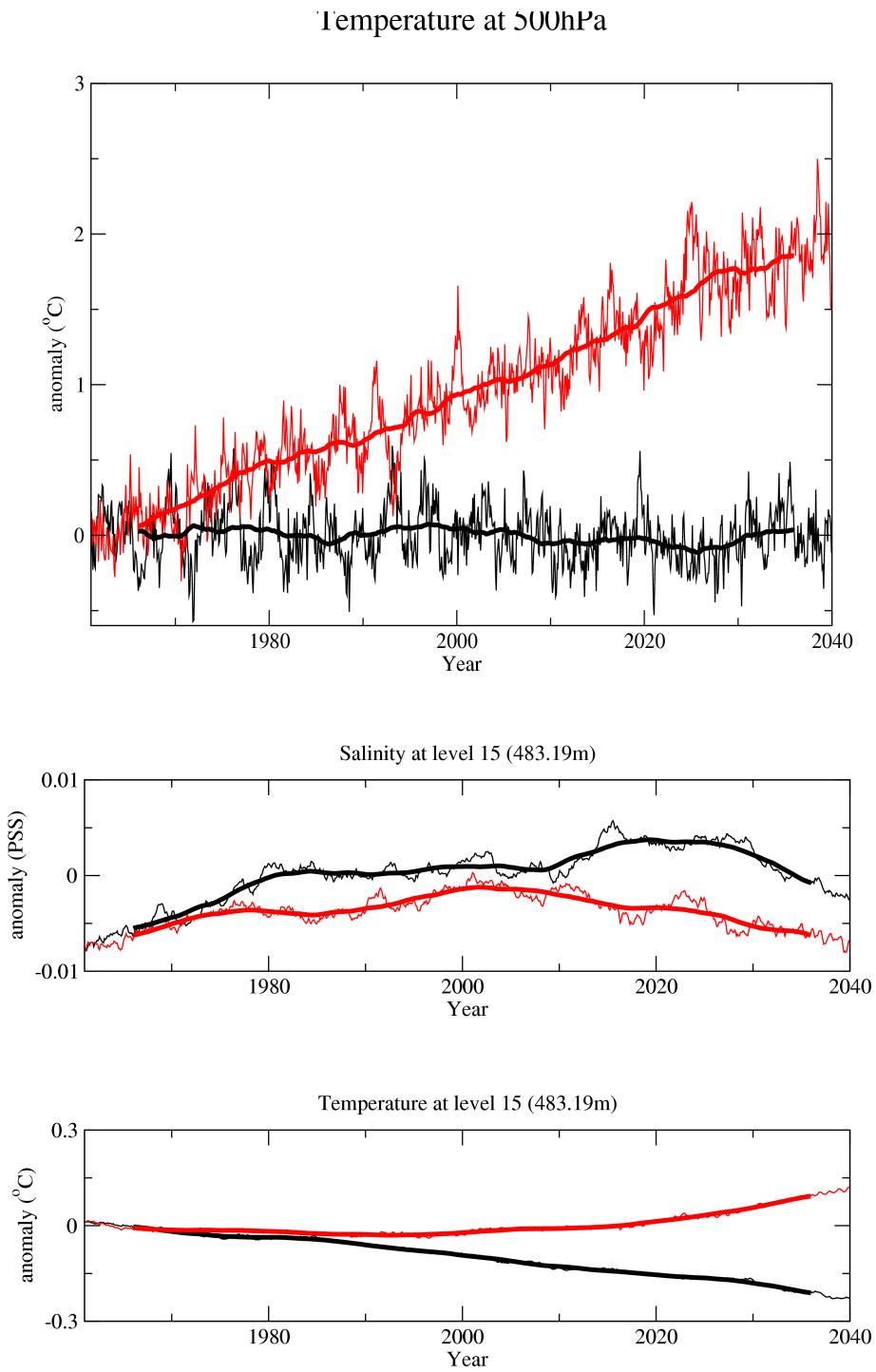

Figure 47: Global area weighted monthly anomaly of 500 hPa air temperature (°C, upper panel) and level 15 salinity (ppt, middle panel) and temperature(°C, lower panel) for control (black curve) and transient (red curve) experiments. For each monthly time-series a 121-month running average has been overlaid.

Acknowledgments

The Australian Greenhouse Office supported this work. The efforts of the Climate Modelling and Applications Team at CSIRO Atmospheric Research in developing the CSIRO Mk3 CSM are gratefully acknowledged, as is the support and facilities of the HPCCC. The authors wish to acknowledge use of the Ferret and Grace programs for analysis and graphics in this paper. Information is available at www.ferret.noaa.gov and plasma-gate.weizmann.ac.il/Grace.

Disclaimer

The CSIRO Mk3 CSM CMIP experimental data may be modified or updated at any time without any prior warning. Users of this model output are urged to check and reassure themselves of its numerical integrity and applicability to their individual research applications. If you have any questions regarding this document or data described within, please contact the author, preferably by e-mail.

References

Cai, W.J., Collier, M.A., Gordon, H.B. and Waterman, L.J.. Strong ENSO variability and a super-ENSO pair in the CSIRO coupled climate model. *Mon. Wea. Rev.*, **131**, 1189–1210, 2002.

Cai, W.J., McPhaden, M.J. and Collier, M.A.. Multidecadal fluctuations of the relationship between equatorial Pacific heat content anomalies and ENSO amplitude. *Geophys. Res. Lett.*, **31**, x–y, 2004.

Cai, W. Collier, M.A., Durack, P.J., Gordon, H.B., Hirst, A.C. O'Farrell, S.P., Whetton, P.J.. The response of climate variability and mean state to climate change: preliminary results from the CSIRO Mark 3 coupled model. *CLIVAR Exchanges*, **28**, 8–11, 2003.

Collier, M.A.. The CSIRO NCEP reanalysis archive. CSIRO Atmospheric Research internal Paper No. 17. 193 pp., 2000.

Collier, M.A.. The CSIRO netCDF archive of the World Ocean Atlas 2001. CSIRO Atmospheric Research internal Paper No. 26. 20 pp., 2003.

Collier, M.A.. The CSIRO NCEP/NCAR/DOE *R-1/R-2* archive. CSIRO Atmospheric Research internal Paper No. 66. 76 pp., 2004.

Conkright, M.E., R.A. Locarnini, H.E. Garcia, T.D. O'Brien, T.P. Boyer, C. Stephens and J.I. Antonov. World OCEAN ATLAS 2001: Objective Analyses, Data Statistics and Figures, CD-ROM Documentation. National Oceanographic Data Center, Silver Spring, MD, **17**, 17 pp., 2002.

Covey, C., AchutaRao, K.M. Cubasch, C. Ulrich, P. Jones, S.J. Lambert, M.E. Mann, T.J. Phillips and K.E. Taylor. An Overview of Results from the Coupled Model Intercomparison Project (CMIP). *Global and Planetary Change*, **37**, 103–133, 2003.

Dorman, J.L., and P.J. Sellers. A global climatology of albedo, roughness length and stomatal resistance for atmospheric general circulation models as represented by the simple biosphere model (SiB). *J. Appl. Meteor.*, **28**, 833–855, 1989.

Gordon, H.B., L.D. Rotstayn, J.L. McGregor, M.R. Dix, E.A. Kowalczyk, S.P. O'Farrell, L.J. Waterman, A.C. Hirst, S.G. Wilson, M.A. Collier, I.G. Watterson, and T.I. Elliott. The CSIRO Mk3 Climate System Model. CSIRO Atmospheric Research technical paper No. 60. 130 pp., 2002.

Kalnay, E., M. Kanamitsu, R. Kistler, W. Collins, D. Deaven, L. Gandin, M. Iredell, S. Saha, G. White, J. Woollen, Y. Zhu, M. Chelliah, W. Ebisuzaki, W. Higgins, J. Janowiak, K.C. Mo, C. Ropelewski, J. Wang, A. Leetmaa, R. Reynolds, R. Jenne and **D. Jospher** The NCEP/NCAR 40-Year Reanalysis Project. *Bul. Amer. Meteor. Soc.*, **3**, 437–471, 1996.

Kanamitsu, M., W. Ebisuzaki, J. Woollen, S-K. Yang, J.J. Hnilo, M. Fiorino and **G.L. Potter**. NCEP-DEO AMIP-II Reanalysis ($R-2$). *Bul. Amer. Meteor. Soc.*, **3**, 437–471, 2002.

Kistler, R., E. Kalnay, W. Collins, S. Saha, G. White, J. Woollen, M. Chelliah, W. Ebisuzaki, M. Kanamitsu, V. Kousky, H. van den Dool, R. Jenne and M. Fiorino. The NCEP-NCAR 50-year Reanalysis: Monthly Means CD-ROM and Documentation. *Bul. Amer. Meteor. Soc.*, **82**, 247–267, 2001.

McGregor, J.L., Gordon, H.B., Watterson, I.G., Dix, M.R., and L.D. Rotstayn The CSIRO 9-level atmospheric general circulation model. CSIRO Atmospheric Research technical paper No. 26. 89 pp., 1993.

Meehl, G.A., C. Covey, M. Latif, B. McAvaney and R.J. Stouffer. CMIP: The Coupled Model Intercomparison Project. *CLIVAR Exchanges*, **26**, 1–4, 2003.

Watterson, I.G. and Dix, M.R.. Effective sensitivity and heat capacity in the response of climate models to greenhouse gas and aerosol forcings. *Q. J. Roy. Met. Soc.*, accepted subject to revision, 2004.

4 Appendix 1: Model grid details

4.1 Atmospheric component grid

Pressure levels

	0	1	2	3	4	5	6	7	8	9
0	4.50	21.60	54.20	100.10	157.40	223.90	297.70	376.50	458.50	541.50
1	623.50	702.30	776.10	842.60	899.90	945.80	978.40	995.50		

Longitudes

	0	1	2	3	4	5	6	7	8	9
0	0.00	1.88	3.75	5.62	7.50	9.38	11.25	13.12	15.00	16.88
1	18.75	20.62	22.50	24.38	26.25	28.12	30.00	31.88	33.75	35.62
2	37.50	39.38	41.25	43.12	45.00	46.88	48.75	50.62	52.50	54.38
3	56.25	58.12	60.00	61.88	63.75	65.62	67.50	69.38	71.25	73.12
4	75.00	76.88	78.75	80.62	82.50	84.38	86.25	88.12	90.00	91.88
5	93.75	95.62	97.50	99.38	101.25	103.12	105.00	106.88	108.75	110.62
6	112.50	114.38	116.25	118.12	120.00	121.88	123.75	125.62	127.50	129.38
7	131.25	133.12	135.00	136.88	138.75	140.62	142.50	144.38	146.25	148.12
8	150.00	151.88	153.75	155.62	157.50	159.38	161.25	163.12	165.00	166.88
9	168.75	170.62	172.50	174.38	176.25	178.12	180.00	181.88	183.75	185.62
10	187.50	189.38	191.25	193.12	195.00	196.88	198.75	200.62	202.50	204.38
11	206.25	208.12	210.00	211.88	213.75	215.62	217.50	219.38	221.25	223.12
12	225.00	226.88	228.75	230.62	232.50	234.38	236.25	238.12	240.00	241.88
13	243.75	245.62	247.50	249.38	251.25	253.12	255.00	256.88	258.75	260.62
14	262.50	264.38	266.25	268.12	270.00	271.88	273.75	275.62	277.50	279.38
15	281.25	283.12	285.00	286.88	288.75	290.62	292.50	294.38	296.25	298.12
16	300.00	301.88	303.75	305.62	307.50	309.38	311.25	313.12	315.00	316.88
17	318.75	320.62	322.50	324.38	326.25	328.12	330.00	331.88	333.75	335.62
18	337.50	339.38	341.25	343.12	345.00	346.88	348.75	350.62	352.50	354.38
19	356.25	358.12								

Latitudes

	0	1	2	3	4	5	6	7	8	9
0	-88.57	-86.72	-84.86	-83.00	-81.14	-79.27	-77.41	-75.54	-73.68	-71.81
1	-69.95	-68.08	-66.22	-64.35	-62.49	-60.62	-58.76	-56.89	-55.02	-53.16
2	-51.29	-49.43	-47.56	-45.70	-43.83	-41.97	-40.10	-38.24	-36.37	-34.51
3	-32.64	-30.78	-28.91	-27.05	-25.18	-23.32	-21.45	-19.59	-17.72	-15.85
4	-13.99	-12.12	-10.26	-8.39	-6.53	-4.66	-2.80	-0.93	0.93	2.80
5	4.66	6.53	8.39	10.26	12.12	13.99	15.85	17.72	19.59	21.45
6	23.32	25.18	27.05	28.91	30.78	32.64	34.51	36.37	38.24	40.10
7	41.97	43.83	45.70	47.56	49.43	51.29	53.16	55.02	56.89	58.76
8	60.62	62.49	64.35	66.22	68.08	69.95	71.81	73.68	75.54	77.41
9	79.27	81.14	83.00	84.86	86.72	88.57				

4.2 Oceanic component grid

Depth levels

	0	1	2	3	4	5	6	7	8	9
0	5.00	15.00	28.25	42.02	59.66	78.54	102.11	127.88	159.47	194.56
1	236.97	284.64	341.69	406.38	483.19	570.87	674.86	793.76	934.08	1095.21
2	1284.65	1502.91	1758.77	2054.29	2400.00	2800.00	3200.00	3600.00	4000.00	4400.00
3	4800.00									

Tracer longitudes

	0	1	2	3	4	5	6	7	8	9
0	-1.88	0.00	1.88	3.75	5.63	7.50	9.38	11.25	13.13	15.00
1	16.88	18.75	20.63	22.50	24.38	26.25	28.13	30.00	31.88	33.75
2	35.63	37.50	39.38	41.25	43.13	45.00	46.88	48.75	50.63	52.50
3	54.38	56.25	58.13	60.00	61.88	63.75	65.63	67.50	69.38	71.25
4	73.13	75.00	76.88	78.75	80.63	82.50	84.38	86.25	88.13	90.00
5	91.88	93.75	95.63	97.50	99.38	101.25	103.13	105.00	106.88	108.75
6	110.63	112.50	114.38	116.25	118.13	120.00	121.88	123.75	125.63	127.50
7	129.38	131.25	133.13	135.00	136.88	138.75	140.63	142.50	144.38	146.25
8	148.13	150.00	151.88	153.75	155.63	157.50	159.38	161.25	163.13	165.00
9	166.88	168.75	170.63	172.50	174.38	176.25	178.13	180.00	181.88	183.75
10	185.63	187.50	189.38	191.25	193.13	195.00	196.88	198.75	200.63	202.50
11	204.38	206.25	208.13	210.00	211.88	213.75	215.63	217.50	219.38	221.25
12	223.13	225.00	226.88	228.75	230.63	232.50	234.38	236.25	238.13	240.00
13	241.88	243.75	245.63	247.50	249.38	251.25	253.13	255.00	256.88	258.75
14	260.63	262.50	264.38	266.25	268.13	270.00	271.88	273.75	275.63	277.50
15	279.38	281.25	283.13	285.00	286.88	288.75	290.63	292.50	294.38	296.25
16	298.13	300.00	301.88	303.75	305.63	307.50	309.38	311.25	313.13	315.00
17	316.88	318.75	320.63	322.50	324.38	326.25	328.13	330.00	331.88	333.75
18	335.63	337.50	339.38	341.25	343.13	345.00	346.88	348.75	350.63	352.50
19	354.38	356.25	358.13	360.00						

Tracer latitudes

	0	1	2	3	4	5	6	7	8	9
0	-87.19	-86.26	-85.33	-84.40	-83.46	-82.53	-81.60	-80.67	-79.74	-78.80
1	-77.87	-76.94	-76.01	-75.08	-74.14	-73.21	-72.28	-71.35	-70.41	-69.48
2	-68.55	-67.62	-66.68	-65.75	-64.82	-63.88	-62.95	-62.02	-61.09	-60.15
3	-59.22	-58.29	-57.36	-56.42	-55.49	-54.56	-53.63	-52.69	-51.76	-50.83
4	-49.90	-48.96	-48.03	-47.10	-46.16	-45.23	-44.30	-43.37	-42.43	-41.50
5	-40.57	-39.64	-38.70	-37.77	-36.84	-35.91	-34.97	-34.04	-33.11	-32.18
6	-31.24	-30.31	-29.38	-28.45	-27.51	-26.58	-25.65	-24.71	-23.78	-22.85
7	-21.92	-20.98	-20.05	-19.12	-18.19	-17.25	-16.32	-15.39	-14.46	-13.52
8	-12.59	-11.66	-10.73	-9.79	-8.86	-7.93	-6.99	-6.06	-5.13	-4.20
9	-3.26	-2.33	-1.40	-0.47	0.47	1.40	2.33	3.26	4.20	5.13
10	6.06	6.99	7.93	8.86	9.79	10.73	11.66	12.59	13.52	14.46
11	15.39	16.32	17.25	18.19	19.12	20.05	20.98	21.92	22.85	23.78
12	24.71	25.65	26.58	27.51	28.45	29.38	30.31	31.24	32.18	33.11
13	34.04	34.97	35.91	36.84	37.77	38.70	39.64	40.57	41.50	42.43
14	43.37	44.30	45.23	46.16	47.10	48.03	48.96	49.90	50.83	51.76
15	52.69	53.63	54.56	55.49	56.42	57.36	58.29	59.22	60.15	61.09
16	62.02	62.95	63.88	64.82	65.75	66.68	67.62	68.55	69.48	70.41
17	71.35	72.28	73.21	74.14	75.08	76.01	76.94	77.87	78.80	79.74
18	80.67	81.60	82.53	83.46	84.40	85.33	86.26	87.19	88.11	

Velocity longitudes

	0	1	2	3	4	5	6	7	8	9
0	-0.94	0.94	2.81	4.69	6.56	8.44	10.31	12.19	14.06	15.94
1	17.81	19.69	21.56	23.44	25.31	27.19	29.06	30.94	32.81	34.69
2	36.56	38.44	40.31	42.19	44.06	45.94	47.81	49.69	51.56	53.44
3	55.31	57.19	59.06	60.94	62.81	64.69	66.56	68.44	70.31	72.19
4	74.06	75.94	77.81	79.69	81.56	83.44	85.31	87.19	89.06	90.94
5	92.81	94.69	96.56	98.44	100.31	102.19	104.06	105.94	107.81	109.69
6	111.56	113.44	115.31	117.19	119.06	120.94	122.81	124.69	126.56	128.44
7	130.31	132.19	134.06	135.94	137.81	139.69	141.56	143.44	145.31	147.19
8	149.06	150.94	152.81	154.69	156.56	158.44	160.31	162.19	164.06	165.94
9	167.81	169.69	171.56	173.44	175.31	177.19	179.06	180.94	182.81	184.69
10	186.56	188.44	190.31	192.19	194.06	195.94	197.81	199.69	201.56	203.44
11	205.31	207.19	209.06	210.94	212.81	214.69	216.56	218.44	220.31	222.19
12	224.06	225.94	227.81	229.69	231.56	233.44	235.31	237.19	239.06	240.94
13	242.81	244.69	246.56	248.44	250.31	252.19	254.06	255.94	257.81	259.69
14	261.56	263.44	265.31	267.19	269.06	270.94	272.81	274.69	276.56	278.44
15	280.31	282.19	284.06	285.94	287.81	289.69	291.56	293.44	295.31	297.19
16	299.06	300.94	302.81	304.69	306.56	308.44	310.31	312.19	314.06	315.94
17	317.81	319.69	321.56	323.44	325.31	327.19	329.06	330.94	332.81	334.69
18	336.56	338.44	340.31	342.19	344.06	345.94	347.81	349.69	351.56	353.44
19	355.31	357.19	359.06	360.94						

Velocity latitudes

	0	1	2	3	4	5	6	7	8	9
0	-86.72	-85.79	-84.86	-83.93	-83.00	-82.07	-81.14	-80.20	-79.27	-78.34
1	-77.41	-76.47	-75.54	-74.61	-73.68	-72.74	-71.81	-70.88	-69.95	-69.01
2	-68.08	-67.15	-66.22	-65.28	-64.35	-63.42	-62.49	-61.55	-60.62	-59.69
3	-58.76	-57.82	-56.89	-55.96	-55.02	-54.09	-53.16	-52.23	-51.29	-50.36
4	-49.43	-48.50	-47.56	-46.63	-45.70	-44.77	-43.83	-42.90	-41.97	-41.04
5	-40.10	-39.17	-38.24	-37.31	-36.37	-35.44	-34.51	-33.57	-32.64	-31.71
6	-30.78	-29.84	-28.91	-27.98	-27.05	-26.11	-25.18	-24.25	-23.32	-22.38
7	-21.45	-20.52	-19.59	-18.65	-17.72	-16.79	-15.85	-14.92	-13.99	-13.06
8	-12.12	-11.19	-10.26	-9.33	-8.39	-7.46	-6.53	-5.60	-4.66	-3.73
9	-2.80	-1.87	-0.93	0.00	0.93	1.87	2.80	3.73	4.66	5.60
10	6.53	7.46	8.39	9.33	10.26	11.19	12.12	13.06	13.99	14.92
11	15.85	16.79	17.72	18.65	19.59	20.52	21.45	22.38	23.32	24.25
12	25.18	26.11	27.05	27.98	28.91	29.84	30.78	31.71	32.64	33.57
13	34.51	35.44	36.37	37.31	38.24	39.17	40.10	41.04	41.97	42.90
14	43.83	44.77	45.70	46.63	47.56	48.50	49.43	50.36	51.29	52.23
15	53.16	54.09	55.02	55.96	56.89	57.82	58.76	59.69	60.62	61.55
16	62.49	63.42	64.35	65.28	66.22	67.15	68.08	69.01	69.95	70.88
17	71.81	72.74	73.68	74.61	75.54	76.47	77.41	78.34	79.27	80.20
18	81.14	82.07	83.00	83.93	84.86	85.79	86.72	87.65	88.57	

5 Appendix 2: Full list of raw monthly and daily data

5.1 Atmospheric variables

Field	Variable	Unit	Experiment label	$x \times y \times z \times t$	monthly	daily
surface albedo	als	ratio	ct3/cm3	192 96 1 t	yes	no
convective cloud	clc	0-1	ct3/cm3	192 96 1 t	yes	no
total cloud	cld	0-1	ct3/cm3	192 96 1 t	yes	no
average total cloud	clda	0-1	ct3/cm3	192 96 1 t	no	yes
high cloud	clh	0-1	ct3/cm3	192 96 1 t	yes	no
low cloud	cll	0-1	ct3/cm3	192 96 1 t	yes	no
middle cloud	clm	0-1	ct3/cm3	192 96 1 t	yes	no
tmlo error	dtm	K	ct3/cm3	192 96 1 t	yes	no
evaporation	evp	mm day^{-1}	ct3/cm3	192 96 1 t	yes	once
monthly ice growth	gro	m	ct3/cm3	192 96 1 t	yes	no
sensible heat flux	hfl	W m^{-2}	ct3/cm3	192 96 1 t	yes	no
ice depth $\times$ concentration	icd	m	ct3/cm3	192 96 1 t	yes	no
ice advection	ich	m	ct3/cm3	192 96 1 t	yes	no
ice concentration	ico	0-1	ct3/cm3	192 96 1 t	yes	no
ice zonal velocity	icu	m s^{-1}	ct3/cm3	192 96 1 t	yes	no
ice meridional velocity	icv	m s^{-1}	ct3/cm3	192 96 1 t	yes	no
ice redistribution	ire	m	ct3/cm3	192 96 1 t	yes	no
ice-ocean salt flux	isf	m	ct3/cm3	192 96 1 t	yes	no
ice-ocean heat flux	itf	W m^{-2}	ct3/cm3	192 96 1 t	yes	no
ice water path	iwp	kg m^{-2}	ct3/cm3	192 96 1 t	yes	no
liquid water path	lwp	kg m^{-2}	ct3/cm3	192 96 1 t	yes	no
soil percolation	per	mm day^{-1}	ct3/cm3	192 96 1 t	yes	no
potential evaporation	pev	mm day^{-1}	ct3/cm3	96 48 1 t	yes	once
moisture puddles	pmc	mm	ct3/cm3	192 96 1 t	yes	no
name	psf	unit	ct3/cm3	96 48 1 t	no	twice
sea-level pressure	psl	hPa	ct3/cm3	192 96 1 t	yes	once
precipitable water	pwc	mm	ct3/cm3	192 96 1 t	yes	no
specific humidity at pressure/sigma level k	q01-q18	kg kg^{-1}	ct3/cm3	192 96 1 t	yes	twice
relative humidity at pressure/sigma level k	r01-r18	percent	ct3/cm3	192 96 1 t	yes	no
net longwave ground clear	rgc	W m^{-2}	ct3/cm3	192 96 1 t	yes	no
downward longwave ground	rgd	W m^{-2}	ct3/cm3	192 96 1 t	yes	no
net longwave at ground	rgn	W m^{-2}	ct3/cm3	192 96 1 t	yes	no
precipitation rate	rnd	mm day^{-1}	ct3/cm3	192 96 1 t	yes	once
screen level relative humidity	rhsa	mm day^{-1}	ct3/cm3	192 96 1 t	yes	once
convective precipitation rate	rnc	mm day^{-1}	ct3/cm3	192 96 1 t	yes	once

Field	Variable	Unit	Experiment label	$x \times y \times z \times t$	monthly	daily
longwave out clear sky	rtc	W m^{-2}	ct3/cm3	192 96 1 t	yes	no
net long-wave at top of atmosphere	rtu	W m^{-2}	ct3/cm3	192 96 1 t	yes	once
runoff	run	mm day^{-1}	ct3/cm3	192 96 1 t	yes	no
net shortwave ground clear	sgc	W m^{-2}	ct3/cm3	192 96 1 t	yes	no
downward short-wave at surface	sgd	W m^{-2}	ct3/cm3	192 96 1 t	no	once
net shortwave at ground	sgn	W m^{-2}	ct3/cm3	192 96 1 t	yes	no
sea-ice depth	sid	m	ct3/cm3	192 96 1 t	yes	no
snow depth	snd	m	ct3/cm3	192 96 1 t	yes	no
snowfall	sno	mm day^{-1}	ct3/cm3	192 96 1 t	yes	no
shortwave out clear sky	soc	W m^{-2}	ct3/cm3	192 96 1 t	yes	no
shortwave out at top	sot	W m^{-2}	ct3/cm3	192 96 1 t	yes	no
temperature at pressure/sigma level k	t01-t18	K	ct3/cm3	192 96 1 t	yes	twice
surface stress east	tax	N m^{-2}	ct3/cm3	192 96 1 t	yes	no
surface stress north	tay	N m^{-2}	ct3/cm3	192 96 1 t	yes	no
soil temperature level 2	tb2	K	ct3/cm3	192 96 1 t	yes	twice
soil temperature level 3	tb3	K	ct3/cm3	192 96 1 t	yes	twice
vegetation ground temperature	tgf	K	ct3/cm3	192 96 1 t	yes	no
bare ground temperature	tgg	K	ct3/cm3	192 96 1 t	yes	no
mean daily maximum surface temperature	thd	K	ct3/cm3	192 96 1 t	yes	no
extreme maximum temperature	thm	K	ct3/cm3	192 96 1 t	yes	no
mean daily minimum surface temperature	tld	K	ct3/cm3	192 96 1 t	yes	no
extreme minimum temperature	tlm	K	ct3/cm3	192 96 1 t	yes	no
surface screen temperature	tsc	K	ct3/cm3	192 96 1 t	yes	no
average screen temperature	tsca	K	ct3/cm3	192 96 1 t	no	once
maximum screen temperature	tsh	K	ct3/cm3	192 96 1 t	no	once
minimum screen temperature	tsl	K	ct3/cm3	192 96 1 t	no	once
surface temperature	tsu	K	ct3/cm3	192 96 1 t	yes	twice
average screen temperature	tsua	K	ct3/cm3	192 96 1 t	no	once
zonal wind at pressure/sigma level k	u01-u18	m s^{-1}	ct3/cm3	192 96 1 t	yes	twice
meridional wind at pressure/sigma level k	v01-v18	m s^{-1}	ct3/cm3	192 96 1 t	yes	twice
average 10m wind speed	v10ma	m s^{-1}	ct3/cm3	192 96 1 t	no	once
surface screen temperature	tsc	°C	ct3/cm3	192 96 1 t	yes	no
surface temperature	tsu	°C	ct3/cm3	192 96 1 t	yes	once
available soil moisture lower	wfb	volumetric ratio	ct3/cm3	192 96 1 t	yes	twice
available soil moisture upper	wfg	volumetric ratio	ct3/cm3	192 96 1 t	yes	twice
surface height	zht	m	ct3/cm3	192 96 1 1	n/a	n/a

5.2 Oceanic variables

Field	Variable	Unit	Experiment label	$x \times y \times z \times t$
salinity	Salt	ppt	ct3/cm3	194 189 31 960
potential temperature	Temp	°C	ct3/cm3	194 189 31 960
meridional velocity	uvel	m s^{-1}	ct3/cm3	194 189 31 960
zonal velocity	vvel	m s^{-1}	ct3/cm3	194 189 31 960
verticl velocity	wvel	m s^{-1}	ct3/cm3	194 189 31 960
surface heat flux	hflx	W m^{-2}	ct3/cm3	194 189 31 960
urface freshwater flux	pme	mm day^{-1}	ct3/cm3	194 189 31 960
zonal windstress	taux	dynes cm^{-2}	ct3/cm3	194 189 31 960
meridional windstress	tauy	dynes cm^{-2}	ct3/cm3	194 189 31 960
stream function	psi	Sv	ct3/cm3	194 189 31 960
topography on T grid	kmt	levels	ct3/cm3	194 189 31 960
topography on U grid	kmu	levels	ct3/cm3	194 189 31 960
meridional overturning streamfunction	vms	Sv	ct3/cm3	0 191 31 960
kinetic energy per unit volume	ke	gm cm^{-1} sec^{-2}	ct3/cm3	0 0 0 29200
global average temperature	tbar	°C	ct3/cm3	0 0 0 29200
global average salinity	sbar	ppm-0.035	ct3/cm3	0 0 0 29200
variance of temperature	tvar	$°C^2$	ct3/cm3	0 0 0 29200
variance of salinity	svar	$(\text{ppm-}0.035)^2$	ct3/cm3	0 0 0 29200
|dT/dt|	abs_cht_t	°C s^{-1}	ct3/cm3	0 0 0 29200
|dS/dt|	abs_chg_s	ppm-0.035 s^{-1}	ct3/cm3	0 0 0 29200
elliptic solver iterations	scans	number	ct3/cm3	0 0 0 29200

6 Appendix 3: Accessing monthly and daily data

All CSIRO Mk3 CSM CMIP data is located on the mass tape storage system operated by the High Performance Computing and Communications Centre, http://www.hpsc.csiro.au/ and accessed through the data server **cherax**.*hpsc.csiro.au*.

All data are found under the directory structure **cherax**:~cec006/ocean/data/{cm3,ct3}, where ct3 and cm3 are the experiment labels referring to the control and transient experiments, respectively.

The basic filename for the monthly data have the following form

type_variable_ybeg_yend.run.nc

where

type is atmos (as in atmospheric) or ocean (as in oceanic)
variable valid CMIP variable[9]
ybeg is the begin year
yend is the end year
run is the experiment label.

The daily data follow a similar naming convention

type-dly_**variable_ybeg_yend.run**.nc

Monthly climatology and anomaly files are also available for specific variables, or subsets of variables that are not listed here. Please contact the lead author of this paper for further information on this matter.

[9] found under the "Experiment label" column heading of the tables in Section 2.1.

CSIRO Atmospheric Research Technical papers

Complete List

(Series title changed from CSIRO Division of Atmospheric Technical papers at number 38)

No. 1 **Galbally, I.E.; Roy, C.R.; O'Brien, R.S.; Ridley, B.A.; Hastie, D.R.; Evans, W.J.F.; McElroy, C.T.; Kerr, J.B.; Hyson, P.; Knight, W.; Laby, J.E.** Measurements of trace composition of the Austral stratosphere: chemical and meteorological data. 1983. 31 pp.

No. 2 **Enting, I.G.** Error analysis for parameter estimates from constrained inversion. 1983. 18 pp.

No. 3 **Enting, I.G.; Pearman, G.I.** Refinements to a one-dimensional carbon cycle model. 1983. 35 pp.

No. 4 **Francey, R.J.; Barbetti, M.; Bird, T.; Beardsmore, D.; Coupland, W.; Dolezal, J.E.; Farquhar, G.D.; Flynn, R.G.; Fraser, P.J.; Gifford, R.M.; Goodman, H.S.; Kunda, B.; McPhail, S.; Nanson, G.; Pearman, G.I.; Richards, N.G.; Sharkey, T.D.; Temple, R.B.; Weir, B.** Isotopes in tree rings. 1984. 86 pp.

No. 5 **Enting, I.G.** Techniques for determining surface sources from surface observations of atmospheric constituents. 1984. 30 pp.

No. 6 **Beardsmore, D.J.; Pearman, G.I.; O'Brien, R.C.** The CSIRO (Australia) Atmospheric Carbon Dioxide Monitoring Program: surface data. 1984. 115 pp.

No. 7 **Scott, J.C.** High speed magnetic tape interface for a microcomputer. 1984. 17 pp.

No. 8 **Galbally, I.E.; Roy, C.R.; Elsworth, C.M.; Rabich, H.A.H.** The measurement of nitrogen oxide (NO, NO2) exchange over plant/soil surfaces. 1985. 23 pp.

No. 9 **Enting, I.G.** A strategy for calibrating atmospheric transport models. 1985. 25 pp.

No. 10 **O'Brien, D.M.** TOVPIX: software for extraction and calibration of TOVS data from the high resolution picture transmission from TIROS-N satellites. 1985. 41 pp.

No. 11 **Enting, I.G.; Mansbridge, J.V.** Description of a two-dimensional atmospheric transport model. 1986. 22 pp.

No. 12 **Everett, J.R.; O'Brien, D.M.; Davis, T.J.** A report on experiments to measure average fibre diameters by optical fourier analysis. 1986. 22 pp.

No. 13 **Enting, I.G.** A signal processing approach to analysing background atmospheric constituent data. 1986. 21 pp.

No. 14 **Enting, I.G.; Mansbridge, J.V.** Preliminary studies with a two-dimensional model using transport fields derived from a GCM. 1987. 47 pp.

No. 15 **O'Brien, D.M.; Mitchell, R.M.** Technical assessment of the joint CSIRO/Bureau of Meteorology proposal for a geostationary imager/sounder over the Australian region. 1987. 53 pp.

No. 16 **Galbally, I.E.; Manins, P.C.; Ripari, L.; Bateup, R.** A numerical model of the late (ascending) stage of a nuclear fireball. 1987. 89 pp.

No. 17 **Durre, A.M.; Beer, T.** Wind information prediction study: Annaburroo meteorological data analysis. 1989. 30 pp. + diskette.

No. 18 **Mansbridge, J.V.; Enting, I.G.** Sensitivity studies in a two-dimensional atmospheric transport model. 1989. 33 pp.

No. 19 **O'Brien, D.M.; Mitchell, R.M.** Zones of feasibility for retrieval of surface pressure from observations of absorption in the A band of oxygen. 1989. 12 pp.

No. 20 **Evans, J.L.** Envisaged impacts of enhanced greenhouse warming on tropical cyclones in the Australian region. 1990. 31 pp. [Out of print]

No. 21 **Whetton, P.H.; Pittock, A.B.** Australian region intercomparison of the results of some general circulation models used in enhanced greenhouse experiments. 1991. 73 pp. [Out of print]

No. 22 **Enting, I.G.** Calculating future atmospheric CO2 concentrations. 1991. 32 pp. available electronically

No. 23 **Kowalczyk, E.A.; Garratt, J.R.; Krummel, P.B.** A soil-canopy scheme for use in a numerical model of the atmosphere 1D stand-alone model. 1992. 56 pp.

No. 24 **Physick, W.L.; Noonan, J.A.; McGregor, J.L.; Hurley, P.J.; Abbs, D.J.; Manins, P.C.** LADM: A Lagrangian Atmospheric Dispersion Model. 1994. 137 pp.

No. 25 **Enting, I.G.** Constraining the atmospheric carbon budget: a preliminary assessment. 1992. 28 pp. Available electronically

No. 26 **McGregor, J.L.; Gordon, H.B.; Watterson, I.G.; Dix, M.R.; Rotstayn, L.D.** The CSIRO 9-level atmospheric general circulation model. 1993. 89 pp.

No. 27 **Enting, I.G.; Lassey, K.R.** Projections of future CO2. with appendix by R.A. Houghton. 1993. 42 pp. Available electronically

No. 28 [Not published]

No. 29 **Enting, I.G.; Trudinger, C.M.; Francey, R.J.; Granek, H.** Synthesis inversion of atmospheric CO2 using the GISS tracer transport model. 1993. 44 pp.

No. 30 **O'Brien, D.M.** Radiation fluxes and cloud amounts predicted by the CSIRO nine level GCM and observed by ERBE and ISCCP. 1993. 37 pp.

No. 31 **Enting, I.G.; Wigley, T.M.L.; Heimann, M.** Future emissions and concentrations of carbon dioxide: key ocean/atmosphere/land analyses. 1994. 120 pp. available electronically

No. 32 **Kowalczyk, E.A.; Garratt, J.R.; Krummel, P.B.** Implementation of a soil-canopy scheme into the CSIRO GCM regional aspects of the model response. 1994. 59 pp.

No. 33 **Prata, A.J.** Validation data for land surface temperature determination from satellites. 1994. 40 pp.

No. 34 **Dilley, A.C.; Elsum, C.C.** Improved AVHRR data navigation using automated land feature recognition to correct a satellite orbital model. 1994. 22 pp.

No. 35 **Hill, R.H.; Long, A.B.** The CSIRO dual-frequency microwave radiometer. 1995. 16 pp.

No. 36 **Rayner, P.J.; Law, R.M.** A comparison of modelled responses to prescribed CO2 sources. 1995. 84 pp.

No. 37 **Hennessy, K.J.** CSIRO Climate change output. 1998. 23 pp.

No. 38 **Enting, I.G.** Attribution of greenhouse gas emissions, concentrations and radiative forcing. 1998. 29 pp. Available electronically

No. 39 **OBrien, D.M.; Tregoning, P.** Geographical distributions of occultations of GPS satellites viewed from a low earth orbiting satellite. 1998. 23 pp.

No. 40 **Enting, I.G.** Characterising the temporal variability of the global carbon cycle. 1999. 23 pp. Available electronically

No. 41 **Enting, I.G.; Law, R.M.** Characteristing Historical Responsibility for the Greenhouse Effect, 2002. 50 pp. Electronic edition only

No. 42 **Mitchell, R.M.** Calibration status of the NOAA AVHRR solar reflectance channels: CalWatch revision 1. 1999. 20 pp.

No. 43 **Hurley, P.J.** The Air Pollution Model (TAPM) Version 1: technical description and examples. 1999. 41 pp. Available electronically

No. 44 **Frederiksen, J.S.; Dix, M.R.; Davies, A.G.** A new eddy diffusion parameterisation for the CSIRO GCM. 2000. 31 pp.

No. 45 **Young, S.A.** Vegetation canopy lidar studies. 2000. 35 pp. Electronic edition only.

No. 46 **Prata, A.J.** Global Distribution of Maximum Land Surface Temperature Inferred from Satellites: Implications for the Advanced Along Tracking Scan Radiometer. 2000. 30 pp. Electronic edition only.

No. 47 **Prata, A.J.** Precipitable water retrieval from multi-filtered shadowband radiometer measurements. 2000. 14 pp. Electronic edition only.

No. 48 **Prata, A.J., Grant, I.F.** Determination of mass loadings and plume heights of volcanic ash clouds from satellite data. 2001. 39 pp. Electronic edition only.

No. 49 **OBrien, D.M.** Numerical calculation of the transfer of polarized radiation by a scattering and absorbing atmosphere. 2001. 65 pp. Electronic edition only.

No. 50 **R.L. Law, Vohralik, P.F.** Methane sources from mass-balance inversions: Sensitivity to transport. 2001 27 pp. Electronic edition only.

No. 51 **Meyer, C.P., Galbally, I.E., Wang, Y.P., Weeks, I.A., Jamie, I., Griffith, D.W.T.** Two automatic chamber techniques for measuring soil-atmosphere exchanges of trace gases and results of their use in the OASIS field experiment. 2001. 33 pp. Electronic edition only.

No. 52 **Mitchell, R.M.** In-flight characteristics of the space count of NOAA AVHRR channels 1 and 2. 2001. 24 pp. Electronic edition only.

No. 53 **Young, S.A.** An investigation into the performance of algorithms used to retrieve cloud parameters from LITE lidar data, and implications for their use with PICASSO-CENA lidar data. 2001. Electronic edition only.

No 54 [Not published]

No. 55 **Hurley, P.** The Air Pollution Model (TAPM) Version 2. Part 1. Technical Description. 2002. Electronic edition only.

No. 56 **Enting, I.G. and Trudinger C.M.** Modelling earth system change. 1, Validating parameterisations for attribution calculations. 2002. Electronic edition only.

No. 57 **Hurley, P., Physick, W.L. and Luhar, A.K.** The Air Pollution Model (TAPM) Version 2. Part 2. Summary of some verification studies. 2002. Electronic edition only.

No. 58 [Not published]

No. 59 **Frederiksen, J.S., Collier, M.A., and Watkins A.B.** Ensemble Prediction Methods based on Fast Growing Perturbations. 2002. Electronic edition only.

No. 60 **Gordon, H.B., et. al.** The CSIRO Mk3 Climate System Model. 2002. Electronic edition only.

No. 61 **Graetz, R.D.** The net carbon dioxide flux from biomass burning on the Australian continent. 2002. Electronic edition only.

No. 62 **Enting, I.G.** Inverse problems in earth system science: A complex systems perspective. 2002. Electronic edition only.

No. 63 [in preparation]

No. 64 **Graetz, R.D., and Skjemstad J.O.** The charcoal sink of biomass burning on the Australian continent. 2003. Electronic edition only.

No. 65 **Young, S.A.** Interpretations of the performance of the hybrid extinction retrieval algorithms (HERA) during the CALIPSO Build 2 tests.

No. 57 **Schmidt, M., King, E.A. and McVicar, T.R.** Development of a Web-based data and product delivery system for the CSIRO AVHRR Time Series (CATS): Architecture, Interface and Processing Descriptions. 2004. Electronic edition only.

No. 67 **Mitchell, R.M, Campbell, S.K., and Daniel P.J.** Selection of a Radiance Source for the Radiometric Calibration Facility at the CSIRO Earth Observation Centre 2004. Electronic edition only.

No. 68 **Collier, M.A.** The CSIRO NCEP/NCAR/DOE *R-1/R-2* archive. 2004. Electronic edition only.